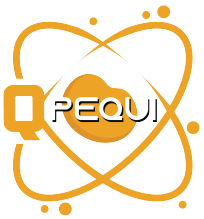

UNIVERSIDADE FEDERAL DE GOIÁS (UFG)
INSTITUTO DE FÍSICA (IF)
PROGRAMA DE PÓS-GRADUAÇÃO EM FÍSICA (PPGF)

RONALDO FERREIRA COSTA

A study on thermodynamics and information in holographic models

GOIÂNIA
2024

UNIVERSIDADE FEDERAL DE GOIÁS
INSTITUTO DE FÍSICA

TERMO DE CIÊNCIA E DE AUTORIZAÇÃO (TECA) PARA DISPONIBILIZAR VERSÕES ELETRÔNICAS DE TESES E DISSERTAÇÕES NA BIBLIOTECA DIGITAL DA UFG

Na qualidade de titular dos direitos de autor, autorizo a Universidade Federal de Goiás (UFG) a disponibilizar, gratuitamente, por meio da Biblioteca Digital de Teses e Dissertações (BDTD/UFG), regulamentada pela Resolução CEPEC nº 832/2007, sem ressarcimento dos direitos autorais, de acordo com a Lei 9.610/98, o documento conforme permissões assinaladas abaixo, para fins de leitura, impressão e/ou download, a título de divulgação da produção científica brasileira, a partir desta data.

O conteúdo das Teses e Dissertações disponibilizado na BDTD/UFG é de responsabilidade exclusiva do autor. Ao encaminhar o produto final, o autor(a) e o(a) orientador(a) firmam o compromisso de que o trabalho não contém nenhuma violação de quaisquer direitos autorais ou outro direito de terceiros.

1. Identificação do material bibliográfico

[X] Dissertação [ ] Tese [ ] Outro*:_____

*No caso de mestrado/doutorado profissional, indique o formato do Trabalho de Conclusão de Curso, permitido no documento de área, correspondente ao programa de pós-graduação, orientado pela legislação vigente da CAPES.

Exemplos: Estudo de caso ou Revisão sistemática ou outros formatos.

2. Nome completo do autor

Ronaldo Ferreira Costa

3. Título do trabalho

A study on thermodynamics and information in holographic models

4. Informações de acesso ao documento (este campo deve ser preenchido pelo orientador)

Concorda com a liberação total do documento [X] SIM [ ] NÃO[1]

[1] Neste caso o documento será embargado por até um ano a partir da data de defesa. Após esse período, a possível disponibilização ocorrerá apenas mediante:
a) consulta ao(à) autor(a) e ao(à) orientador(a);
b) novo Termo de Ciência e de Autorização (TECA) assinado e inserido no arquivo da tese ou dissertação.
O documento não será disponibilizado durante o período de embargo.
Casos de embargo:
- Solicitação de registro de patente;
- Submissão de artigo em revista científica;
- Publicação como capítulo de livro;
- Publicação da dissertação/tese em livro.

Obs. Este termo deverá ser assinado no SEI pelo orientador e pelo autor.

Documento assinado eletronicamente por **Romulo Cesar Rougemont Pereira**, **Professor do Magistério Superior**, em 03/02/2025, às 12:44, conforme horário oficial de Brasília, com fundamento no § 3º do art. 4º do Decreto nº 10.543, de 13 de novembro de 2020.

Documento assinado eletronicamente por **Ronaldo Ferreira Costa**, **Discente**, em 04/02/2025, às 20:42, conforme horário oficial de Brasília, com fundamento no § 3º do art. 4º do Decreto nº 10.543, de 13 de novembro de 2020.

A autenticidade deste documento pode ser conferida no site https://sei.ufg.br/sei/controlador_externo.php?acao=documento_conferir&id_orgao_acesso_externo=0, informando o código verificador **5120262** e o código CRC **5610AA64**.

RONALDO FERREIRA COSTA

A study on thermodynamics and information in holographic models

Um estudo sobre termodinâmica e informação em modelos holográficos

Dissertação apresentada ao Programa de Pós-Graduação em Física do Instituto de Física da Universidade Federal de Goiás (UFG), como requisito parcial para obtenção do título de mestre em física.

Área de Concentração: Física.
Linha de Pesquisa: Partículas e Campos.

Orientador: Prof. Dr. Rômulo Cesar Rougemont Pereira
Coorientador: Prof. Dr. Lucas Chibebe Céleri

GOIÂNIA
2024

Ficha de identificação da obra elaborada pelo autor, através do
Programa de Geração Automática do Sistema de Bibliotecas da UFG.

Costa, Ronaldo Ferreira
A Study on Thermodynamics and Information in Holographic Models [manuscrito] / Ronaldo Ferreira Costa. - 2024.
95 f.: il.

Orientador: Prof. Dr. Rômulo Cesar Rougemont Pereira; co orientador Dr. Lucas Chibebe Céleri.
Dissertação (Mestrado) - Universidade Federal de Goiás, Instituto de Física (IF), Programa de Pós-Graduação em Física, Goiânia, 2024.
Bibliografia.
Inclui lista de figuras, lista de tabelas.

1. Information. 2. Thermodynamics. 3. Gauge/Gravity duality. I. Pereira, Rômulo Cesar Rougemont, orient. II. Título.

CDU 539.12

UNIVERSIDADE FEDERAL DE GOIÁS

INSTITUTO DE FÍSICA

ATA DE DEFESA DE DISSERTAÇÃO

Ata nº 222 da sessão de Defesa de Dissertação de Ronaldo Ferreira Costa, que confere o título de Mestre em Física, na área de concentração em Física.

Aos 20 dias do mês de dezembro de 2024, a partir das 10h00min, por meio de videoconferência, realizou-se a sessão pública de Defesa de Dissertação intitulada “A study on thermodynamics and information in holographic models”. Os trabalhos foram instalados pelo Orientador, Professor Doutor Romulo Cesar Rougemont Pereira (IF/UFG), com a participação dos demais membros da Banca Examinadora: Professor Doutor Marcelo Santos Guimarães (IF/UERJ), membro titular externo; e Professor Doutor Willians Oswaldo Barreto Acevedo (CCNH/UFABC), membro titular externo. Durante a arguição, os membros da banca não fizeram sugestão de alteração do título do trabalho. A Banca Examinadora reuniu-se em sessão secreta a fim de concluir o julgamento da Dissertação, tendo sido o candidato aprovado pelos seus membros. Proclamados os resultados pelo Professor Doutor Romulo Cesar Rougemont Pereira, Presidente da Banca Examinadora, foram encerrados os trabalhos e, para constar, lavrou-se a presente ata que é assinada pelos membros da Banca Examinadora, aos 20 dias do mês de dezembro de 2024.

TÍTULO SUGERIDO PELA BANCA

Documento assinado eletronicamente por **Romulo Cesar Rougemont Pereira**, **Professor do Magistério Superior**, em 20/12/2024, às 14:33, conforme horário oficial de Brasília, com fundamento no § 3º do art. 4º do Decreto nº 10.543, de 13 de novembro de 2020.

Documento assinado eletronicamente por **Willians Oswaldo Barreto Acevedo**, **Usuário Externo**, em 20/12/2024, às 15:30, conforme horário oficial de Brasília, com fundamento no § 3º do art. 4º do Decreto nº 10.543, de 13 de novembro de 2020.

Documento assinado eletronicamente por **Marcelo Santos Guimarães**, **Usuário Externo**, em 20/12/2024, às 15:56, conforme horário oficial de Brasília, com fundamento no § 3º do art. 4º do Decreto nº 10.543, de 13 de novembro de 2020.

A autenticidade deste documento pode ser conferida no site https://sei.ufg.br/sei/controlador_externo.php?acao=documento_conferir&id_orgao_acesso_externo=0, informando o código verificador **5001906** e o código CRC **2784836B**.

"To my grandmother Joana, who loved everyone equally and who, unfortunately, couldn't accompany me on this journey to the end."

Acknowledgements

Many people collaborated to make this work possible, and without them, it likely wouldn't exist. First, I would like to thank my parents, Maria and Domingos, for all their support and encouragement. Even without understanding anything about what I do, they always supported me unconditionally. To Camila, my companion through all moments, good, bad, sad, or happy, thank you for always being by my side and helping me see the world differently. I am grateful to my advisors, Rômulo and Lucas, for showing me what physics research truly entails and for their patience in explaining and correcting my doubts countless times. Thanks to Professors Marcos Castro and Márcio Adriano, for their teachings, good conversations, and help in supervising my mandatory internship. To my fellow graduate students, who made the difficulties more bearable, especially my colleagues from room 219 and the QPequi Group: Anderson (Paizão), Gabriel (Gabs), and Pedro. I also want to mention Marcelo (Matielo), Vinícius (Vinição), Gustavo de Oliveira, Gustavo Marques (Gustavão), Alexandre, Samuel, Rodrigo, and Igor.

To my lifelong friends, who will always be with me, no matter what: Alexander (Miltin), Rafael, and Johnny.

Finally, I would like to acknowledge CAPES for funding this work through a master's scholarship.

Resumo

Esta dissertação aborda aspectos da teoria da informação e da termodinâmica no contexto da dualidade calibre/gravidade, focando em dois modelos holográficos específicos: 1RCBH e 2RCBH. O estudo analisa conceitos fundamentais da teoria da informação, como a entropia de emaranhamento, e discute a dualidade calibre/gravidade como uma ferramenta para analisar propriedades termodinâmicas e de informação desses modelos.

Inicialmente, revisamos em detalhe a termodinâmica do modelo 1RCBH, que é um "toy-model" para uma teoria de campo quântico fortemente acoplada a temperatura e densidade finitas e que possui um ponto crítico em seu diagrama de fase, enquanto o modelo 2RCBH descreve uma teoria de campo quântico fortemente acoplada diferente, também definida a temperatura e densidade finitas, mas sem um ponto crítico em seu diagrama de fase. O foco principal da pesquisa é calcular observáveis termodinâmicos e de informação utilizando a dualidade holográfica calibre/gravidade nesses modelos.

Também revisamos a entropia de emaranhamento do modelo 1RCBH e, como uma contribuição original, propomos um novo método de cálculo mais eficiente do que o considerado anteriormente na literatura. Devido a dificuldades numéricas ainda a serem entendidas e resolvidas, uma análise detalhada da entropia de emaranhamento nos modelos 1RCBH e 2RCBH será adiada para um artigo a ser desenvolvido em breve.

Palavras-chave: Informação; Termodinâmica; Dualidade Calibre/Gravidade.

Abstract

This dissertation addresses aspects of information theory and thermodynamics in the context of gauge/gravity duality, focusing on two specific holographic models: 1RCBH and 2RCBH. The study analyzes fundamental concepts of information theory, such as entanglement entropy and discusses gauge/gravity duality as a tool for analyzing thermodynamic and information properties of these models.

Initially, we review in detail the thermodynamics of the 1RCBH model, which is a toy-model for a strongly-coupled quantum field theory at finite temperature and density and has a critical point in its phase diagram, while the 2RCBH model describes a different strongly-coupled quantum field theory, also defined at finite temperature and density, but without a critical point in its phase diagram. The main focus of the research is to calculate thermodynamic and information observables using holographic gauge/gravity duality in these models.

We also review the entanglement entropy of the 1RCBH model, and, as an original contribution, we propose a new and more efficient method to evaluate it than previously considered in the literature. Due to some numerical issues still to be understood and solved, a detailed analysis of the entanglement entropy in the 1RCBH and 2RCBH models will be postponed to an upcoming work intended for publication.

Keywords: Information; Thermodynamics; Gauge/Gravity Duality.

Contents

List of Figures

List of Tables

Chapter 1

Introduction

Information theory has played a fundamental role in theoretical physics. Among the most relevant concepts of this theory are entanglement entropy and mutual information, which we will review in the second chapter, along with other fundamental concepts of information theory, focusing on their subsequent applications. Entanglement entropy measures how much a quantum state differs from a separable state, reaching its maximum value when a state is a superposition of all possible quantum states with equal weights. This concept is particularly relevant for the study of phase transitions in quantum systems.

Holographic gauge/gravity duality, also known as AdS/CFT correspondence, is one of the most notable developments in theoretical physics in recent decades. It establishes a relationship between strongly-coupled quantum gauge theories, and gravitational theories in higher-dimensional spacetimes. This duality has allowed for a deeper understanding of different regimes of theories, providing a bridge between two seemingly distinct areas of physics. In the third chapter, we review some essential aspects of gauge/gravity duality, using it as a tool for the study of our models.

The main focus of this work is the calculation of thermodynamic and information observables by using the holographic gauge/gravity duality in two specific toy-models: 1 R-charge Black Hole (1RCBH) and 2 R-charge Black Hole (2RCBH). In the fourth chapter, we will address the 1RCBH model, which consists of a rigorous top-down holographic construction. It is defined at finite temperature and density, having a critical point in its phase diagram.

In the fifth chapter, we will explore the 2RCBH model, which, like the previous one, is a rigorous top-down holographic construction. However, this model does not have a critical point in its phase diagram. We will compare the calculations of the thermodynamics of this model with those of the 1RCBH model, highlighting the differences and similarities between them.

This work aims to review the literature, explicitly verifying the thermodynamics of the 1RCBH and 2RCBH models, which are already known. We also present new perspectives for the numerical calculation of entanglement entropy in both models, which will be submitted for publication as a research article in the near future.

We define here our notation and conventions used throughout this dissertation, unless otherwise specified. We adopt the natural unit system, i.e., $c = k_B = \hbar = 1$. The metric signature is mostly plus, i.e., $(- + + \cdots)$.

Chapter 2

Basic Aspects of Information Theory

Every physical system has the capacity to record bits of information[1], where this recording can be the configuration of balls on a pool table, the passage of electric current, light in a switch, an atom, an electron, and even a photon. The information that the physical system carries can be classified as classical, quantum, or a hybrid combination, depending on the system's characteristics [1], [2]. We can confidently assert that both the position of a ball on a pool table and a road map record only classical information. Electrons, atoms, or even superconducting systems are capable of recording information, which can be quantum due to the application of quantum theory to each of these systems or classical, as it is always possible for a quantum system to make such a recording [1], [3]. It is worth noting that this entire section is strongly based on [1]–[4], though not exclusively on these sources. In particular, all the proofs of the claims discussed here can be found in Ref. [1].

In the sequence we discuss some features of classical information theory, also known as Shannon theory, before discussing its quantum aspects. We have no intention to be complete here, but just providing some tools that will be important for us in the next chapters.

2.1 Shannon's Theory

Let us consider a random variable X. Each realization[2] x of the random variable X belongs to a set $\mathcal{X}$ that we will call the alphabet. Each occurrence

[1] In the context of information theory, the term "information" acquires a meaning that differs somewhat from our day-to-day experience. It is important to remember that the concept of a physical bit refers to the physical representation of a bit, while the information bit is a measure of the amount we learn from the outcome of a random experiment [1]. Eventually, the term *surprise* can more precisely convey the idea of information as applied in the context of information theory.

[2] In our context, it refers to the manifestation of a specific process or event that transmits/possesses data, knowledge or meaning.

is said to be independent and identically distributed (i.i.d.). Let $p_X(x)$ be the probability density function of X, where $p_X(x)$ indicates the probability of occurrence of the realization x. We then define the information content $i(x)$ of a realization (or occurrence) x as a measure of the surprise one has when learning the result of a random experiment, expressed by [1], [2]

$$i(x) \equiv -\log\left[p_X(x)\right]. \tag{2.1}$$

The logarithm used throughout the text is taken to base two, and this selection implies that we are measuring surprise, or information, in units of bits.

The measure of surprise (2.1) behaves as expected: it is bigger for events with lower probability and thus surprises us more, and it is smaller for events with higher probability whose occurrence does not surprise us as much [1], [2]. By carefully analyzing the previously stated sentence, we can also see that the information content is non-negative for any realization x. Equation (2.1) also shows that the information content has the property of additivity, due to the choice of the logarithmic function. Consider two independent random events (i.e., events that are uncorrelated), with two symbols, x_1 and x_2, which are associated, respectively, with the random variables X_1 and X_2. Then, the events occur according to the joint probability $p_{X_1X_2}(x_1, x_2)$, such that [1]

$$\begin{aligned} i(x_1, x_2) &= -\log\left[p_{X_1X_2}(x_1, x_2)\right] \\ &= -\log\left[p_{X_1}(x_1)\, p_{X_2}(x_2)\right] \\ &= -\log\left[p_{X_1}(x_1)\right] - \log\left[p_{X_2}(x_2)\right] \\ &= i(x_1) + i(x_2), \end{aligned} \tag{2.2}$$

where the independence was used in the second equality.

The information content is a useful measure of surprise for specific occurrences of the random variable X, but it does not encompass a general notion of the amount of surprise that a given random variable X has [1], [2]. The Shannon entropy $S_{sh}(X)$ captures this general idea of the surprise of a random variable X —which is the expected information content of the random variable X [1], [2]— defined as

$$S_{sh}(X) \equiv \mathbb{E}_X\left[i(X)\right], \tag{2.3}$$

where $\mathbb{E}_X$ is the expected value, also known as expectation. Thus, the entropy of a discrete random variable X with probability distribution $p_X(x)$ is given by

$$S_{sh}(X) \equiv -\sum_x p_X(x) \log\left[p_X(x)\right], \tag{2.4}$$

which is the general definition of Shannon entropy for a probability distribution of a random variable X. Since the probability density function describes the likelihood of a random variable X falling within a certain range or assuming a specific value x, this definition is valid and consistent.

Throughout the text, we will adopt the convention that $0 \cdot \log(0) = 0$ for occurrences with zero probability. The fact that $\lim_{\varepsilon \to 0} \varepsilon \cdot \log(1/\varepsilon) = 0$ intuitively justifies this last convention, or it can be interpreted as a statement that the zero probability of an event is much more important or relevant than being infinitely surprised if such an event were to occur [1], [2].

2.1.1 Conditional Entropy

Now, let us introduce another important quantity in Information Theory. To do so, let us consider a schematic communication scenario where we have a sender and a receiver, whom we will call Alice and Bob[3], respectively.

Alice wants to communicate with Bob and sends him a message that consists of many symbols, each being an instance of a random variable X whose possible values are $x_1, \cdots, x_n$. She transmits the message through a noisy channel, so what Bob receives are several copies of a random variable Y, drawn from an alphabet with symbols $y_1, \cdots, y_k$, as Bob may confuse some of the symbols he received from Alice due to the noise in the channel as well as misunderstand others [1], [3], [4]. The question that needs to be answered is how many bits of information will Bob gain after Alice has transmitted a message with N symbols.

To answer this question, let's assume that $P_{X,Y}(x, y)$ is the probability that, on a given occurrence, Alice sends a message $X = x$ and Bob receives it as $Y = y$. Then, the probability that Bob receives $Y = y$, summing over all the choices of what Alice intended to send, is given by

$$P_Y(y) = \sum_x P_{X,Y}(x, y). \tag{2.5}$$

[3] Alice and Bob are names given to fictional characters that are used to help understand a given concept. Their invention is credited to R.L. Rivest, A. Shamir, and L. Adleman presented in [5].

If Bob can receive $Y = y$, he will then be able to measure the probability that Alice sent x, given by the conditional probability [1], [2]

$$P_{X|Y}\left(x \mid y\right) = \frac{P_{X,Y}\left(x, y\right)}{P_{Y}\left(y\right)}.$$

Once Bob has received $Y = y$, the result of his estimate of the remaining uncertainty in Alice's signal, which is the Shannon entropy of the conditional probability distribution, is given by

$$S(X \mid Y = y) = -\sum_{x} P_{X|Y}\left(x \mid y\right) \log\left(P_{X|Y}\left(x \mid y\right)\right). \tag{2.6}$$

Averaging over all possible values of Y, once Bob has received Y, will result in the average remaining entropy, given by

$$\begin{aligned}\sum_{y} P_{Y}\left(y\right) S(X \mid Y = y) &= -\sum_{y} P_{Y}\left(y\right) \sum_{x} \frac{P_{X,Y}\left(x, y\right)}{P_{Y}\left(y\right)} \log\left(\frac{P_{X,Y}\left(x, y\right)}{P_{Y}\left(y\right)}\right) \qquad (2.7)\\ &= -\sum_{x,y} P_{X,Y}\left(x, y\right) \log\left(P_{X,Y}\left(x, y\right)\right)\\ &\quad + \sum_{x,y} P_{X,Y}\left(x, y\right) \log\left(P_{Y}\left(y\right)\right) \qquad (2.8)\end{aligned}$$

which results in the conditional entropy [1], [2]

$$S(X \mid Y) = S(X, Y) - S_{sh}(Y), \tag{2.9}$$

which is the entropy that remains in the probability distribution X once Y is known [1], [2], [4], and also

$$S(X, Y) \equiv -\sum_{x,y} P_{X,Y}\left(x, y\right) \log\left(P_{X,Y}\left(x, y\right)\right) \tag{2.10}$$

is the joint entropy while $S_{sh}(Y)$ is the Shannon entropy of the probability distribution $P_{Y}\left(y\right) = \sum_{x} P_{X,Y}\left(x, y\right)$ for Y.

As the quantities from which (2.9) were obtained are sums of entropies, which in turn have positive coefficients, we have that the conditional entropy is always positive [1], [2], so that

$$S(X, Y) - S_{Sh}(Y) \geq 0. \tag{2.11}$$

2.1.2 Relative Entropy

Given the random variables X and Y, associated with the symbols x and y, which are given according to the probability distributions $p_X(x)$ and $p_Y(y)$, respectively, we define the relative entropy as [1], [2]

$$S(X\|Y) \equiv -\sum_{x,y} p_X(x) \log\left[p_Y(y)\right] - S_{sh}(X). \tag{2.12}$$

Using (2.4), we can rewrite (2.12) as [2]

$$S(X\|Y) = \sum_{x,y} p_X(x) \log\left(\frac{p_X(x)}{p_Y(y)}\right). \tag{2.13}$$

Relative entropy is not symmetric in the exchange of $p_X(x)$ and $p_Y(y)$. Therefore, relative entropy is not a distance measure in the strict mathematical sense because it is not symmetric and does not satisfy the triangle inequality. Relative entropy measures how much the probability distribution $p_Y(y)$ differs from a second distribution $p_X(x)$. Note that if the set of all values of the probability distribution over X is not contained in the set of all values of the probability distribution over Y, this quantity gives an infinite value. For this reason, it is also called divergence [1], [2], [4].

For example, if we have a model that estimates the probability distribution of some data, but for some reason this model is not very good and the true distribution is slightly different, we can then use relative entropy to measure the difference between this estimated distribution and the true one [3].

Additionally, there is an interesting property satisfied by relative entropy, which is the fact that $S(X\|Y)$ is non-negative and it is zero if and only if $Y = X$ [1], [2]. As the difference between these two probability distributions increases, the relative entropy will become larger, always assuming positive values.

Finally, given a uniform probability distribution $p_Y(y) = 1/|\mathcal{X}|$ ($|\mathcal{X}|$ is the cardinality of the alphabet) and $p_X(x)$ a probability distribution for X. Then

$$\begin{aligned} S(X\|Y) &= \sum_{x,y} p_X(x) \log\left(\frac{p_X(x)}{p_Y(y)}\right) \\ &= \sum_{x} p(x) \log\left(p(x) \cdot |\mathcal{X}|\right) \\ &= \sum_{x} p(x) \log p(x) + \sum_{x} p(x) \log|\mathcal{X}|. \end{aligned} \tag{2.14}$$

and since $\log|\mathcal{X}|$ is a constant, and $\sum_x p(x) = 1$, we have

$$S(X\|Y) = \sum_x p(x)\log p(x) + \log|\mathcal{X}|. \tag{2.15}$$

Since the Shannon entropy $S_{sh}(X)$ is given by (2.4), we can then express

$$\sum_x p(x)\log p(x) = -S_{sh}(X), \tag{2.16}$$

which substituting into (2.15), we have

$$S(X\|Y) = \log|\mathcal{X}| - S_{sh}(X). \tag{2.17}$$

Since $0 \leq S(X\|Y)$, we have that

$$0 \leq \log|\mathcal{X}| - S_{sh}(X), \tag{2.18}$$

and then

$$S_{sh}(X) \leq \log|\mathcal{X}|, \tag{2.19}$$

which is the maximum value that entropy can reach [1], [2].

2.1.3 Mutual Information

Now let's address a measure of information entropy that is *common* or *mutual* to the two parts that contain it. We define the mutual information between two random variables X and Y as [1], [2]

$$I(X;Y) \equiv S_{sh}(X) - S(X \mid Y). \tag{2.20}$$

Mutual information measures how much dependence or correlation there is between two random variables, in our case X and Y. It can be said that it measures how much knowledge we have of one random variable that will imply a reduction in uncertainty about the other random variable. In this sense, it is the common information between the two random variables. If Y is known and X is not, there is an uncertainty $S(X \mid Y)$ about the variable X. Therefore, knowing Y will provide a gain of information of $S(X \mid Y)$ bits about X and consequently will reduce the total uncertainty $S_{sh}(X)$ about X. If we think that X has a great dependence on Y, knowing Y will significantly change the

knowledge we have about X. These arguments suggest that mutual information is also defined as a measure of dependence between its random variables.

Two random variables X and Y have zero bits of mutual information if they are statistically independent (it is worth remembering that the joint density factors as $p_{X,Y}(x,y) = p_X(x)p_Y(y)$ when X and Y are independent). That is, the knowledge of Y does not provide any information about X when the random variables are statistically independent. In fact, knowing Y does not provide any information about X when both are disjoint.

We can also show that [1], [2]

$$\begin{aligned} I(X;Y) &= S_{sh}(X) + S_{sh}(Y) - S(X,Y) \\ &= S_{sh}(Y) - [S(X,Y) - S_{sh}(X)] \\ &= S_{sh}(Y) - S(Y \mid X) \qquad (2.21) \\ &= I(Y;X), \qquad (2.22) \end{aligned}$$

showing that mutual information is symmetric. From (2.21) , we have that the mutual information is non-negative, so that, for any two random variables, X and Y,

$$I(X;Y) \geq 0, \qquad (2.23)$$

with equality if, and only if, X and Y are independent [1], [2]. We can still rewrite the mutual information $I(X;Y)$ as

$$\begin{aligned} I(X;Y) &= \sum_{x,y} p_{XY}(x,y) \log \frac{p_{XY}(x,y)}{p_X(x)p_Y(y)} \\ &= \sum_{x,y} p_{XY}(x,y) \log \frac{p_{XY}(x \mid y)}{p_X(x)} \\ &= -\sum_{x,y} p_{XY}(x,y) \log p_X(x) + \sum_{x,y} p_{XY}(x,y) \log p_{XY}(x \mid y) \\ &= -\sum_{x} p_X(x) \log p_X(x) - \left(-\sum_{x,y} p_{XY}(x,y) \log p_{XY}(x \mid y) \right) \\ &= S_{Sh}(X) - S_{Sh}(X \mid Y). \qquad (2.24) \end{aligned}$$

So far, we have presented some basic concepts of information measures from Shannon's information theory. In the next section, we will continue to explore the topic of information, now in the quantum context.

2.2 Quantum Information

There are several measures of information that are important for measuring the amount of information and the correlations present in quantum systems. The fundamental measure we will discuss is the von Neumann entropy (also known as quantum entropy). It is a generalization of Shannon entropy applied to the quantum world and brings with it not only classical uncertainty but also encompasses the quantum uncertainty in a quantum state. When we talk about classical entropy, our smallest unit of information is the bit [2]. This measure of entropy when associated with the quantum world is called a qubit [4]. It is worth remembering that a physical qubit is different from an information qubit. The physical qubit describes the quantum state of a system, like a photon or an electron. The information qubit is the most fundamental unit of measure of quantum information present in a quantum system. It is also worth noting that this entire section is strongly based on [1], [3], [6], [7], but not solely on them. In particular, all the proofs can be found in [1], [6], [7].

2.2.1 Density Matrices

The most general representation of a quantum system is written in terms of an operator ρ called the density operator, or density matrix. It is constructed in such a way that it naturally encompasses quantum and classical probabilities [1]. So, even if we do not have classical uncertainties, we will eventually find the need to deal with density matrices. For this reason, it is said that the density matrix is one of the most important concepts in quantum theory [1], [8].

As motivation, let's imagine that we have a machine that prepares quantum systems in certain states. For example, this could be an oven producing spin 1/2 particles, or a quantum optics setup producing photons. Suppose this device is imperfect, so it does not always produce the same state. That is, suppose it produces a state $|\psi_1\rangle$ with a certain probability p_1 or a state $|\psi_2\rangle$ with a certain probability p_2 and so on. Note that here we are introducing a classical uncertainty [8]. The $|\psi_i\rangle$ are quantum states, but we do not know which states we will get from the machine. We can have as many p's as we want. All we need to assume is that they satisfy the expected properties of a probability [3], [8]:

$$p_i \in [0,1], \quad \text{e} \quad \sum_i p_i = 1. \tag{2.25}$$

Now let A be an observable. If the state is $|\psi_1\rangle$, then the expected value of A will be $\langle\psi_1|A|\psi_1\rangle$. However, if it is $|\psi_2\rangle$ then it will be $\langle\psi_2|A|\psi_2\rangle$. To calculate the actual expected value of A we must then average the quantum averages, given by

$$\langle A\rangle = \sum_i p_i \langle\psi_i|A|\psi_i\rangle\,, \tag{2.26}$$

where we weigh the possible expected values $\langle\psi_i|A|\psi_i\rangle$ by the relative probabilities p_i that each one occurs [8].

This type of average cannot be written as $\langle\phi|A|\phi\rangle$ for some ket $|\phi\rangle$. If we want to assign a "state" to our system, then we must generalize the idea of ket. To do this, let's introduce the idea of trace.

The trace of an operator is defined as the sum of its diagonal entries

$$\mathrm{Tr}(A) = \sum_i \langle i|A|i\rangle. \tag{2.27}$$

It turns out that the trace is the same, no matter which basis is used. You can see this using completeness, for example: if $|a\rangle$ is some other basis, then

$$\sum_i \langle i|A|i\rangle = \sum_i \sum_a \langle i \mid a\rangle\langle a|A|i\rangle = \sum_i \sum_a \langle a|A|i\rangle\langle i \mid a\rangle = \sum_a \langle a|A|a\rangle. \tag{2.28}$$

Therefore, we conclude that

$$\mathrm{Tr}(A) = \sum_i \langle i|A|i\rangle = \sum_a \langle a|A|a\rangle. \tag{2.29}$$

The trace is a property of the operator, not of the basis we use [8]. Since it doesn't matter which basis is used, let's choose the basis $|\lambda_i\rangle$ that diagonalizes the operator A. Then $\langle\lambda_i|A|\lambda_i\rangle = \lambda_i$ will be an eigenvalue of A.

Thus, we also see that

$$\mathrm{Tr}(A) = \sum_i \lambda_i = \text{ sum of all eigenvalues of } A. \tag{2.30}$$

A useful property of the trace is that it is cyclic

$$\mathrm{Tr}(AB) = \mathrm{Tr}(BA). \tag{2.31}$$

Using the cyclic property above, it is also possible to move an arbitrary number of operators, but only in cyclic permutations [8]. We have as an example

$$\mathrm{Tr}(ABC) = \mathrm{Tr}(CAB) = \mathrm{Tr}(BCA). \tag{2.32}$$

where we are moving them in a specific order: $\mathrm{Tr}(ABC) \neq \mathrm{Tr}(BAC)$. Another example we have is a trace of the form $\mathrm{Tr}\left(UAU^{\dagger}\right)$, where U is a unitary operator. In this case, it follows from the cyclic property that

$$\mathrm{Tr}\left(UAU^{\dagger}\right) = \mathrm{Tr}\left(AU^{\dagger}U\right) = \mathrm{Tr}(A). \tag{2.33}$$

Therefore, the trace of an operator is invariant under unitary transformations and also agrees with the fact that the trace is the sum of the eigenvalues and the unitaries preserve the eigenvalues [8].

Finally, using $|\psi\rangle$ and $|\phi\rangle$ arbitrary kets, we can calculate the trace of the outer product $|\psi\rangle\langle\phi|$, as

$$\mathrm{Tr}(|\psi\rangle\langle\phi|) = \sum_i \langle i \mid \psi\rangle\langle\phi \mid i\rangle = \sum_i \langle\phi \mid i\rangle\langle i \mid \psi\rangle. \tag{2.34}$$

The sum over $|i\rangle$ becomes 1 due to completeness and then we have that

$$\mathrm{Tr}(|\psi\rangle\langle\phi|) = \langle\phi \mid \psi\rangle. \tag{2.35}$$

Returning to the discussion about density matrices, using (2.35) to write

$$\langle\psi_i|A|\psi_i\rangle = \mathrm{Tr}\left[A\,|\psi_i\rangle\,\langle\psi_i|\right]. \tag{2.36}$$

Then (2.26) can be written as

$$\langle A\rangle = \sum_i p_i \,\mathrm{Tr}\left[A\,|\psi_i\rangle\,\langle\psi_i|\right] = \mathrm{Tr}\left\{A\sum_i p_i\,|\psi_i\rangle\,\langle\psi_i|\right\}. \tag{2.37}$$

We then define the density matrix as [8]

$$\rho = \sum_i p_i\,|\psi_i\rangle\,\langle\psi_i|\,. \tag{2.38}$$

Then we can finally write (2.26) as

$$\langle A\rangle = \mathrm{Tr}(A\rho), \tag{2.39}$$

which is the same as $\mathrm{Tr}(\rho A)$ since the trace is cyclic.

With this idea, we can now reformulate all of quantum mechanics in terms of density matrices, instead of kets [8]. If it happens that a density matrix can be written as $\rho = |\psi\rangle\langle\psi|$, we say that we have a pure state [8]. And in this case it is not necessary to use ρ and we can simply continue to use $|\psi\rangle$. For example, (2.39) reduces to $\mathrm{Tr}(A\rho) = \langle\psi|A|\psi\rangle$. A state that is not pure is usually called a mixed state. In this case, we must use ρ.

The density matrix satisfies several properties [3], [8]. We will comment on two main ones. First, the density matrix is a Hermitian operator

$$\rho^\dagger = \rho. \tag{2.40}$$

Second,

$$\mathrm{Tr}(\rho) = \sum_i p_i \,\mathrm{Tr}\left(|\psi_i\rangle\,\langle\psi_i|\right) = \sum_i p_i \,\langle\psi_i \mid \psi_i\rangle = \sum_i p_i = 1. \tag{2.41}$$

This is the normalization condition of the density matrix. Another way to see this starting from (2.39) choosing $A = 1$. Then, as $\langle 1\rangle = 1$ we obtain again $\mathrm{Tr}(\rho) = 1$.

2.2.2 Entanglement Entropy

There are several measures of entanglement. Even measuring entanglement is not trivial, as the understanding of what entanglement is has changed over the years [9]. In 1935, Schrödinger named the effects of the so-called non-classical manifestations of quantum formalism as *"Verschränkung"*, which we know today as entanglement [10]. Several renowned scientists of the past century have written their opinions on entanglement, among whom we list [11]:

- *Asher Peres*: a trick that quantum magicians use to produce phenomena that classical magicians cannot imitate [12];
- *Artur Ekert*: a tool for secure communication [13];
- *Charles Bennett*: a resource that enables quantum teleportation [14];
- *David Mermin*: a correlation that contradicts the theory of elements of reality [15];

- *Einstein/Podolsky/Rosen* (EPR): an entangled wave function does not describe physical reality completely [16];
- *Erwin Schrödinger*: for an entangled state, ″the best possible knowledge of the whole does not include the best possible knowledge of its parts‶ [10];
- *Horodecki's*: the necessity for the first applications of positive maps in physics [17];
- *John Bell*: a correlation stronger than any classical correlation [18];
- *Peter Shor*: a global structure of the wave function that allows faster algorithms [19].

Over the years, we have seen that the view on entanglement has been changing and we still do not have a single, definitive definition of what entanglement is.

Entanglement is essential for quantum theory, especially information, cryptography, and computing, with the latter having its heart in entanglement [9], [20], [21]. However, entanglement alone does not solve our problems; it is necessary to quantify entanglement in order to develop theory and calculations. The main issue is precisely this: we do not fully understand what entanglement is, but we know its mathematical definition and how it manifests, for example, via Bell's inequality [9].

In the case of pure states, which is the interest of this dissertation, it is possible to distinguish between entangled and non-entangled states. A pure state is said to be entangled if its state vector $|\psi\rangle$ cannot be written as $|\psi\rangle = |\psi_A\rangle \otimes |\psi_B\rangle$; otherwise, it is a product state [6].

To quantitatively measure entanglement, one considers the entanglement entropy, which for a pure state is uniquely given by the von Neumann entropy [6]. The von Neumann entropy of a density matrix ρ_A is defined similarly to the Shannon entropy of a probability distribution, given by

$$S(\rho_A) = -\operatorname{Tr} \rho_A \log \rho_A. \tag{2.42}$$

Using an analogy, let's suppose that Alice has an alphabet $A = \{a_1, a_2, \ldots, a_N\}$, where the letters ρ_i are the density matrix operators describing quantum states, each of which can occur with probability p_i [22]. Suppose Alice sends a "letter" (quantum state) to Bob, and Bob only knows that the letters were taken from the set $\{\rho_i, p_i\}$, where $\rho_i = |i\rangle\langle i|$. The quantum state he describes is,

therefore [22]

$$\rho = \sum_i p_i \rho_i = \sum_i p_i |i\rangle\langle i| = \begin{pmatrix} p_1 & 0 & \dots & 0 \\ 0 & p_2 & \cdots & 0 \\ \vdots & \vdots & \ddots & \vdots \\ 0 & 0 & \cdots & p_N \end{pmatrix}, \tag{2.43}$$

and the von Neumann entropy is

$$S(\rho) = -\operatorname{Tr}\rho\log\rho = -\operatorname{Tr}\left\{\sum_i p_i|i\rangle\left\langle i\left|\log\sum_j p_i\right|j\right\rangle\langle j|\right\}. \tag{2.44}$$

Since $\rho|j\rangle = p_j|j\rangle, F(\rho)|j\rangle = F(p_j)|j\rangle$, we can see from the above expression, with $F(\rho) = \log\rho$

$$S(\rho) = -\sum_i p_i\langle i|\log\rho|i\rangle = -\sum_i p_i \log p_i. \tag{2.45}$$

We then see the similarity between von Neumann entropy and Shannon entropy [22].

We have analogously, as is the case for Shannon entropy,

$$S(\rho_A) \geq 0, \tag{2.46}$$

and being equal only for a pure state, which in other words, one of the p being 1 and the others 0. Equation (2.42) also implies the same upper bound that we have classically for a system with d states, given by [1], [7]

$$S(\rho_A) \leq \log d, \tag{2.47}$$

being equal only if the populations are equally distributed, so that

$$\rho_A = \frac{1}{d}\begin{pmatrix} 1 & & & \\ & 1 & & \\ & & 1 & \\ & & & \ddots \end{pmatrix}. \tag{2.48}$$

In this case, we have that A is in a maximally mixed state (2.42). As presented, von Neumann entropy has many properties analogous to Shannon entropy; however, it has more subtle details and fundamental differences, which are presented in [1], [7].

An interesting property of von Neumann entropy that has no classical analog is: given a bipartite system AB that is in a pure state, then

$$|\psi_{AB}\rangle = \sum_i \sqrt{p_i} \left|\psi_A^i\right\rangle \otimes \left|\psi_B^i\right\rangle \in \mathcal{H}_A \otimes \mathcal{H}_B, \tag{2.49}$$

we then have that the density matrices of systems A and B are given by

$$\rho_A = \sum_i p_i \left|\psi_A^i\right\rangle \left\langle\psi_A^i\right|, \tag{2.50}$$

and similarly

$$\rho_B = \sum_i p_i \left|\psi_B^i\right\rangle \left\langle\psi_B^i\right|. \tag{2.51}$$

And since the same constants p_i appear in each, we have that

$$S(\rho_A) = S(\rho_B). \tag{2.52}$$

Note that, in this situation, as the system AB is in a pure state, its entropy S_{AB} is zero [1].

In this chapter, we provided a brief introduction to the fundamental concepts of information theory, exploring the notions of entropy, mutual information, and entanglement, both in the classical context and in quantum mechanics. We discussed entropy as a measure of uncertainty in a system, while mutual information quantifies the degree of correlation between two variables. In the quantum realm, we addressed entanglement, a unique characteristic that describes non-classical correlations between systems. After presenting these fundamental ideas, we will return to these concepts in a more advanced context within the holographic principle, where we will show how these principles apply and transform into holographic theory.

Chapter 3

Basic Aspects of the Gauge/Gravity Duality

Throughout physics, there are limitations, whether from an experimental or theoretical standpoint. When we reach these limits, it is very natural to resort to effective models and/or other alternative theoretical approaches to gain some qualitative insight and even some quantitative predictions for the behavior of the observable or theory in question. One of these alternative approaches, which is the theoretical tool considered in this dissertation, is called *gauge-gravity holographic duality*, also often referred to as AdS-CFT correspondence, holographic correspondence, or Maldacena duality [23]–[26]. It is worth emphasizing that in the first subsection, we will briefly approach the gauge/gravity duality closely following the discussions presented in [27].

3.1 Overview of the Duality

The gauge-gravity holographic duality is motivated by the structure of string theory, which in its original formulation had a relation with the strong interaction. Fundamentally, string theory (note that we are not referring to superstring theory) was originally developed as an S-matrix theory for the strong nuclear interaction between hadrons, which were empirically known to fall on linear Regge trajectories that related their total angular momentum J to their squared mass m^2, known as Chew-Frautschi plots [28]. By modeling a meson as a relativistic open string rotating around its center, it is possible to reproduce the observed Chew-Frautschi relation, $J = \alpha_0 + \alpha' m^2$, where the relativistic string tension is given in terms of the measured slope of the linear Regge trajectory, $\sigma = (2\pi\alpha')^{-1} \approx (440\text{MeV})^2$ [29]. Its slope is practically the same for the different Regge trajectories defined by the different measured values of the

Regge intercept, α_0, which will depend on the flavor quantum numbers of the considered hadrons. Hadrons with the same flavor quantum numbers fall on the same Regge trajectory and can be seen as resonances of this trajectory with different values of mass and angular momentum. However, as this simple string model also predicts results that contradict hadron experiments, such as an incorrect (albeit smooth) exponential fall-off for the associated Veneziano scattering amplitude in the high-energy limit of hard hadron scattering at fixed angles, it was abandoned as a model for hadrons, being replaced by the advent of QCD, with its theoretical and experimental successes as the fundamental description of the strong interaction [27].

Subsequently, theoretical interest in string theory reappeared more significantly, but this time in a very different context. This revival is associated with the so-called first and second superstring revolutions, which correspond, respectively [27]:

1. to the discovery of five different consistent supersymmetric quantum string theories in 10 spacetime dimensions, namely: Type I, Type IIA, Type IIB, Heterotic $SO(32)$, and Heterotic $E_8 \otimes E_8$;

2. to the subsequent discovery that these five 10-dimensional superstring theories are related through a network of duality transformations, and are also related to a membrane theory defined in 11 spacetime dimensions called M-theory, whose low-energy limit corresponds to a unique 11-dimensional supergravity theory.

It is worth noting that all superstring theories share a very interesting common feature: a massless spin-2 particle in their spectrum, known as the graviton, which is the hypothetical vibrational mode of the string responsible for mediating the gravitational interaction at the quantum level. Due to this, and also because of the fundamental fact that at low energies, superstring theory reduces to supergravity, thus incorporating general relativity as the classical and low-energy description of gravity, superstring theory is considered a promising candidate for a quantum gravity theory [30]–[34].

In its original formulation, the so-called AdS-CFT correspondence [23]–[26] relates Type IIB superstring theory defined on the product of a 5-dimensional Anti-de Sitter (AdS) spacetime and a 5-dimensional sphere, $AdS_5 \times S^5$, to a conformal quantum field theory (CFT) corresponding to $\mathcal{N} = 4$ Supersymmetric Yang-Mills (SYM) theory with gauge group $SU(N_c)$, where N_c is the number

of color charges and is related to the local symmetry of the system, along with $\mathcal{N} = 4$ referring to the number of different supersymmetries in the theory, defined on the conformally flat 4-dimensional boundary of AdS_5 [27]. Two other early realizations of the AdS-CFT duality also involve the relation between M-theory defined on $AdS_4 \times S^7$ and the Aharony-Bergman-Jafferis-Maldacena (ABJM) superconformal field theory defined on the 3-dimensional boundary of AdS_4, as well as the relation between M-theory defined on $AdS_7 \times S^4$ and the so-called $6D$ (2,0) superconformal field theory defined on the 6-dimensional boundary of AdS_7 [27].

Now, let's present some aspects of the original proposal, in which the standard review [35] is also indicated, as well as the following works for more details [36]–[39]. Let's take as an example the relationship between the Type IIB superstring theory compactified on $AdS_5 \times S^5$ and the $\mathcal{N} = 4$ SYM theory that lives on the boundary of AdS_5. First, consider the Type IIB string theory in the flat Minkowski spacetime $\mathbb{R}^{1,9}$ and a collection of N_c coincident parallel D3-branes in this background[1] [42].

The excitations of the so-called perturbative string theory in this system correspond to vibrational modes of both: closed strings and also open strings with their endpoints attached to the D3-branes [27]. If we consider the system defined at low energies compared to the characteristic scale of the string, $(\alpha')^{-1/2} \equiv (l_s)^{-1}$, only massless string modes can be excited, which, for the closed strings, will generate a gravitational supermultiplet, and for the open strings with their endpoints attached to the $(3+1)$ dimensional volume of the coincident N_c D3-branes, will yield an $\mathcal{N} = 4$ vector supermultiplet with gauge group $SU(N_c)$. A low-energy effective action for these massless string excitations in the considered background can be schematically written by integrating

[1] An endpoint of an open string must satisfy either Dirichlet or Neumann boundary conditions. Considering Neumann boundary conditions on p spatial dimensions plus time, then the remaining $D - p - 1$ dimensions must satisfy Dirichlet boundary conditions. Since for Dirichlet boundary conditions a string endpoint is fixed in space, while for Neumann boundary conditions it must move at the speed of light, then with Neumann boundary conditions on $p + 1$ dimensions, the open string endpoints are constrained to move within a $(p + 1)$-dimensional hypersurface, which is a dynamical object called a Dp-brane [27]. Dp-branes are shown to be related to black p-branes [40], [41], which are solutions of higher-dimensional (super)gravity that generalize the concept of black holes by having extended event horizons that are translationally invariant through p spatial dimensions [27]. They actually provide different descriptions of a single object, in which a perturbative string regime is accurately described by Dp-branes not backreacting on the background spacetime, while at low energies, corresponding to taking $\alpha' \equiv l_s^2$ to be small, where l_s is the fundamental string length, so that massive string states can be neglected, and also large gravitational fields, the backreaction of the Dp-branes on the background produces a black p-brane geometry.

out the massive string modes [27],

$$S_{\text{eff}} = S_{\mathbb{R}^{1,9}\ \text{bulk}} + S_{\mathbb{R}^{1,3}\ \text{brane}} + S_{\text{int}}\ , \tag{3.1}$$

where $S_{\mathbb{R}^{1,9}\ \text{bulk}}$ is the low-energy action for the gravitational supermultiplet, corresponding to Type IIB supergravity (SUGRA) in $\mathbb{R}^{1,9}$ along with higher-order derivative corrections arising from integrating out the massive string modes; $S_{\mathbb{R}^{1,3}\ \text{brane}}$ is the low-energy action for the $\mathcal{N}=4$ vector supermultiplet residing in the $\mathbb{R}^{1,3}$ volume of the coincident N_c D3-branes, corresponding to the $\mathcal{N}=4$ SYM theory with gauge group $SU(N_c)$ plus higher-order derivative corrections arising from integrating out the massive string modes; and S_{int} is an interaction term between the bulk and brane modes [27].

Higher-order derivative corrections to the bulk and brane actions arising from integrating out the massive string modes are proportional to positive powers of α', while the interaction action is proportional to positive powers of the square root of Newton's gravitational constant in $10D$, $\kappa_{10} \equiv \sqrt{8\pi G_{10}} \sim g_s \alpha'^2$, where g_s is the string coupling, so that by considering the so-called decoupling limit in which $\alpha' \equiv l_s^2 \to 0$ with N_c and g_s fixed, we have that $S_{\mathbb{R}^{1,9}\ \text{bulk}} \to S_{\mathbb{R}^{1,9}\ \text{IIB SUGRA}}$, $S_{\mathbb{R}^{1,3}\ \text{brane}} \to S_{\mathbb{R}^{1,3}\mathcal{N}=4\text{SYM}}$, and $S_{\text{int}} \to 0$, so we are left with two decoupled actions [27]

$$\lim_{\alpha' \to 0 (\text{fixed } N_c, g_s)} S_{\text{eff}} = S_{\mathbb{R}^{1,9}\ \text{IIB SUGRA}} + S_{\mathbb{R}^{1,3}\mathcal{N}=4\text{SYM}}. \tag{3.2}$$

For a given number N_c of coincident D3-branes, the 't Hooft coupling, which effectively controls the strength of interactions in the $\mathcal{N}=4$ SYM $SU(N_c)$ gauge theory, is given by $\lambda_t \equiv N_c g_{\text{SYM}}^2 = N_c g_s$, where this latter relation can be inferred from the fact that a closed string, governed by the coupling g_s, can be formed by the collision between the endpoints of two open strings moving on the D3-branes, with g_{SYM} being the non-Abelian gauge field coupling corresponding to the massless mode of open strings on these branes [37]. This reasoning holds for any value of λ_t and as the SYM theory is a CFT, its 't Hooft coupling remains constant for any energy value, so in fact, there are infinitely many different SYM theories, each defined at some given value of λ_t [27].

We can consider another perspective for the same system as follows. The effective gravitational field generated by the collection of N_c coincident D3-branes is $\sim N_c g_s \left(l_s/r\right)^4$ [38], [39], and by considering a very large N_c such that

$\lambda_t = N_c g_s \gg 1$ even for small values of g_s, so that we can ignore the contributions of quantum string loops in the bulk, very close to the D3-branes for $r \to 0$, the gravitational field is very intense, and its backreaction on the background spacetime highly distorts its geometry, producing a curved manifold. In this limit, it is necessary to replace the perturbative string description of D3-branes in flat Minkowski spacetime with the associated supergravity solution of the black 3-brane, whose near-horizon geometry, i.e., near the black brane, precisely approximates that of $AdS_5(L) \times S^5(L)$, with the same curvature radius L for both the AdS_5 and S^5 manifolds. On the other hand, far from the black brane, the background geometry is still that of Minkowski $\mathbb{R}^{1,9}$ [27]. In both regions, near and far from the black brane, considering that the string coupling g_s is small, so that string loops can be discarded, by taking the decoupling limit as before, with $l_s \to 0$ and N_c, g_s fixed, the bulk spacetime is inhabited only by Type IIB supergravity fields [27].

By comparing the two perspectives above for the same system, when defined in the same regime corresponding to low energies, low string coupling value, large N_c, and with strong 't Hooft coupling ($\alpha' \equiv l_s^2 \to 0$ with N_c,g_s fixed, but such that g_s is small, N_c is large and $\lambda_t = N_c g_{\text{SYM}}^2 = N_c g_s \gg 1$), we notice that in both views there is a common element, which is Type IIB supergravity defined in $\mathbb{R}^{1,9}$, and it is then conjectured that the remaining pieces in each perspective must be dual to each other: the strongly coupled, large N_c, $\mathcal{N} = 4$ SYM theory with gauge group SU (N_c), defined in $\mathbb{R}^{1,3}$, which is equivalent, up to a conformal factor, to the boundary of AdS_5, and the classical, weakly coupled Type IIB supergravity defined in $AdS_5(L) \times S^5(L)$ [27]. The duality involved in this comparison comprises, in fact, a detailed mathematical dictionary that translates the evaluation of physical observables in a classical supergravity theory, defined at weak coupling over a background given by the product of an AdS spacetime and a compact manifold, into the calculation of other observables in a different conformal quantum gauge field theory defined at strong coupling and with a large number of colors on the conformally flat boundary of the AdS manifold. Thus, the notion of the hologram understood in the AdS-CFT duality refers to the fact that the gravitational information of a higher-dimensional bulk spacetime can be encoded in its boundary [27].

This is the weakest form of the AdS-CFT holographic correspondence and a particular case of the broader gauge-gravity duality, being widely supported by

a large amount of consistency checks [35]–[38]. The stronger version of the AdS-CFT conjecture corresponds to a particular case of the so-called gauge-string duality, which is more general than the gauge-gravity duality and proposes that the duality should be valid for all values of g_s and N_c, thus relating the $\mathcal{N}=4$ SYM theory in $\mathbb{R}^{1,3}$ with arbitrary 't Hooft coupling and an arbitrary number of colors for the gauge group $SU(N_c)$, and the full quantum Type IIB string theory, generally formulated non-perturbatively in $AdS_5(L) \times S^5(L)$, instead of just its low-energy limit corresponding to Type IIB supergravity. It is also postulated that higher derivative/curvature corrections in the bulk correspond to the inverse of 't Hooft coupling corrections in the dual CFT, as according to the detailed holographic dictionary, $\alpha'/L^2 = \left\{ l_s / \left[l_s \left(N_c g_s \right)^{1/4} \right] \right\}^2 = 1/\sqrt{\lambda_t}$, and that quantum string loop corrections in the bulk correspond to the inverse of N_c corrections in the dual CFT, as $g_s \left(l_s/L \right)^4 = g_s \left(l_s / \left[l_s \left(N_c g_s \right)^{1/4} \right] \right)^4 = 1/N_c$ [27].

The AdS-CFT holographic duality has a striking feature, which is the fact that complicated non-perturbative calculations in a strongly coupled quantum CFT can be translated, through the detailed mathematical holographic dictionary, into much simpler calculations (although at no point do we claim that these calculations are necessarily easy) involving weakly coupled classical gravity in higher dimensions [27].

More generally, the holographic gauge-gravity duality is not restricted to AdS spacetimes in the bulk and dual CFTs on the boundary. For example, by considering the backreaction of effective $5D$ massive fields living in AdS_5, which are associated with the Kaluza-Klein (KK) reduction on S^5 of the originally massless $10D$ modes of SUGRA, the AdS_5 background metric is generally deformed within the bulk, and the effective $5D$ bulk spacetime geometry becomes only asymptotically AdS, with the AdS_5 metric being asymptotically recovered near the bulk spacetime boundary [27]. Usually, there is also a corresponding deformation of the dual QFT theory on the asymptotically AdS bulk spacetime boundary induced by considering relevant or marginal operators, which can break conformal symmetry and supersymmetry, and whose scale dimension is associated through the holographic dictionary to the masses of the effective $5D$ bulk fields [27]. In this sense, we have a broader holographic gauge-gravity duality relating a strongly coupled QFT that is not necessarily conformal or supersymmetric, living on the boundary of an asymptotically AdS higher-dimensional spacetime, whose geometry is dynamically determined by a classical gravity theory interacting with different matter fields in the bulk [27].

In the holographic gauge-gravity duality, the extra dimension connecting the asymptotically AdS bulk spacetime to its boundary plays the role of a geometrization of the energy scale of the renormalization group flow in the QFT living on the boundary [43], with low/high energy processes in the QFT being mapped to the deep interior/near-boundary regions of the bulk spacetime, respectively [27].

The main motivation for employing holography is to calculate observables that are unfeasible to obtain through perturbation theory in strongly coupled quantum field theories (QFTs). Holographic calculations involve general relativity and, although they can be complicated in some cases, at least they are, in principle, possible to be carried out. In contrast, perturbation theory under strong coupling conditions in QFTs is simply an inapplicable approach.

A certain class of holographic models is determined by a specific class of gravity-matter actions, usually in asymptotically AdS spacetimes, which require the use of a negative cosmological constant in the gravitational action, in D spacetime dimensions. Although we usually work with bulk spacetimes with five dimensions or less, at least one more dimension is always used than the flat spacetime of the target theory or target phenomenology that we want to model holographically. It is worth noting that, in the case of strongly interacting systems in condensed matter, effective descriptions of the system in low dimensions are often considered, therefore, in such cases the dual gravitational holographic model will have less than five dimensions.

A holographic model is defined by a specific gravity-matter action within a particular class of holographic models. For example, the class of EMD (Einstein-Maxwell-Dilaton) actions has infinitely many different specific actions, just as the class of sinusoidal functions $\sin(\alpha x)$ contains infinitely many distinct sine functions, each determined by a value of the parameter α. Each action within a class is specified by a set of functions and parameters that can be free, as in bottom-up phenomenological models, or can be fixed by formal low-energy constructions originating from string theory, as in top-down models. The latter is exactly the case of the two models we will discuss throughout the text. By specifying the form of these functions and the values of these parameters, a model within a class of actions is determined. Each specific holographic model describes a different physical system, whether it exists in our universe or not. Therefore, in addition to holographic models of direct relevance to different

phenomenologies [2], we can also consider some top-down holographic toy models. The latter, although of no direct phenomenological relevance, may be used to investigate possible general properties of strongly coupled quantum systems in simpler setups where the holographic dictionary has been more rigorously justified. Such calculations in toy models are also typically a first step towards more complicated calculations in realistic models.

In other words, once a holographic gravitational model is specified, delimiting the target QFT on the boundary of the higher-dimensional bulk spacetime to be emulated holographically by the specified classical gravity-matter model, we have a physical system holographically dual to this QFT on the boundary, with this boundary QFT being necessarily strongly coupled. The boundary QFT observables can be evaluated through calculations involving classical gravity, by using the holographic dictionary presented in Fig. 3.1.

Each holographic model and/or dual physical system can be specified under different dynamic conditions. The specification of these different dynamic conditions do not involve any modification of the model's action but are implemented through the choice of different ansätze and boundary conditions for the fields of the considered action. This, in turn, leads to different field equations and, consequently, to different physical results that arise as solutions of these differential equations, or from mathematical operations performed with them. These solutions can be analytical or numerical, depending on the model and the type of physical and/or dynamic condition we are interested in analyzing.

For example, if the ansätze for the gravitational bulk fields involve only a dependence on the extra dimension, often called the holographic radial coordinate, and if the form of the ansatz for the metric does not admit an event horizon, then the physical situation in the dual boundary QFT will correspond to the vacuum state. Correspondingly, in the bulk, the equations of motion will be a coupled system of ODEs (Ordinary Differential Equations) with no blackening function in this case. If the ansatz for the metric admits an event horizon, with the bulk system still depending only on the holographic coordinate, we will have black holes or, more generally, black branes[3] in equilibrium, and the dual boundary QFT will be defined in a given state of thermodynamic equilibrium, whose specific state will depend on the properties of the black hole considered

[2] Which are typically much more difficult to formulate and also often less rigorous from the standpoint of the holographic dictionary, since the vast majority of phenomenologically realistic holographic models are bottom-up constructions.

[3] Black branes are solutions of the Einstein equations with extended event horizons with spatial translation symmetry along directions parallel to the gravitational bulk's boundary.

Boundary QFT				Bulk Gravity
Operator	$\mathcal{O}(x)$	$\longleftrightarrow$	$\Phi(x,r)$	Field
Spin	$s_{\mathcal{O}}$	$\longleftrightarrow$	s_Φ	Spin
Global Charge	$q_{\mathcal{O}}$	$\longleftrightarrow$	q_Φ	Gauge Charge
Scaling dimension	$\Delta_{\mathcal{O}}$	$\longleftrightarrow$	m_Φ	Mass
Source	$J(x)$	$\longleftrightarrow$	$\Phi(x,r)\|_\partial$	Boundary Value (B.V.)
Expectation Value	$\langle\mathcal{O}(x)\rangle$	$\longleftrightarrow$	$\Pi_\Phi(x,r)\|_\partial$	B.V. of Radial Momentum
Global Symmetry Group	G	$\longleftrightarrow$	G	Gauge Symmetry Group
Source for Global Current	$\mathcal{A}_\mu(x)$	$\longleftrightarrow$	$A_\mu(x,r)\|_\partial$	B.V. of Gauge Field
Expectation of Current	$\langle\mathcal{J}^\mu(x)\rangle$	$\longleftrightarrow$	$\Pi^\mu_A(x,r)\|_\partial$	B.V. of Momentum
Stress Tensor	$T^{\mu\nu}(x)$	$\longleftrightarrow$	$g_{\mu\nu}(x,r)$	Spacetime Metric
Source for Stress-Energy	$h_{\mu\nu}(x)$	$\longleftrightarrow$	$g_{\mu\nu}(x,r)\|_\partial$	B.V. of Metric
Expected Stress-Energy	$\langle T^{\mu\nu}(x)\rangle$	$\longleftrightarrow$	$\Pi^{\mu\nu}_g(x,r)\|_\partial$	B.V. of Momentum
# of Degrees of Freedom Per Spacetime Point	N^2	$\longleftrightarrow$	$\left(\frac{L}{\ell_p}\right)^{d-1}$	Radius of Curvature In Planck Units
Characteristic Strength of Interactions	λ	$\longleftrightarrow$	$\left(\frac{L}{\ell_s}\right)^{d}$	Radius of Curvature In String Units
QFT Partition Function with Sources $J_i(x)$	$Z_{\mathrm{QFT_d}}[J_i]$	$\longleftrightarrow$	$Z_{\mathrm{QG_{d+1}}}[\Phi_i[J_i]]$	QG Partition Function in AdS w/ $\Phi_i\|_\partial = J_i$
QFT Partition Function at Strong Coupling	$Z^{\lambda,N\gg1}_{\mathrm{QFT_d}}[J_i]$	$\longleftrightarrow$	$e^{-I_{\mathrm{GR_{d+1}}}[\Phi[J_i]]}$	Classical GR Action in AdS w/ $\Phi_i\|_\partial = J_i$
QFT n-Point Functions at Strong Coupling	$\langle\mathcal{O}_1(x_1)\ldots\mathcal{O}_n(x_n)\rangle$	$\longleftrightarrow$	$\frac{\delta^n I_{\mathrm{GR_{d+1}}}[\Phi[J_i]]}{\delta J_1(x_1)\ldots\delta J_n(x_n)}\Big\|_{J_i=0}$	Classical Derivatives of the On-Shell Classical Gravitational Action
Thermodynamic State		$\longleftrightarrow$		Black Hole
Temperature	T	$\longleftrightarrow$	T_H	Hawking Temperature $\sim$ Mass
Chemical Potential	μ	$\longleftrightarrow$	Q	Charge of Black Hole
Free Energy	F	$\longleftrightarrow$	$I_{\mathrm{GR}}\|_{(\mathrm{on-shell})}$	On-Shell Bulk Action
Entropy	S	$\longleftrightarrow$	A_H	Area of Horizon

FIGURE 3.1: Some entries of the holographic dictionary, taken from [44].

in the bulk, which emerges as a solution of the field equations from a given choice of initial data. For each set of initial data, a black hole solution with certain properties is generated—for example, charge and mass values—which translate into specific thermal states of the boundary QFT, with given values of chemical potentials, temperature, pressure, among others. In this case, the field equations are still just coupled ODEs.

If we consider quadratic perturbations at the level of the action, around thermodynamic equilibrium, the bulk fields will be written as background terms, obtained through the procedure described above, plus the perturbation terms. If, for these bulk field perturbations, we adopt an ansatz with temporal and/or spatial dependence in the coordinates parallel to the boundary (and orthogonal to the holographic radial coordinate) in the form of a plane wave, the linearized equations of motion for these perturbations in the bulk will initially be coupled PDEs (Partial Differential Equations). However, since the spatial and temporal dependence of the perturbations in this case has already been specified in the form of plane waves, these equations of motion are reduced again to coupled ODEs, now also depending on the frequency ω and the wave number k of these plane wave ansätze. These (ω, k) are characteristics of the considered perturbations and, by solving their equations of motion subjected to certain boundary conditions, one can obtain, through the holographic dictionary, both several hydrodynamic transport coefficients and also characteristic equilibration times of the dual system in the boundary QFT perturbed around thermodynamic equilibrium. These equilibration times indicate how the system relaxes to equilibrium according to different observables. This relaxation dynamics near thermodynamic equilibrium is associated with the calculation of the quasinormal modes (QNMs) of the perturbed black holes [45]–[55].

On the other hand, if we assume a generic dependence of the bulk fields in coordinates beyond the holographic radial coordinate, we will necessarily have to deal with coupled PDEs. This is because the holographic coordinate will always be present, and, in this case, there will be at least one more coordinate, usually the time. More ambitiously, one could consider including all the coordinates of the bulk spacetime, which would allow for a fully non-trivial dependence on all the coordinates of the target QFT at the boundary. However, increasing the number of variables/coordinates in the PDE system brings considerable difficulties for the numerical evaluation of these equations, as well as increasing computational time costs. In this case of coupled PDEs, the

dual boundary QFT can initially be defined in a state far from thermodynamic equilibrium, where neither thermodynamics nor hydrodynamics are applicable descriptions for the system. However, generally, the analyzed systems evolve to acquire, from a certain moment in time, an effective hydrodynamic description, at which point we say that the system has "hydrodynamized", although the hydrodynamization of different observables usually occurs on different time scales. Subsequently, the system assumes an effective thermodynamic description, and we generally say that the system has "thermalized" only when the system's observable that equilibrates the latest has definitively converged, within a certain numerical tolerance, to its thermodynamic equilibrium value. Thus, it is possible to study different equilibration dynamics of initial states far from equilibrium from the specification of different multi-coordinate ansätze for the bulk fields and different boundary conditions [53], [56]–[69].

Since its original proposal by Maldacena in 1997 [23], the holographic gauge-gravity duality has established itself as one of the most important discoveries in theoretical physics in recent decades, being applied to obtain various insights into the non-perturbative physics of different strongly coupled quantum systems, including studies in the context of strong interaction [27], [44], [70]–[75], condensed matter systems [76]–[81], and more recently, in information theory [82]–[85].

3.2 Black Holes and Thermodynamics: a bird's eye view

First, we will provide a convenient shortcut to derive the Hawking temperature, which involves arguing that, in the Euclidean black hole metric, the Wick-rotated imaginary time coordinate must be periodic in the imaginary direction, and this imaginary time periodicity implies that the black hole has a temperature. This shortcut is entirely correct, and its formal justification from the path integral can be found in [86]. This discussion will be closely following section 11 of Ramallo's review [39].

Given t belonging to the reals, we have that under a Wick rotation [87]

$$t \in \mathbb{R} \xrightarrow{W.R.} \bar{t} = -it_E \in i\mathbb{R} \quad \therefore \quad t_E = i\bar{t}. \tag{3.3}$$

$$\mathrm{e}^{-iHt} \xrightarrow{W.R.} \mathrm{e}^{-iH\bar{t}} = \mathrm{e}^{-iH(-it_E)} = \mathrm{e}^{-Ht_E} \tag{3.4}$$

where W.R. is a Wick rotation. Then, e^{-Ht_E} is formally equivalent to the Boltzmann factor $\mathrm{e}^{-H/T}$ under the identification $t_E = i\bar{t} \equiv 1/T$.

Let us consider the partition function of a thermal field theory, $Z = \mathrm{Tr}[\mathrm{e}^{-H/T}]$, then the thermal expectation value of a given observable $\mathcal{O}$ is given by

$$\begin{aligned}\langle\mathcal{O}\rangle_T = \frac{\mathrm{Tr}\left[\mathcal{O}\mathrm{e}^{-H/T}\right]}{Z} &\sim \int_{\psi_i=\psi_f=\psi}[D\psi]\left\langle\psi(x),t\left|\mathcal{O}e^{-\frac{H}{T}}\right|\psi(x),t\right\rangle \\ &\sim \int[D\psi]\left\langle\psi(x),t|\mathcal{O}|\psi(x),t+\frac{i}{T}\right\rangle\end{aligned} \tag{3.5}$$

and the restriction $\psi_i = \psi\left(x, t + i/T\right) = \psi_f = \psi\left(x,t\right)$ implies that the functional integral must be performed over all periodic functions ψ over a circle of radius $\beta \equiv 1/T$. Notice that for $T \to 0 \Rightarrow \beta \to \infty$ and effectively there is no compactification of the Euclidean time dimension in the vacuum, that is, the compactification of Euclidean time corresponds to $T \neq 0$.

Let us now consider a stationary black hole metric with Euclidean time t_E. It is worth noting that in this case, the time component of the metric has the same sign as the spatial components, so that

$$ds^2 = g(r)\left[f(r)dt_E^2 + d\vec{x}^2\right] + \frac{1}{h(r)}dr^2 \tag{3.6}$$

where the functions $f(r)$ and $h(r)$ have a first-order zero at the event horizon, such that

$$f(r \to r_H) \approx f'\left(r_H\right)\left(r - r_H\right), \quad h(r \to r_H) \approx h'\left(r_H\right)\left(r - r_H\right), \tag{3.7}$$

so that near the horizon the metric becomes

$$ds^2 \approx g\left(r_H\right)\left[f'\left(r_H\right)\left(r - r_H\right)dt_E^2 + d\vec{x}^2\right] + \frac{dr^2}{h'\left(r_H\right)\left(r - r_H\right)}. \tag{3.8}$$

We define a new radial coordinate $\rho \in \mathbb{R}_+$ through the relation

$$d\rho^2 \equiv \frac{dr^2}{h'\left(r_H\right)\left(r - r_H\right)} \implies d\rho = \frac{dr}{\sqrt{h'\left(r_H\right)\left(r - r_H\right)}} \tag{3.9}$$

which can be integrated to give the following relationship between ρ and r:

$$\rho = 2\sqrt{\frac{r - r_H}{h'(r_H)}}. \tag{3.10}$$

We now define an angular coordinate $\theta \in [0, 2\pi]$ through the relation

$$g(r_H) f'(r_H)(r - r_H) dt_E^2 = \frac{4(r - r_H)}{h'(r_H)} d\theta^2 \tag{3.11}$$

then

$$d\theta = \frac{\sqrt{g(r_H) f'(r_H) h'(r_H)}}{2} dt_E \quad \therefore \quad \theta = \frac{\sqrt{g(r_H) f'(r_H) h'(r_H)} t_E}{2}. \tag{3.12}$$

In terms of the coordinates (ρ, θ), the part depending on (r, t_E) in the metric near the horizon (3.8) takes the form

$$g(r_H) f'(r_H)(r - r_H) dt_E^2 + \frac{dr^2}{h'(r_H)(r - r_H)} = \rho^2 d\theta^2 + d\rho^2, \tag{3.13}$$

which is locally the metric of a plane. Note from (3.10) that the horizon is at $\rho = 0$ and for this to be a regular point of the geometry without curvature singularities, the angular variable θ must be periodic with period 2π, otherwise, there would be a conical singularity at the origin associated with an angular deficit of the geometry. But from (3.12), if θ is periodic, t_E is periodic, and we saw earlier that having a periodic Euclidean time corresponds to having the system at a finite temperature, $T \neq 0$. Thus, we conclude that we can assign a temperature T to the black hole, which is the Hawking temperature. Note that t_E must be periodic under $t_E \to t_E + 1/T$ where T is the temperature given by

$$\frac{1}{T} = \frac{4\pi}{\sqrt{g(r_H) f'(r_H) h'(r_H)}}, \tag{3.14}$$

so that when $t_E \to t_E + 1/T \implies \theta \to \theta + 2\pi$ by (3.14) and (3.12).

From (3.14) and (3.8) we have that

$$T = \frac{\sqrt{g(r_H) f'(r_H) h'(r_H)}}{4\pi} = \frac{\sqrt{g'_{t_E t_E}(r_H) g'^{rr}(r_H)}}{4\pi} = \frac{\sqrt{-g'_{tt}(r_H) g'^{rr}(r_H)}}{4\pi}. \tag{3.15}$$

As the area of the event horizon of a black hole increases if its mass increases, we have that $dM \propto dA_H$ for a black hole. By multiplying dM by the gravitational constant G , we have that GdM has the dimension of acceleration times area

and therefore, $GdM \propto \kappa dA_H$, where κ must have the dimension of acceleration and it is therefore natural to associate it with the surface gravity at the event horizon of the black hole as seen by an asymptotically distant observer (in our case, by an observer at the boundary of the gravitational bulk). Considering various specific geometries of black holes, it turns out that in practice $\kappa = 2\pi T$ and (see section 3 of [38] and section 11 of [39])

$$GdM = \frac{\kappa}{8\pi} dA_H = \frac{T}{4} dA_H \quad \therefore \quad dM = Td\left(\frac{A_H}{4G}\right), \tag{3.16}$$

which is the first law of black hole thermodynamics, analogous to the first law of usual thermodynamics,

$$dE = TdS. \tag{3.17}$$

Identifying the mass of a stationary black hole with its internal energy ($E = Mc^2$, where we are considering natural units $c = \hbar = k_B = 1$), by comparing (3.16) and (3.17) we identify the Bekenstein-Hawking expression [88], [89] for the entropy of a stationary black hole [38] [39]

$$S_H \equiv \frac{A_H}{4G}. \tag{3.18}$$

Black holes with conserved charges under a $U(1)$ symmetry group are solutions of the Einstein-Maxwell equations (along with other possible matter fields in the gravitational bulk). On the other hand, in field theories, charges are expressed as volume integrals of charge densities,

$$Q = \int_{\mathbb{R}^3} d^3x\, \rho = \int_{\mathbb{R}^3} d^3x\, J^0. \tag{3.19}$$

The conserved current $J^\mu(x)$ of the QFT living at the boundary $\partial\mathcal{M}_5$ of a 5-dimensional manifold minimally couples with the boundary value of the Maxwell field of the gravitational bulk, so that by choosing the ansatz $A^\mu = \Phi(r)\delta^\mu_0$, where r is the holographic radial coordinate in terms of which the boundary of the gravitational bulk is located at $r \to \infty$, we have that the interaction Lagrangian between A^μ and J_μ at the boundary is,

$$L_{int}\,|_{\partial\mathcal{M}_5} \propto \lim_{r\to\infty} \int_{\mathbb{R}^3} d^3x A^\mu J_\mu = \lim_{r\to\infty} \Phi(r) Q. \tag{3.20}$$

The first law of thermodynamics for charged black holes is (see sections 3 and 9 of [38]),

$$dE = dM = TdS + \mu dQ, \tag{3.21}$$

or in terms of volume densities $\varepsilon = E/V$, $s = S/V$ and $\rho = Q/V$,

$$d\varepsilon = Tds + \mu d\rho. \tag{3.22}$$

By comparing (3.22) and (3.20), it is proposed that the chemical potential in the homogeneous and isotropic strongly-coupled QFT in thermodynamic equilibrium at the boundary is calculated as

$$\mu = \lim_{r\to\infty} A^0(r) = \lim_{r\to\infty} \Phi(r). \tag{3.23}$$

Since the chemical potential and charge density are conjugate thermodynamic variables, it is proposed that the charge density in the homogeneous and isotropic QFT in thermodynamic equilibrium at the boundary is calculated as the boundary value of the radial canonical momentum conjugate to the temporal component of the Maxwell field in the gravitational bulk [4],

$$\rho = \langle J^0 \rangle \equiv \lim_{r\to\infty} \frac{\partial \mathcal{L}}{\partial \left(\partial_r A^0(r)\right)} = \lim_{r\to\infty} \frac{\partial \mathcal{L}}{\partial \left(\partial_r \Phi(r)\right)}. \tag{3.24}$$

Up to this point, we have heuristically discussed some of the thermodynamic entries of the holographic dictionary presented in Fig. 3.1.

In the next chapter, we will apply some concepts discussed here to calculate several thermodynamic observables for a top-down holographic toy-model. It is defined at finite temperature and density, having a critical point in its phase diagram. Subsequently, we will focus on our main goal which is the calculation of information observables.

3.3 Heuristic Aspects of Holographic Entanglement Entropy

As discussed in Sec. 2.2.2, the entanglement entropy is defined for pure states as the von Neumann entropy $S_A \equiv -Tr_A[\rho_A \ln(\rho_A)]$ of the reduced density

[4] In equation (3.24) $\sqrt{-g}$ is included in $\mathcal{L}$, i.e., $S = \int_{\mathcal{M}_5} d^5x\mathcal{L}$.

matrix $\rho_A \equiv Tr_B(\rho)$ obtained by tracing out the degrees of freedom of a d-dimensional spacelike submanifold B, in a given QFT in $D = d+1$ dimensions, where B is the complement of A. S_A measures how the subsystems A and B are correlated to each other. In a QFT, the leading divergence of $S_A \propto$ Area of the subsystem A (what is known as the "Area Law" [90], [91] see also the reviews [92]–[99]). In 2D CFTs, the entanglement entropy is proportional to the central charge of the QFT [5] [100]–[103]. Unlike thermodynamic entropy, which vanishes in most cases at zero temperature [6], the entanglement entropy is non-zero at $T = 0$ and can therefore be used to investigate the properties of the ground state of a given quantum system (for example, it can be used as an order parameter for quantum phase transitions at zero temperature - see, for instance, section 4 of [82]). The Ryu-Takayanagi formula for the holographic entanglement entropy provides an answer to the following question: "Which part of an asymptotically AdS spacetime is related to the calculation of S_A (for a QFT on the boundary) on the gravitational side of the gauge-gravity holographic duality?" The proposal of Ryu and Takayanagi (R-T) is that [82]

$$S_A = \frac{\text{Area}\,(\gamma_A)}{4G_N^{(D+1)}}, \tag{3.25}$$

where $D + 1 = d + 2$ is the dimension of the asymptotically AdS spacetime (d is the spatial dimension and $D = d + 1$ is the spacetime dimension of the boundary) and Area (γ_A) is the hyperarea of the minimal hypersurface γ_A in the bulk, whose boundary coincides with the boundary of the subsystem A, see Fig. 3.2,

$$\partial\gamma_A = \partial A. \tag{3.26}$$

The area law for S_A [90], [91] is naturally encompassed by the holographic entanglement entropy formula (3.25).

Since entanglement entropy is always divergent for continuous systems, we introduce an ultraviolet cutoff a (analogous to a lattice spacing) to regularize its expression, obtaining from numerical analyses [90], [91] (see also [104]–[106]),

$$S_A = \lambda \cdot \frac{\text{Area}(\partial A)}{a^{d-1}} + \text{subleading terms as } a \to 0, \tag{3.27}$$

[5] The central charge c is a numerical parameter that characterizes the Virasoro Algebra of the symmetry generators of the CFT.

[6] This is not always valid, since, for example, the entropy of the Reissner-Nordström black hole remains finite when $T \to 0$, see, for example, section 3.3.3 of [82].

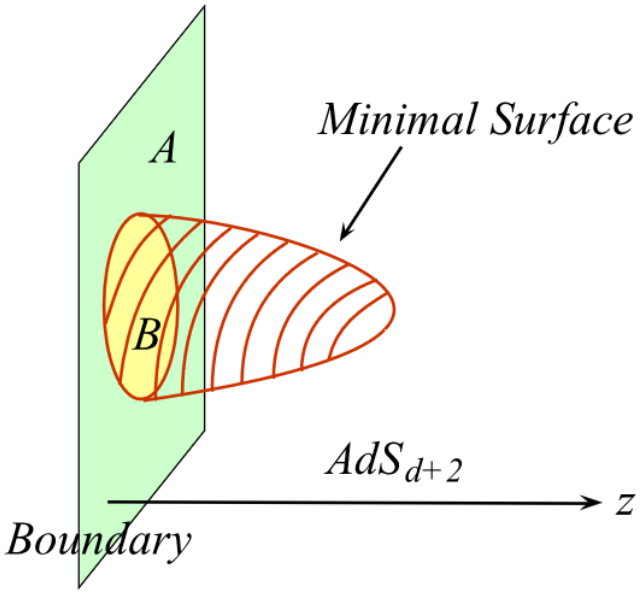

FIGURE 3.2: The holographic calculation of entanglement entropy via AdS/CFT, taken from [82].

where λ is a constant which depends on the considered system. For CFTs, being ∂A a smooth and compact manifold, the R-T formula (3.25) for holographic entanglement entropy predicts that [82]

$$\begin{aligned} S_A &= p_1(l/a)^{d-1} + p_3(l/a)^{d-3} + \cdots \\ &\cdots + \begin{cases} p_{d-1}(l/a) + p_d, & d: \text{ even} \\ p_{d-2}(l/a)^2 + \tilde{c}\log(l/a), & d: \text{ odd} \end{cases} \end{aligned} \tag{3.28}$$

where l is the typical length scale of ∂A and $\tilde{c}$ is given in terms of CFTs central charges, in particular $\tilde{c} = c/3$ for $d = 1$ which leads to $S_A^{2D\ CFTs} = c/3 \log(l/a)$, which is a well-known result for $2D$ CFTs.

Since the metric of asymptotically AdS backgrounds diverges at the boundary ($u = 0$), we impose an ultraviolet cutoff in the bulk, $u \geq a \in \mathbb{R}_+^*$, which we identify as the ultraviolet cutoff of the QFT on the boundary [7]. To obtain a gravitational dual of the entanglement entropy S_A of the boundary QFT, we extend ∂A in Fig. 3.2 to the gravitational bulk with the condition that γ_A is the smallest possible surface in the bulk, such that $\partial\gamma_A = \partial A$, and propose that S_A is calculated by means of (3.25). It can be shown that the leading divergence

[7] The argument considered here is proposed for static asymptotically AdS backgrounds (for time-dependent backgrounds, see section 6 of the review [82]).

obtained from the calculation of (3.25) is proportional to $a^{-(d+1)}\text{Area}\,(\partial A)$, reproducing the area law in (3.27) [82].

The form of (3.25) is identical to the Bekenstein-Hawking formula for the entropy of a black hole, replacing the hyperarea of the black hole's event horizon with the hyperarea of the minimal surface γ_A. This formula can be heuristically motivated as follows [82], [107]. Being the reduced density matrix ρ_A of the QFT normalized such that $\text{Tr}_A\,(\rho_A) = 1$, we consider the replica trick, in which we take n-replicas of the subsystem A, so that,

$$S_A = -\,\text{Tr}_A[\rho_A \ln \rho_A] = -\left.\frac{\partial}{\partial n}\,\text{Tr}_A\,\rho_A^n\right|_{n=1} = -\left.\frac{\partial}{\partial n}\log \text{Tr}_A\,\rho_A^n\right|_{n=1}, \tag{3.29}$$

where using the functional integration formalism it can be shown that [82] $\text{Tr}\,(\rho_A^n) = Z_n/Z_1^n$, being Z_n a partition function in a space with conical singularities, obtained as the Riemann surface R_n corresponding to the gluing of n copies of the original space ∂A with negative angular deficit $\delta = 2\pi(1-n)$ [8]. Thus, on the gravitational side of the holographic duality, it is proposed to construct a $(d+2)$-dimensional asymptotically AdS_{d+2} geometry with angular deficit δ located on a codimension-2 surface [9] [107]. Using the fundamental holographic Gubser-Klebanov-Polyakov-Witten (GKPW) relation [24], [25],

$$Z_{QFT} \sim \mathrm{e}^{-S_{SUGRA}^{on-shell}} \quad \therefore \quad \ln Z_{QFT} \sim -S_{SUGRA}^{on-shell}, \tag{3.30}$$

which relates the partition function of a strongly coupled QFT on the boundary to the dual on-shell supergravity (SUGRA) action in the gravitational bulk, it is shown that [82], [107]

$$S_A = -\left.\frac{\partial}{\partial n}\log \text{Tr}\,\rho_A^n\right|_{n=1} = -\frac{\partial}{\partial n}\left[\frac{(1-n)\,\text{Area}\,(\gamma_A)}{4G_N^{d+2}}\right]_{n=1} = \frac{\text{Area}\,(\gamma_A)}{4G_N^{(d+2)}} \tag{3.31}$$

where the Hamilton's principle of least action, used to calculate the on-shell gravitational action, implies that the $\text{Area}(\gamma_A)$ is the surface of minimal hyperarea in the bulk with border $\partial\gamma_A = \partial A$ on the boundary.

Finally, equation (3.31) will be used in Sections 4.3 and 5.3 to evaluate the holographic entanglement entropy in the 1RCBH and 2RCBH models, respectively.

[8] This angular deficit is used to construct the Riemann surface - see for example fig. 2b of [82].

[9] Codimension $(\gamma_A) \equiv \text{dimension}(\mathcal{M}_{d+2}) - \text{dimension}(\gamma_A)$.

Chapter 4

1RCBH model

In the present chapter, we will deal with a top-down holographic construction, which it is defined at finite temperature and density, having a critical point in its phase diagram. This top-down holographic model may be viewed as a simple and safe playground where several physical observables for a strongly coupled QFT at finite temperature and density may be evaluated using the holographic dictionary. In fact, we will present the calculations of thermodynamic observables, and later, we will focus on our main objective, which is information observables.

In the low energy limit of type IIB strings, all quantum loops of strings are discarded, resulting in type IIB Supergravity theory. When defined on $AdS_5 \times S^5$, a compactification of the fields of the type IIB supergravity theory is performed on the S^5 sphere, generating an infinite tower of massive Kaluza-Klein modes. The Kaluza-Klein reduction of the type IIB supergravity theory on the S^5 sphere can be consistently truncated by considering only the lowest mass modes, generating an effective theory for these modes, namely $5D$ maximally supersymmetric $\mathcal{N} = 8$ gauged supergravity [108], [109], see also [110], [111].

The isometry group of the S^5 sphere is $SO(6)$, and the Cartan subgroup of $SO(6)$ is $SO(2) \times SO(2) \times SO(2)$. As mentioned in section 3, the $\mathcal{N} = 4$ SYM theory with gauge group $SU(N)$, with large N and strong coupling, is dual to type IIB supergravity theory in $AdS_5 \times S^5$. This $\mathcal{N} = 4$ SYM theory in the vacuum has a global R-symmetry[1] $SU(4)$.

There are black brane solutions that are charged only under the Cartan subgroup $U(1) \times U(1) \times U(1)$ of the $SU(4)$ R-symmetry group. Since $U(1)$ and $SO(2)$ are isomorphic, $U(1) \times U(1) \times U(1) \simeq SO(2) \times SO(2) \times SO(2)$, and the Cartan subgroup of S^5 isometries is isomorphic to the Cartan subgroup of the

[1] R-symmetry is a symmetry that transforms the generators of supersymmetry, called supercharges, in a supersymmetric theory.

$\mathcal{N} = 4$ SYM R-symmetry. These black brane solutions[2] in the bulk, therefore, break the $SU(4)$ R-symmetry group of the $\mathcal{N} = 4$ SYM in the vacuum to only its Cartan subgroup $U(1) \times U(1) \times U(1)$ at finite temperature and finite R-charge densities. The effective bulk theory in $5D$ that provides these charged black brane solutions is known as the STU model[3] [108], [109], see also [110], [111].

The STU model with three generic conserved R-charges has three Maxwell gauge fields (associated with each $U(1)$ of the Cartan subgroup of $SU(4)$), two scalar fields, and the metric. We can set two of these R-charges to zero and keep only one non-trivial R-charge, in which case the R-symmetry of the system is further reduced to just $U(1)$. This particular case of the STU model is called the 1 R-charge Black Hole (1RCBH) model [110], [111].

In this chapter, we will address the 1RCBH model, and in the next chapter, we will discuss another particular case of the STU model corresponding to setting one R-charge to zero and keeping the other two R-charges different from zero but equal to each other, which is called the 2 R-charge Black Hole (2RCBH) model [110], [111]. Setting all the charges of the STU model to zero yields the purely thermal SYM theory. It is worth noting that in this case, the dual gravitational action is the pure Einstein-Hilbert action with a negative cosmological constant in five dimensions, which, in turn, has a unique solution corresponding to the AdS_5-Schwarzschild spacetime.

4.1 The 1RCBH model

Given a certain simplicity and also the fact that it is a rigorous top-down holographic construction that describes a strongly coupled quantum medium at finite temperature and density, which has a critical point in its phase diagram, the 1RCBH model has been extensively explored in the holographic literature in recent times. For example, its thermodynamics was analyzed in [52], [110],

[2] In particular, the solutions of "black holes" in the 1RCBH and 2RCBH models are actually black brane solutions. Thus, it would be correct to call them black branes, but in holography, these solutions are typically referred to as "black holes" .

[3] The bosonic part of $5D$ $\mathcal{N} = 2$ gauged Supergravity is given by equation (1) of [108], where the potential of the scalar fields of the theory is given by equation (2) of the same reference, which satisfy the general constraint (3). In the particular case of this constraint being given by equation (38) of the same reference, we have the so-called STU model, where S, T, U are three scalar fields of which only 2 are independent, due to the constraint (38), $STU = 1$. Although it originally appears as a particular case of $5D$ $\mathcal{N} = 2$ gauged SUGRA with the constraint $STU = 1$, the STU model can also be embedded in the $5D$ $\mathcal{N} = 8$ gauged SUGRA.

hydrodynamic transport coefficients were calculated in [110], [112], the spectra of quasinormal modes were obtained in [52], [53], various observables of quantum information theory were evaluated in [113]–[115], chaotic properties and the pole-skipping phenomenon were addressed in [116], [117], while the holographic renormalization and far from equilibrium numerical simulations of homogeneous isotropization dynamics and inhomogeneous Bjorken flow were discussed in [53], [65], [68], [69].

The 1RCBH model [110], [111] is described by a bulk Einstein-Maxwell-dilaton (EMD) action plus two boundary terms as follows

$$S = \frac{1}{2\kappa_5^2}\int_{\mathcal{M}_5} d^5x\sqrt{-g}\left[R - \frac{f(\phi)}{4}F_{\mu\nu}F^{\mu\nu} - \frac{1}{2}\left(\partial_\mu\phi\right)^2 - V(\phi)\right] + S_{GHY} + S_{ct}, \tag{4.1}$$

where R is the Ricci curvature scalar, the dilaton ϕ is a real scalar field, $F_{\mu\nu} = \partial_\mu A_\nu - \partial_\nu A_\mu$, with A_μ being the Maxwell gauge field, and $\kappa_5^2 = 8\pi G_5$, where G_5 is the Newtonian gravitational constant in 5 dimensions. The Maxwell-dilaton coupling[4] and the dilaton potential, which define the top-down construction corresponding to the model, are given, respectively, by

$$f(\phi) = \mathrm{e}^{-2\sqrt{\frac{2}{3}}\phi}, \quad V(\phi) = -\frac{1}{L^2}\left(8\mathrm{e}^{\frac{\phi}{\sqrt{6}}} + 4\mathrm{e}^{-\sqrt{\frac{2}{3}}\phi}\right), \tag{4.2}$$

where L is the asymptotic AdS_5 radius and S_{GHY} is the Gibbons-Hawking-York boundary action [86], [118], see also [119], which is necessary for the Hamilton's Principle to yield the Einstein equations consistently with Dirichlet boundary conditions in a spacetime with a boundary, as it is the case for asymptotically AdS spaces. The last term in (4.1), denoted by S_{ct}, is the counterterm action that is added to the EMD action to remove the divergences of the on-shell action at the boundary [53]. For simplicity, we will consider $L = 1$.

Varying the EMD action with respect to the metric, we obtain the Einstein equations,

$$R_{\mu\nu} - \frac{1}{2}g_{\mu\nu}R = \kappa_5^2 T_{\mu\nu}, \tag{4.3}$$

where the energy-momentum tensor of the matter fields A^μ and ϕ is defined by,

$$T_{\mu\nu} \equiv -\frac{2}{\sqrt{-g}}\frac{\delta\left(\sqrt{-g}\mathcal{L}_{\mathrm{Matter}}/2\kappa_5^2\right)}{\delta g^{\mu\nu}}, \tag{4.4}$$

[4]Since the dilaton is a real scalar field, it is not charged under the $U(1)$ gauge symmetry group associated with the Maxwell field, and therefore, there is no minimal coupling between the dilaton and Maxwell field.

wherein

$$T_{\mu\nu} = \frac{1}{\kappa_5^2}\left[\frac{f(\phi)}{2}F_{\mu\alpha}F_{\nu}{}^{\alpha} + \frac{1}{2}\partial_\mu\phi\partial_\nu\phi - \frac{1}{2}g_{\mu\nu}\left(\frac{f(\phi)}{4}F_{\alpha\beta}F^{\alpha\beta} + \frac{1}{2}\left(\partial_\alpha\phi\right)^2 + V(\phi)\right)\right]. \tag{4.5}$$

Often, it is simpler to work with the form given by the trace-reversed Einstein equations. Contracting both sides of (4.3) with the inverse metric $g^{\mu\nu}$ we have the following

$$\begin{aligned} g^{\mu\nu}R_{\mu\nu} - \frac{1}{2}g^{\mu\nu}g_{\mu\nu}R &= \kappa_5^2 g^{\mu\nu}T_{\mu\nu} \\ R - \frac{1}{2}\underbrace{\delta_\mu^\mu}_{D=5}R &= \kappa_5^2 T_\mu^\mu \\ -\frac{R}{2} &= \frac{\kappa_5^2}{3}T_\rho^\rho. \end{aligned} \tag{4.6}$$

Substituting in (4.3) the expression on the right-hand side of the above equality we have

$$R_{\mu\nu} = \kappa_5^2\left(T_{\mu\nu} - \frac{1}{3}g_{\mu\nu}T_\rho^\rho\right). \tag{4.7}$$

By substituting (4.5) in (4.7), we rewrite Einstein equations as

$$R_{\mu\nu} - \frac{g_{\mu\nu}}{3}\left[V(\phi) - \frac{f(\phi)}{4}F_{\rho\sigma}F^{\rho\sigma}\right] - \frac{1}{2}\partial_\mu\phi\partial_\nu\phi - \frac{f(\phi)}{2}F_{\mu\sigma}F_{\nu}{}^{\sigma} = 0. \tag{4.8}$$

We can also obtain the Maxwell equations by varying the EMD action with respect to the Maxwell field, getting

$$\partial_\mu\left(\sqrt{-g}f(\phi)F^{\mu\nu}\right) = 0. \tag{4.9}$$

The dilaton field equation, obtained by varying the EMD action with respect to the scalar field is,

$$\frac{1}{\sqrt{-g}}\partial_\mu\left(\sqrt{-g}g^{\mu\nu}\partial_\nu\phi\right) - \partial_\phi V(\phi) - \frac{F_{\rho\sigma}F^{\rho\sigma}}{4}\partial_\phi f(\phi) = 0. \tag{4.10}$$

It is worth noting that any model of the EMD class satisfies the equations of motion given by (4.8), (4.9) and (4.10). To treat a strongly coupled QFT on the boundary, dual to the EMD theory defined in the gravitational bulk, in the particular case of this QFT being in a homogeneous and isotropic configuration in thermodynamic equilibrium at finite temperature and density, in the absence

of external electromagnetic fields, we use as an ansatz for the bulk fields

$$ds^2 = \mathrm{e}^{2A(r)}\left(-h(r)dt^2 + d\vec{x}^2\right) + \frac{\mathrm{e}^{2B(r)}}{h(r)}dr^2, \quad \phi = \phi(r), \quad A^\mu = \Phi(r)\delta^\mu_0, \quad (4.11)$$

where the fields depend only on the holographic radial coordinate (this fact justifies why there is no variation in time and space for the QFT state considered on the boundary). The gauge field has only the non-zero time component, whose boundary value will provide the chemical potential in the QFT. The metric, which has a blackening function, describes charged black hole backgrounds, which are the gravitational duals to thermal states at finite temperature and density in the boundary QFT in thermodynamic equilibrium.

Substituting (4.2) (which specify the 1RCBH model within the class of EMD models) and (4.11) (which specify that the system in equilibrium) into the general EMD field equations (4.8), (4.9) and (4.10), we obtain a set of coupled ODEs for the bulk fields, whose solutions are of the form specified below [5]

$$A(r) = \ln r + \frac{1}{6}\ln\left(1 + \frac{Q^2}{r^2}\right), \quad (4.12)$$

$$B(r) = -\ln r - \frac{1}{3}\ln\left(1 + \frac{Q^2}{r^2}\right), \quad (4.13)$$

$$h(r) = 1 - \frac{M^2}{r^2\left(r^2 + Q^2\right)}, \quad (4.14)$$

$$\phi(r) = -\sqrt{\frac{2}{3}}\ln\left(1 + \frac{Q^2}{r^2}\right), \quad (4.15)$$

$$\Phi(r) = \left(-\frac{MQ}{r^2 + Q^2} + \frac{MQ}{r_H^2 + Q^2}\right). \quad (4.16)$$

These solutions are specified in terms of two data that we can choose for the black holes: their mass denoted by M and their charge denoted by Q. Each black hole solution generated in the gravitational bulk from the choices of the pair (M, Q) is dual, via the holographic dictionary, to a specific thermal state of the boundary QFT, which is located at $r \to \infty$. In the solutions given by (4.12) to (4.16) we have that r_H is the radial location of the event horizon of the black hole solution, which is obtained by the condition of vanishing of the g_{tt} component of the metric, which corresponds to the vanishing of the blackening

[5] The presented solutions were explicitly checked by direct substitution into the ODEs, thus showing that these functions, in fact, solve the field equations.

function at $r = r_H$

$$\left(1 - \frac{M^2}{r_H^2\left(r_H^2 + Q^2\right)}\right) = 0. \tag{4.17}$$

Since the above expression is a quartic equation for r_H, it therefore has four roots. Since the holographic radial coordinate r is real and non-negative, we take from these four roots the one that corresponds to a real and non-negative value for the radial location of the event horizon, which is given by

$$r_H = \sqrt{\frac{\sqrt{Q^4 + 4M^2} - Q^2}{2}}. \tag{4.18}$$

We can use (4.18) to express M as a function of r_H and Q and, alternatively to the description of black hole backgrounds in terms of (M, Q), we can describe them in terms of (r_H, Q), resulting

$$M = r_H\sqrt{Q^2 + r_H^2}. \tag{4.19}$$

In the next section, we will discuss the calculation of thermodynamic observables, the phase diagram and R-charge susceptibilities for the 1RCBH model.

4.2 Thermodynamics

4.2.1 Basic thermodynamic variables

We can obtain the Hawking temperature of the black hole in terms of the charge Q and the radial location of the event horizon r_H through (3.15) with the identification of the metric coefficients given below (4.20), which follows from (4.11),

$$T = \left.\frac{\sqrt{-\left(g_{tt}\right)'\left(g^{rr}\right)'}}{4\pi}\right|_{r=r_H}, \tag{4.20}$$

where $g_{tt} = -e^{2A(r)}h(r)$, $g^{rr} = e^{-2B(r)}h(r)$ and $'$ denotes the derivative with respect to r. Substituting these quantities into expression (4.20), we have that

$$T = \left.\frac{\sqrt{-\left(-e^{2A(r)}h(r)\right)'\left(e^{-2B(r)}h(r)\right)'}}{4\pi}\right|_{r=r_H} \tag{4.21}$$

$$= \left.\frac{\sqrt{\left(2e^{2A(r)}h(r)A'(r)+e^{2A(r)}h'(r)\right)\left(e^{-2B(r)}h'(r)-2e^{-2B(r)}h(r)B'(r)\right)}}{4\pi}\right|_{r=r_H}, \tag{4.22}$$

which applying (4.12),(4.13),(4.14) and performing the calculation of the respective derivatives, we obtain

$$T = \left.\frac{\sqrt{\frac{M^4(2Q^4+9Q^2r^2+9r^4)+M^2(5Q^6r^2+23Q^4r^4+36Q^2r^6+18r^8)+r^4(Q^2+r^2)^2(2Q^4+9Q^2r^2+9r^4)}{r^4(Q^2+r^2)^3}}}{6\pi}\right|_{r=r_H}. \tag{4.23}$$

Substituting (4.18),(4.19) into the above expression, evaluating at $r = r_H$ and simplifying, we have

$$T = \frac{Q^2+2r_H^2}{2\pi\sqrt{Q^2+r_H^2}}. \tag{4.24}$$

For the chemical potential of R-charges $U(1)$ by using (3.23), we have

$$\mu = \lim_{r\to\infty}\Phi(r) = \lim_{r\to\infty}\left(-\frac{MQ}{r^2+Q^2}+\frac{MQ}{Q^2+r_H^2}\right), \tag{4.25}$$

where $\Phi(r)$ was given by (4.16). Calculating the limit, we have that

$$\mu = \frac{MQ}{Q^2+r_H^2}, \tag{4.26}$$

and substituting (4.19) and simplifying, we will have the chemical potential given by

$$\mu = \frac{Qr_H}{\sqrt{Q^2+r_H^2}}. \tag{4.27}$$

The entropy S can be obtained through the Bekenstein-Hawking formula presented in (3.18), as

$$S = \frac{A_H}{4G_5}, \tag{4.28}$$

being the hypersurface of the event horizon A_H given by

$$A_H = \int_{\mathcal{M}_H} \sqrt{|\gamma_H|} d^3x = \int_{\mathcal{M}_H} \sqrt{g_{xx} g_{yy} g_{zz}} d^3x = \int_{\mathcal{M}_H} \sqrt{\mathrm{e}^{2A(r_H)} \mathrm{e}^{2A(r_H)} \mathrm{e}^{2A(r_H)}} d^3x$$
$$= \mathrm{e}^{3A(r_H)} \int_{\mathcal{M}_H} d^3x, \tag{4.29}$$

which substituting (4.12) and simplifying we will have

$$A_H = r_H^2 \sqrt{Q^2 + r_H^2} \int_{\mathcal{M}_H} d^3x. \tag{4.30}$$

As the integral is in three dimensions, we will have a volume denoted by V, therefore

$$A_H = r_H^2 \sqrt{Q^2 + r_H^2} V. \tag{4.31}$$

Substituting (4.31) into (4.28), we have

$$S = \frac{r_H^2 \sqrt{Q^2 + r_H^2} V}{4G_5}. \tag{4.32}$$

Dividing the entropy S by the volume V we will have the entropy density s, given by

$$s = \frac{r_H^2 \sqrt{Q^2 + r_H^2}}{4G_5}. \tag{4.33}$$

We can still rewrite the Newton constant in five dimensions as follows

$$\kappa_5^2 = 8\pi G_5 \Rightarrow 4G_5 = \frac{\kappa_5^2}{2\pi}.$$

Therefore, we have the entropy density given by the expression

$$s = \frac{2\pi}{\kappa_5^2} r_H^2 \sqrt{Q^2 + r_H^2}. \tag{4.34}$$

We also have that the R-charge density given by expression (3.24), which is the radially conjugate momentum

$$\rho = \lim_{r \to \infty} \frac{\delta S}{\delta \Phi'}. \tag{4.35}$$

The Lagrangian density for the Maxwell field is

$$\mathcal{L}_{\text{Maxwell}} = -\frac{\sqrt{|g|}}{2\kappa_5^2} \frac{f(\phi)}{4} F_{\mu\nu} F^{\mu\nu}. \tag{4.36}$$

We need to find the momentum conjugate to the field A_μ, denoted by π^μ and given by [120]

$$\pi^\mu = \frac{\partial \mathcal{L}_{\text{Maxwell}}}{\partial(\partial_r A_\mu)}, \tag{4.37}$$

where r is the radial coordinate, so that

$$\begin{aligned}\pi^\mu = \frac{\partial}{\partial(\partial_r A_\mu)}\left(-\frac{\sqrt{|g|}}{2\kappa_5^2}\frac{f(\phi)}{4}F_{\mu\nu}F^{\mu\nu}\right) &= -\frac{\sqrt{|g|}}{2\kappa_5^2}\frac{f(\phi)}{4}\frac{\partial}{\partial(\partial_r A_\mu)}\left(F_{\mu\nu}F^{\mu\nu}\right) \\ &= -\frac{\sqrt{|g|}}{2\kappa_5^2}\frac{f(\phi)}{4}\cdot 2\left(\partial^r A^\mu - \partial^\mu A^r\right),\end{aligned} \tag{4.38}$$

then, we have that

$$\pi^\mu = -\frac{\sqrt{|g|}}{2\kappa_5^2}\frac{f(\phi)}{2}F^{r\mu}. \tag{4.39}$$

Now, as in (3.24), we will consider the $\mu = 0$ component of the conjugate momentum,

$$\rho = \lim_{r\to\infty}\pi^0 = \frac{1}{2\kappa_5^2}\lim_{r\to\infty}\sqrt{|g|}\frac{f(\phi)}{2}F^{0r}. \tag{4.40}$$

Therefore, the R-charge density ρ is given by [120]

$$\begin{aligned}\rho = \frac{1}{2\kappa_5^2}\lim_{r\to\infty}\left(\mathrm{e}^{3A(r)}\cdot\mathrm{e}^{-2\sqrt{\frac{2}{3}}\phi}\cdot\partial^0 A^r\right) &= \frac{1}{2\kappa_5^2}\lim_{r\to\infty}\mathrm{e}^{3A(r)}\cdot\mathrm{e}^{-2\sqrt{\frac{2}{3}}\phi}\cdot\partial_t\left(\Phi(r)dt\right) \\ &= \frac{1}{2\kappa_5^2}\lim_{r\to\infty}\mathrm{e}^{3A(r)}\cdot\mathrm{e}^{-2\sqrt{\frac{2}{3}}\phi}\cdot\Phi(r)\end{aligned} \tag{4.41}$$

which substituting (4.11), (4.12), (4.13), (4.15) and (4.16) into the above expression and simplifying, will result in

$$\rho = \frac{1}{2\kappa_5^2}\lim_{r\to\infty}\frac{2MQr^{2/3}}{\left(Q^2+r^2\right)^{1/3}} = \frac{2MQ}{2\kappa_5^2}, \tag{4.42}$$

which substituting (4.19) we have

$$\rho = \frac{Qr_H}{\kappa_5^2}\sqrt{Q^2+r_H^2}. \tag{4.43}$$

4.2.2 Phase diagram and equation of state

The black hole solutions of the 1RCBH model can be parameterized in terms of the dimensionless ratio Q/r_H. To obtain the ratio, we divide (4.27) by (4.24),

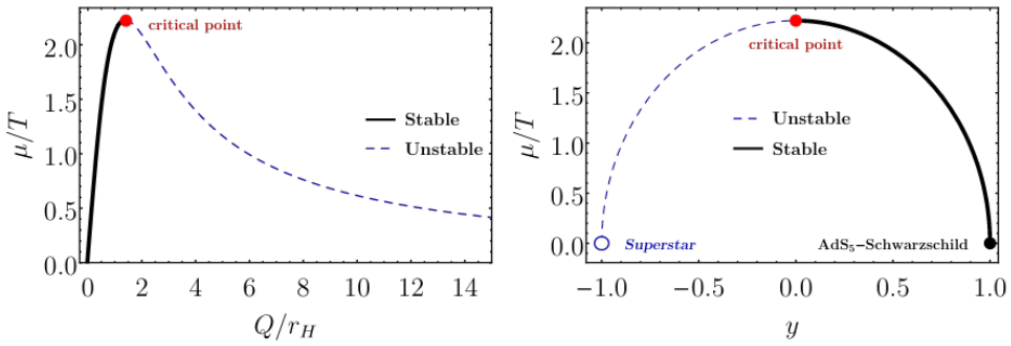

FIGURE 4.1: Phase structure for the 1RCBH model (following closely the discussions presented in [52], [110] and taken from [52]): (a) The only dimensionless control parameter of the QFT phase diagram, μ/T, as a function of the dimensionless ratio that corresponds to Q/r_H on the gravity side for the stable and unstable branches. It is worth noting that the superstar solution is at $Q/r_H \to \infty$; (b) The same discussion, but in terms of the alternative variable y defined in (4.46).

resulting in

$$\frac{\mu}{T} = \frac{2\pi Q r_H}{Q^2 + 2r_H^2}. \tag{4.44}$$

We can obtain from (4.44) the quantity Q/r_H,

$$\frac{Q}{r_H} = \sqrt{2}\left(\frac{1 \pm \sqrt{1 - \left(\frac{\mu/T}{\pi/\sqrt{2}}\right)^2}}{\frac{\mu/T}{\pi/\sqrt{2}}}\right). \tag{4.45}$$

Since the quantity Q/r_H is non-negative, it implies that $\mu/T \in [0, \pi/\sqrt{2}]$. Still looking at the same expression, we have that for each value of the ratio $\mu/T \in [0, \pi/\sqrt{2})$, there are two different values of Q/rH, each associated with different branches of black hole solutions.

We introduce through the parametric relation below a variable y that smoothly connects the two branches of solutions

$$y^2 + \left(\frac{\mu/T}{\pi/\sqrt{2}}\right)^2 = 1 \quad \text{with} \quad y \in [-1, 1], \tag{4.46}$$

where $y = 0$ will parameterize the critical region of the background geometry, in which $\mu/T = \pi/\sqrt{2}$. [6] For $y = 1$, we have the parameterization of the background geometry of the AdS$_5$-Schwarzschild without charge, which in turn

[6] Later it will be clear why this is a critical point of the phase diagram.

has $Q = 0$ and $r_H \neq 0$ implying directly in $\mu/T = 0$. If $y = -1$, we have that $\mu/T = 0$, however, it is $r_H = 0$ and $Q \neq 0$, which will indeed correspond to a supersymmetric BPS solution known in the literature as "superstar" [121] instead of a black hole. We can still write (4.46) in terms of μ/T, as

$$\mu/T = \frac{\pi}{\sqrt{2}}\sqrt{1-y^2}. \tag{4.47}$$

Isolating the charge Q from (4.44) we obtain two possible solution branches,

$$Q = \frac{\pi r_H}{\mu/T} \pm \frac{\sqrt{\pi^2 r_H^2 - 2r_H^2(\mu/T)^2}}{\mu/T}, \tag{4.48}$$

and substituting (4.47) into the above expression, we have

$$Q = \mp\frac{\sqrt{2}r_H(y \pm 1)}{\sqrt{1-y^2}}. \tag{4.49}$$

From the temperature expression (4.24), we can isolate the radial location of the event horizon r_H, and substituting the charge Q by the expression (4.49) we have

$$r_H = \frac{\pi T}{2}\sqrt{(3 \mp y)(y \pm 1)}. \tag{4.50}$$

which are two solutions corresponding to the upper or lower signs.

We can rewrite (4.49) in terms of (4.50), which becomes

$$Q = \frac{\pi T\sqrt{(y \mp 3)(y \mp 1)}}{\sqrt{2}}. \tag{4.51}$$

Finally, we can write the mass M of the black hole given in (4.19) by substituting r_H by the expression given in (4.50)

$$M = \frac{\pi^2 T^2}{4}\sqrt{y \pm 1}(3 \mp y)^{3/2}. \tag{4.52}$$

It is known in the literature [122] that for a SYM plasma, we have

$$\frac{1}{\kappa_5^2} = \frac{N_c^2}{4\pi^2}, \tag{4.53}$$

where N_c is the number of color charges of the boundary QFT, which is very large in the classical limit of the holographic duality.

By substituting (4.53), (4.49) and (4.50) in the entropy density relation (4.34), we will have

$$s = \frac{1}{16} N c^2 \pi^2 T^3 (3 \mp y)^2 (1 \pm y), \tag{4.54}$$

being able to rewrite the same in terms of μ/T using (4.46), and after some algebraic manipulations we will have

$$\frac{s}{N_c^2 T^3} = \frac{\pi^2}{16} \left(3 \pm \sqrt{1 - \left(\frac{\mu/T}{\pi/\sqrt{2}} \right)^2} \right)^2 \left(1 \mp \sqrt{1 - \left(\frac{\mu/T}{\pi/\sqrt{2}} \right)^2} \right), \tag{4.55}$$

where the lower/upper signs will denote the branches that are stable/unstable, as in (4.45). Later we will justify why the mentioned signs represent the thermodynamically stable or unstable branches.

For the R-charge density given in (4.43), substituting by (4.53), (4.49) and (4.50), we have

$$\rho = \frac{\mu/T}{16} N_c^2 T^3 (3 - y)^2 \tag{4.56}$$

which can be rewritten in terms of μ/T using (4.46)

$$\frac{\rho}{N_c^2 T^3} = \frac{\mu/T}{16} \left(3 \pm \sqrt{1 - \left(\frac{\mu/T}{\pi/\sqrt{2}} \right)^2} \right)^2 . \tag{4.57}$$

It is worth noting here that for this model, given any dimensionless ratio, it will always be written in terms of μ/T, as expected, since this is a model with conformal symmetry, and therefore does not have an intrinsic mass scale with respect to which temperature and chemical potential can be measured independently. In a conformal theory, when temperature is introduced, it becomes a scale of the theory with respect to which variations in the chemical potential can be measured. For this reason, the phase diagram of the model is not a plane, but a line parameterized by values of μ/T, which, being limited between $\left[0, \pi/\sqrt{2}\right]$ forms, in the case of the model in question, a line segment.

Starting from the Gibbs-Duhem thermodynamic relation, $dp = sdT + \rho d\mu$, it is possible to calculate the pressure. To do this, it is necessary to obtain the entropy and the chemical potential, as presented below.

For an entropy density given by $s = s(T, y)$ we have

$$\left(\frac{\partial s}{\partial \mu}\right)_T = \left(\frac{\partial s}{\partial y}\right)_T \frac{dy}{d(\mu/T)} \left(\frac{\partial(\mu/T)}{\partial \mu}\right)_T = -\frac{{N_c}^2 \pi T^2 (3 \mp y)(3y \mp 1)(\mu/T)}{8\sqrt{\pi^2 - 2(\mu/T)^2}}$$
$$= \frac{N_c^2 T^2 (3 \mp y)(3y \mp 1)(\mu/T)}{8y}. \quad (4.58)$$

Now, for the charge density given by $\rho = \rho(T, \mu/T, y)$ we have that

$$\left(\frac{\partial \rho}{\partial T}\right)_\mu = \left(\frac{\partial \rho}{\partial T}\right)_{\frac{\mu}{T}, y} + \left(\frac{\partial \rho}{\partial(\mu/T)}\right)_{T,y} \left(\frac{\partial(\mu/T)}{\partial T}\right)_\mu + \left(\frac{\partial \rho}{\partial y}\right)_{T, \frac{\mu}{T}} \frac{dy}{\mathrm{d}(\mu/T)} \left(\frac{\partial(\mu/T)}{\partial T}\right)_\mu \quad (4.59)$$

$$= \frac{N_c^2 T}{16} (3 \mp y) \left[\mp 3T(y \mp 3)(\mu/T) \pm \mu \left((y \mp 3) - \frac{4(\mu/T)^2}{\pi\sqrt{\pi^2 - 2(\mu/T)^2}}\right)\right], \quad (4.60)$$

which rewriting in terms of μ/T using (4.46)

$$\left(\frac{\partial \rho}{\partial T}\right)_\mu = \frac{N_c^2 T^2 (3 \mp y)(3y \mp 1)(\mu/T)}{8y}. \quad (4.61)$$

From expressions (4.58) and (4.61) we obtain the following Maxwell relation

$$\left(\frac{\partial s}{\partial \mu}\right)_T = \left(\frac{\partial \rho}{\partial T}\right)_\mu. \quad (4.62)$$

By the Gibbs-Duhem relation, the quantities s, ρ, are partial derivatives of the pressure with respect to T and μ, respectively. Writing the pressure as a function of T and y, then $p = p(T, y)$, therefore

$$p = \left(\int \left[s + \rho \left(\frac{\partial \mu}{\partial T}\right)_{\frac{\mu}{T}}\right] dT\right)_y + F(y) = \left(\int \left[\rho \left(\frac{\partial \mu}{\partial(\mu/T)}\right)_T \frac{d(\mu/T)}{dy}\right] dy\right)_T + G(T). \quad (4.63)$$

Let's define

$$I_1 = \left(\int \left[s + \rho \left(\frac{\partial \mu}{\partial T}\right)_{\frac{\mu}{T}}\right] dT\right)_y + F(y), \quad I_2 = \left(\int \left[\rho \left(\frac{\partial \mu}{\partial(\mu/T)}\right)_T \frac{d(\mu/T)}{dy}\right] dy\right)_T + G(T). \quad (4.64)$$

where I_1 is an expression for the pressure, in which the first term of the integrand is the entropy density which is integrated with respect to temperature, which

results in

$$I_1 = -\frac{\pi^2 N_c^2 T^4}{128}(y \mp 3)^3(y \pm 1) + F(y). \tag{4.65}$$

For I_2, we also have an expression for the pressure, where we have in the integrand the charge density integrated with respect to the chemical potential, so that

$$I_2 = -\frac{\pi^2 N_c^2 T^4}{128} y^2 \left[(y \mp 8)y + 18\right] + G(T). \tag{4.66}$$

As I_1 and I_2 are different expressions for the pressure, therefore, when subtracting $I_1 - I_2$ we must obtain zero.

$$I_1 - I_2 = \frac{27}{128}\pi^2 N_c^2 T^4 + F(y) - G(T) = 0, \tag{4.67}$$

while $F(y) = 0$ we have that $G(T) = \frac{27}{128}\pi^2 N_c^2 T^4$. Substituting $F(y) = 0$ in (4.65) we obtain

$$p = \frac{\pi^2 N_c^2 T^4}{128}(3 \pm y)^3(1 \mp y), \tag{4.68}$$

which can be rewritten in terms of μ/T using (4.46)

$$\frac{p}{N_c^2 T^4} = \frac{\pi^2}{128}\left(3 \pm \sqrt{1 - \left(\frac{\mu/T}{\pi/\sqrt{2}}\right)^2}\right)^3 \left(1 \mp \sqrt{1 - \left(\frac{\mu/T}{\pi/\sqrt{2}}\right)^2}\right). \tag{4.69}$$

Using (4.34), (4.57) and (4.69), we can calculate the internal energy density $\varepsilon = Ts - p + \mu\rho$,

$$\varepsilon = \frac{3}{128}\pi^2 N_c^2 T^4 (3 \pm y)^3 (y \mp 1), \tag{4.70}$$

again rewriting in terms of μ/T using (4.46), we have

$$\frac{\varepsilon}{N_c^2 T^4} = \frac{3\pi^2}{128}\left(3 \pm \sqrt{1 - \left(\frac{\mu/T}{\pi/\sqrt{2}}\right)^2}\right)^3 \left(1 \mp \sqrt{1 - \left(\frac{\mu/T}{\pi/\sqrt{2}}\right)^2}\right). \tag{4.71}$$

As $\varepsilon - 3p$ is the trace of the 4D boundary QFT energy-momentum tensor, which is non-zero in general, but vanishes for conformal theories, we verify that $\varepsilon - 3p = 0$, which was expected since the 1RCBH is a conformal model [53].

The specific heat at fixed chemical potential and constant volume is given by

$$C_\mu = \frac{1}{V}\left(\frac{\partial Q}{\partial T}\right)_{\mu,V} = T\left(\frac{\partial s}{\partial T}\right)_\mu = T\left[\left(\frac{\partial s}{\partial T}\right)_y + \left(\frac{\partial s}{\partial y}\right)_T \frac{\mathrm{d}y}{\mathrm{d}(\mu/T)}\left(\frac{\partial(\mu/T)}{\partial T}\right)_\mu\right] \tag{4.72}$$

and substituting the expressions and performing the same mathematical manipulations done previously and applying (4.46), we have that

$$\frac{C_\mu}{N_c^2 T^3} = \frac{\pi^2}{16}\left[\frac{\left(3 \pm \sqrt{\left(\frac{\mu/T}{\pi/\sqrt{2}}\right)^2}\right)\left(1 \mp \sqrt{\left(\frac{\mu/T}{\pi/\sqrt{2}}\right)^2}\right)\left(1 \mp 5\sqrt{\left(\frac{\mu/T}{\pi/\sqrt{2}}\right)^2}\right)}{\left(\sqrt{\left(\frac{\mu/T}{\pi/\sqrt{2}}\right)^2}\right)}\right]. \quad (4.73)$$

Whereas the R-charge susceptibility of order $n+1$ is given by

$$\chi_{n+1} = \left(\frac{\partial^n \rho}{\partial \mu^n}\right)_T = \left(\frac{\partial \chi_n}{\partial \mu}\right)_T \quad (4.74)$$

where we calculate up to $n = 7$, and $\chi_1 = \rho$, as presented below. For χ_2 we have

$$\chi_2 = \left(\frac{\partial \rho}{\partial \mu}\right)_T = \left(\frac{\partial \rho}{\partial(\mu/T)}\right)_{T,y}\left(\frac{\partial(\mu/T)}{\partial \mu}\right)_T + \left(\frac{\partial \rho}{\partial y}\right)_{T,(\mu/T)} \frac{\mathrm{d}y}{\mathrm{d}(\mu/T)}\left(\frac{\partial(\mu/T)}{\partial \mu}\right)_T, \quad (4.75)$$

where after performing the calculations we have

$$\chi_2 = \frac{N_c^2 T^2}{16}(3 \pm y)\left(3(1 \pm y) \mp \frac{2}{y}\right), \quad (4.76)$$

and applying (4.46), we have that

$$\chi_2 = \frac{N_c^2 T^2}{16}\left(3 \pm \sqrt{1 - \left(\frac{\mu/T}{\pi/\sqrt{2}}\right)^2}\right)\left(3\left(1 \pm \sqrt{1 - \left(\frac{\mu/T}{\pi/\sqrt{2}}\right)^2}\right) \mp \frac{2}{\sqrt{1 - \left(\frac{\mu/T}{\pi/\sqrt{2}}\right)^2}}\right). \quad (4.77)$$

Since we obtain (4.77) as a function of μ/T we have that $\partial/\partial\mu = T^{-1}\partial/\partial(\mu/T)$ and that under successive application of this operator all other orders of susceptibilities below are obtained.

We then have that χ_3 will be given by

$$\chi_3 = \frac{3{N_c}^2 T}{4\pi\sqrt{2}}\sqrt{1 - y^2}\left(\mp\frac{1}{y^3} \mp \frac{2}{y} - 1\right), \quad (4.78)$$

again applying (4.46), we have that

$$\chi_3 = \frac{3{N_c}^2 T}{4\pi\sqrt{2}}\sqrt{1-\left(\sqrt{1-\left(\frac{\mu/T}{\pi/\sqrt{2}}\right)^2}\right)^2}\left(\mp\frac{1}{\left(\sqrt{1-\left(\frac{\mu/T}{\pi/\sqrt{2}}\right)^2}\right)^3}\mp\frac{2}{\left(\sqrt{1-\left(\frac{\mu/T}{\pi/\sqrt{2}}\right)^2}\right)}-1\right). \tag{4.79}$$

We have that χ_4 is given by

$$\chi_4 = \frac{3{N_c}^2}{4\pi^2}\left(-1\mp\frac{3}{y^5}\right), \tag{4.80}$$

and applying (4.46), we have

$$\chi_4 = \frac{3{N_c}^2}{4\pi^2}\left(-1\mp\frac{3}{\left(\sqrt{1-\left(\frac{\mu/T}{\pi/\sqrt{2}}\right)^2}\right)^5}\right). \tag{4.81}$$

Similarly, χ_5, which results

$$\chi_5 = \mp\frac{45{N_c}^2}{2\sqrt{2}\pi^3 T}\frac{\sqrt{1-y^2}}{y^7}, \tag{4.82}$$

where applying (4.46), we have

$$\chi_5 = \mp\frac{45{N_c}^2}{2\sqrt{2}\pi^3 T}\frac{\sqrt{1-\left(\sqrt{1-\left(\frac{\mu/T}{\pi/\sqrt{2}}\right)^2}\right)^2}}{\left(\sqrt{1-\left(\frac{\mu/T}{\pi/\sqrt{2}}\right)^2}\right)^7}. \tag{4.83}$$

In the same way, χ_6, resulting

$$\chi_6 = \mp\frac{45{N_c}^2}{2\pi^4 T^2}\left(\frac{7}{y^9}-\frac{6}{y^7}\right), \tag{4.84}$$

applying (4.46), we have that

$$\chi_6 = \mp\frac{45{N_c}^2}{2\pi^4 T^2}\left(\frac{7}{\left(\sqrt{1-\left(\frac{\mu/T}{\pi/\sqrt{2}}\right)^2}\right)^9}-\frac{6}{\left(\sqrt{1-\left(\frac{\mu/T}{\pi/\sqrt{2}}\right)^2}\right)^7}\right), \tag{4.85}$$

And finally, we have $\chi 7$ given by

$$\chi_7 = \mp \frac{945 {N_c}^2}{\sqrt{2}\pi^5 T^3} \left(\frac{\sqrt{1-y^2}\,(-3+2y^2)}{y^{11}} \right) \tag{4.86}$$

and applying (4.46), we have that

$$\chi_7 = \mp \frac{945 {N_c}^2}{\sqrt{2}\pi^5 T^3} \left(\frac{\sqrt{1-\left(\sqrt{1-\left(\frac{\mu/T}{\pi/\sqrt{2}}\right)^2}\right)^2}\left[-3+2\left(\sqrt{1-\left(\frac{\mu/T}{\pi/\sqrt{2}}\right)^2}\right)^2\right]}{\left(\sqrt{1-\left(\frac{\mu/T}{\pi/\sqrt{2}}\right)^2}\right)^{11}} \right). \tag{4.87}$$

As we approach the critical point, we observe, for example, that the free energy density that corresponds to minus the pressure of our system becomes non-analytic, which means that we cannot express this quantity by means of a convergent power series. During a phase transition, this non-analyticity arises due to either a discontinuity or a divergence in the derivatives of the free energy.

If this discontinuity is present in a first derivative, this transition is called a first-order phase transition. On the other hand, if the divergence is in the second derivative or in another higher-order derivative, we have a second-order phase transition. It is worth noting that the specific heat and the susceptibilities all diverge at the critical point of this model, which is therefore a point of second-order phase transition, since the specific heat and the susceptibilities are second-order or higher derivatives of the pressure, in the case of χ_3, χ_4 onwards.

The phase diagram of the 1RCBH model is a line segment that extends from the initial point when $\mu/T = 0$ to the final point at $\pi/\sqrt{2}$, where it ends abruptly. At this final point, the second derivative of the pressure with respect to the chemical potential, which gives us the susceptibility, and the second derivative of the pressure with respect to the temperature, diverge, as shown in fig. 4.2 and fig. 4.3, indicating a second-order phase transition. However, in this model, there is no genuine phase transition, as the phase diagram ends when the critical point is reached and therefore the critical point does not separate two distinct stable phases [110].

When $\mu = 0$, we have the purely thermal SYM theory if we are in the stable branch; if we are in the unstable branch, we have the superstar solution [121], as already mentioned in Sec. 4.2.2. When we consider a finite chemical potential, we obtain different solutions of charged black holes that go up to the critical

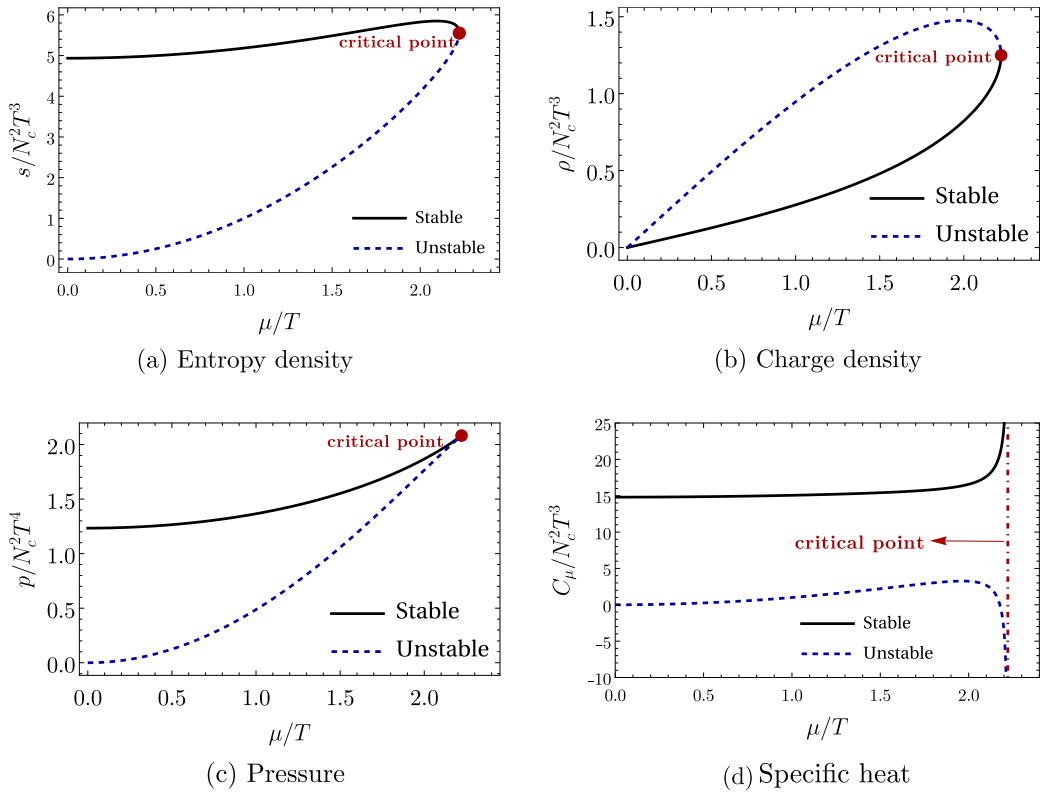

(a) Entropy density (b) Charge density

(c) Pressure (d) Specific heat

FIGURE 4.2: Distribution of thermodynamic quantities for the 1RCBH model.

point [110].

Global thermodynamic stability requires that in a region of the phase diagram with competing solutions (as occurs in this model for all values of μ/T) the globally stable phase is the one that minimizes the free energy, or correspondingly, maximizes the pressure of the system. Local thermodynamic stability with respect to thermal fluctuations corresponds to requiring the positivity of the Jacobian of the susceptibility matrix. In other words, if the Jacobian is negative we know that we have a thermodynamically unstable phase. It is worth noting that in general the Jacobian does not allow us to decide which phase is stable or metastable, since in both cases the Jacobian is positive. In the particular case of the 1RCBH, since there are only two branches of competing solutions, and also, one of these branches has a positive Jacobian and the other negative for each value of μ/T, the Jacobian test can directly distinguish which branch is stable and which is unstable [123]

$$\mathcal{J} = \frac{\partial(s,\rho)}{\partial(T,\mu)} = \begin{pmatrix} \frac{\partial s}{\partial T} & \frac{\partial s}{\partial \mu} \\ \frac{\partial \rho}{\partial T} & \frac{\partial \rho}{\partial \mu} \end{pmatrix}. \tag{4.88}$$

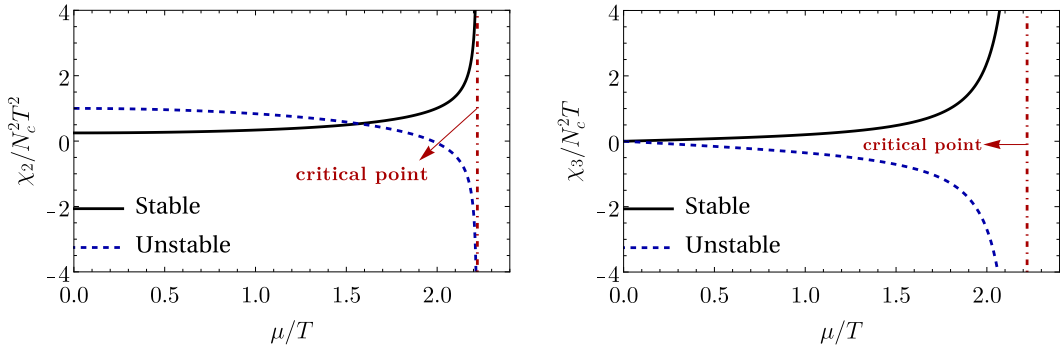

(a) 2nd-order susceptibility

(b) 3rd-order susceptibility

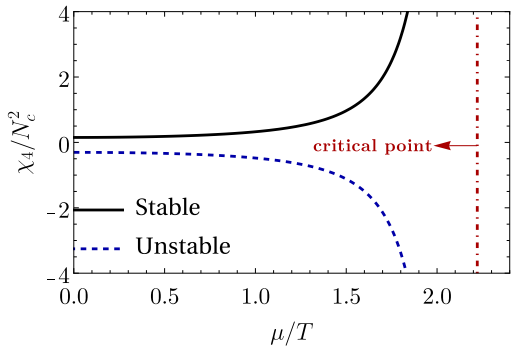

(c) 4th-order susceptibility

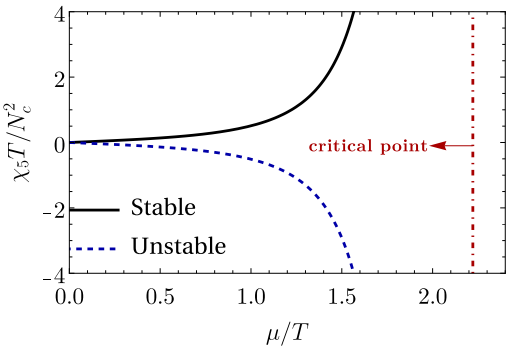

(d) 5th-order susceptibility

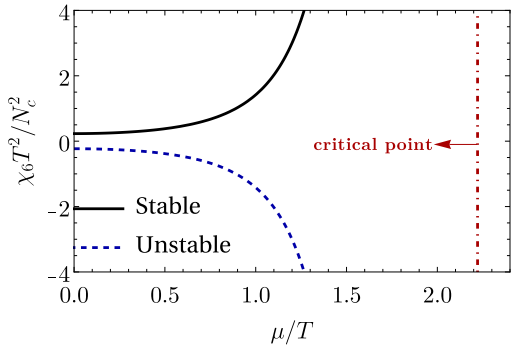

(e) 6th-order susceptibility

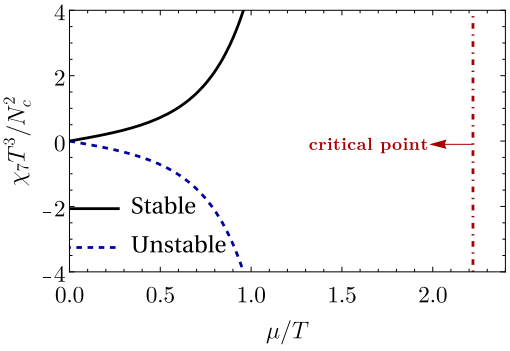

(f) 7th-order susceptibility

FIGURE 4.3: Susceptibilities of order n for the 1RCBH model.

Its expression for the 1RCBH model is given by

$$\mathcal{J} = \frac{3N_c^4\pi^2T^4}{256}(3-y)^4\left(1+\frac{1}{y}\right), \tag{4.89}$$

where the term that is raised to the fourth power is always positive, while the expression that is in parentheses will be negative for $y \in (-1,0)$, corroborating with the previous division of the stable and unstable branches. Applying (4.46), we have that

$$\frac{\mathcal{J}}{N_c^4T^4} = \frac{3\pi^2}{256}\left[3 \mp \left(\sqrt{1-\left(\frac{\mu/T}{\pi/\sqrt{2}}\right)^2}\right)\right]^4\left(1 \mp \frac{1}{\left(\sqrt{1-\left(\frac{\mu/T}{\pi/\sqrt{2}}\right)^2}\right)}\right). \tag{4.90}$$

4.3 Aspects of Holographic Entanglement Entropy for the 1RCBH Model

In this section, we review the calculation of Holographic Entanglement Entropy (HEE) in the 1RCBH model [114] (see also [117]). Although the calculation of entanglement entropy from the holographic point of view and the Wilson loop are obtained in a similar way in gauge/gravity duality, their physical interpretations are distinct. The Wilson loop depends on the position of the particles. For example, a probe quark-antiquark pair in the dual theory on the gravitational side represents the movement of an open string, whose ends is described by an open string sagging into the bulk, with its ends attached to the boundary representing the probe particles. Holographic entanglement entropy S_A, on the other hand, depends on the choice of the subsystem in the gauge theory, and on the gravitational theory side, the holographic entanglement entropy will depend on the spacetime properties of the bulk [124].

4.3.1 Poincare Coordinates

It is convenient for the following discussion to work in the so-called Poincare coordinates, where the new holographic radial coordinate is defined as $u = 1/r$ and, therefore, the bulk fields in (4.11) now read as follows

$$ds^2 = \mathrm{e}^{2A(u)}\left(-h(u)dt^2 + d\vec{x}^2\right) + \frac{\mathrm{e}^{2B(u)}}{h(u)}\frac{1}{u^4}du^2, \quad \phi = \phi(u), \quad A^\mu = \Phi(u)\delta^\mu_0, \tag{4.91}$$

where the boundary $r \to \infty$ is at $u = 0$ in terms of the new holographic coordinate u [114], [117].

Substituting (4.2) (which specify the 1RCBH model within the class of EMD models) and (4.91) (which specify that the system is in equilibrium in the new coordinate system) into the general EMD field equations (4.8), (4.9), and (4.10), we obtain a set of coupled ODEs for the bulk fields, whose solutions are of the form specified below [115] [7],

$$A(u) = \ln\left(\frac{1}{u}\right) + \frac{1}{6}\ln\left(1 + Q^2u^2\right), \tag{4.92}$$

$$B(u) = -\ln\left(\frac{1}{u}\right) - \frac{1}{3}\ln\left(1 + Q^2u^2\right), \tag{4.93}$$

$$h(u) = 1 - \frac{M^2u^4}{1 + Q^2u^2}, \tag{4.94}$$

$$\phi(u) = -\sqrt{\frac{2}{3}}\ln\left(1 + Q^2u^2\right), \tag{4.95}$$

$$\Phi(u) = \frac{MQu_H^2}{(1 + Q^2u_H^2)} - \frac{MQu^2}{(1 + Q^2u^2)}. \tag{4.96}$$

In the solutions given by (4.92) to (4.96), we have that u_H is the radial location of the event horizon of the black hole solution, which is obtained by the condition that the g_{tt} component of the metric vanishes, which corresponds to the vanishing of the blackening function at $u = u_H$, so that

$$\left(1 - \frac{M^2u_H^4}{1 + Q^2u_H^2}\right) = 0. \tag{4.97}$$

Since the above expression is a quartic equation for u_H, it therefore has four roots. Since the holographic radial coordinate u is real and non-negative, we take from among these four roots the one that corresponds to a real and non-negative value for the radial location of the event horizon, which is given by [114], [115],

$$u_H = \sqrt{\frac{Q^2 + \sqrt{Q^4 + 4M^2}}{2M^2}}. \tag{4.98}$$

We can use (4.98) to express M as a function of u_H and Q, and as an alternative to the description of black hole backgrounds in terms of (M, Q), we can describe

[7] Again, as in Sec. 4.1, the solutions presented were explicitly verified by direct substitution into the ODEs, thus showing that these functions do, in fact, solve the field equations.

them in terms of (u_H, Q), resulting in

$$M = \frac{\sqrt{Q^2 u_H^2 + 1}}{u_H^2}. \tag{4.99}$$

4.3.2 Holographic Entanglement Entropy

In this subsection, we review in more detail the original results presented in Section 3 of [114], which were also subsequently reviewed in Section 3 of [117]. Starting from the expression given in (3.25) to calculate the HEE, we need to obtain the hyperarea of the minimal hypersurface in the bulk with the boundary given by $\partial\gamma_A = \partial A$ (see Fig. 4.4), using the background geometry discussed in section 4.3.1.

We consider here a subsystem $A \in \mathbb{R}^3$ corresponding to a slab (parallelepiped) geometry defined as,

$$X^1 \equiv x^1 \equiv x(u) \in \left[-\frac{l}{2}, \frac{l}{2}\right], \qquad X^i = x^i \in \left[-\frac{R}{2}, \frac{R}{2}\right], \; i = 2, 3, \tag{4.100}$$

where $x^\mu = X^\mu(\sigma^1, \sigma^2, \sigma^3)$ is the parametric equation of the hypersurface γ_A illustrated in Fig. 4.4. Considering that R is sufficiently large, so that $\frac{R}{l} \gg 1$, we can then state that the surface given by γ_A will be invariant under translations in the x^i coordinates [114], [117], [125].

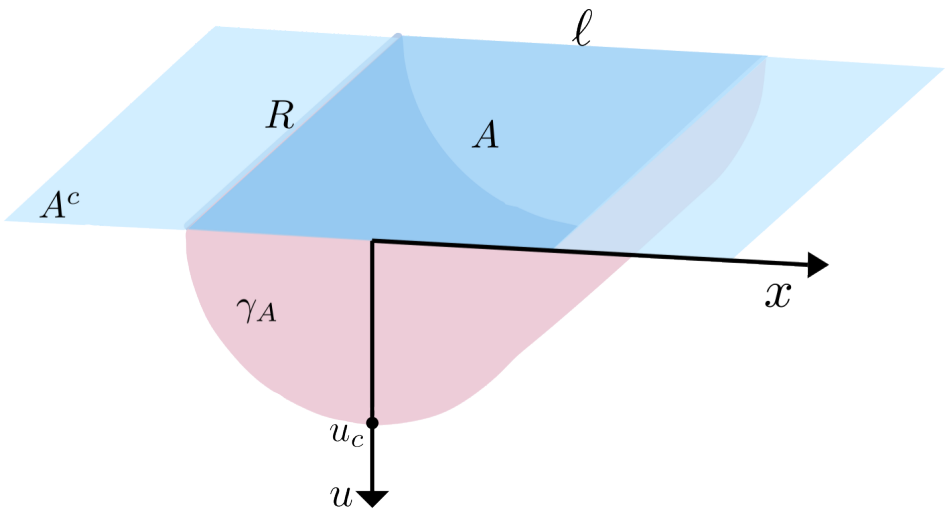

FIGURE 4.4: A simplified cartoon of region A with characteristic length l, where A^c is the complement of the spatial region $A \in \mathbb{R}^3$, and u_c is the turning point of γ_A in the bulk. The minimal surface γ_A is shown extending into the bulk. The figure omits an additional dimension of size R which cannot be visually represented.

By following [124], we choose to parametrize the hypersurface γ_A by taking the parameters $\sigma^1 = u$, $\sigma^2 = x^2 = y$, $\sigma^3 = x^3 = z$, so that the hyperarea of the hypersurface γ_A in an arbitrary curved background geometry is given by,

$$A(\gamma_A) = \int_{\gamma_A} d^3\sigma \sqrt{\det(\gamma_{ab})} = \int_{\gamma_A} d\sigma^1 d\sigma^2 d\sigma^3 \sqrt{\det(\gamma_{ab})}; \quad \gamma_{ab} := g_{\mu\nu}\partial_a X^\mu \partial_b X^\nu, \tag{4.101}$$

where γ_{ab} is the induced metric (or pullback) on γ_A, the indices $a, b \in \{\sigma^1 = u, \sigma^2 = y, \sigma^3 = z\}$, and the HEE will be calculated over a constant time slice.

Using (4.91), we obtain for the induced metric,

$$\gamma_{yy} = g_{yy}\partial_y X^y \partial_y X^y = \mathrm{e}^{2A(u)}, \quad \gamma_{zz} = g_{zz}\partial_z X^z \partial_z X^z = \mathrm{e}^{2A(u)}, \tag{4.102}$$

where $\partial_y X^y = \partial_z X^z = 1$, i.e., $\gamma_{yy} = \gamma_{zz}$, and,

$$\gamma_{uu} = g_{xx}\partial_u X^x \partial_u X^x + g_{uu}\partial_u X^u \partial_u X^u = \mathrm{e}^{2A(u)} \left(x'(u)\right)^2 + \frac{\mathrm{e}^{2B(u)}}{u^4 h(u)}, \tag{4.103}$$

where $\partial_u X^x = x'(u)$, $\partial_u X^u = 1$, and all the non-diagonal components of the induced metric γ_{ab} vanish.

With γ_{ab} at hand, we can calculate its determinant,

$$\begin{aligned} \det(\gamma_{ab}) &= \gamma_{uu}\gamma_{yy}\gamma_{zz} + \text{cross terms} \\ &= \left(\mathrm{e}^{2A(u)} \left(x'(u)\right)^2 + \frac{\mathrm{e}^{2B(u)}}{u^4 h(u)}\right) \mathrm{e}^{2A(u)}\mathrm{e}^{2A(u)} + 0 \\ &= \mathrm{e}^{6A(u)} \left(\left(x'(u)\right)^2 + \frac{\mathrm{e}^{2B(u)-2A(u)}}{u^4 h(u)}\right). \end{aligned} \tag{4.104}$$

Calculating the square root of the expression obtained by (4.104), we have that

$$\sqrt{\det(\gamma_{ab})} = \mathrm{e}^{3A(u)} \sqrt{\left(\left(x'(u)\right)^2 + \frac{\mathrm{e}^{2B(u)-2A(u)}}{u^4 h(u)}\right)}, \tag{4.105}$$

which, substituting into (4.101), gives us the expression for the area of the surface γ_A [114], [117]

$$\begin{aligned} A(\gamma_A) &= \int_{\gamma_A} d\sigma^1 d\sigma^2 d\sigma^3 \sqrt{\det(\gamma_{ab})} \\ &= 2\int_0^{u_c} du \int_{-R/2}^{R/2} dy \int_{-R/2}^{R/2} dz\ \mathrm{e}^{3A(u)} \sqrt{(x'(u))^2 + \frac{\mathrm{e}^{2B(u)-2A(u)}}{u^4 h(u)}} \\ &= 2R^2 \int_0^{u_c} du\ \underbrace{\mathrm{e}^{3A(u)} \sqrt{(x'(u))^2 + \frac{\mathrm{e}^{2B(u)-2A(u)}}{u^4 h(u)}}}_{\equiv \mathcal{L}(x(u),x'(u),u)}, \end{aligned} \tag{4.106}$$

where the factor of 2 comes from the u-integration with respect to the symmetric configuration of the U-shaped profile for γ_A depicted in Fig. 4.4, with u_c being the turning point of the hypersurface γ_A. The area functional (4.106) is extremized by solving the Euler-Lagrange equation for $\mathcal{L}$,

$$\frac{\partial \mathcal{L}}{\partial x(u)} - \partial_u \frac{\partial \mathcal{L}}{\partial (x'(u))} = 0. \tag{4.107}$$

Since the integrand $\mathcal{L}$ of the area functional (4.106) does not explicitly depend on $x(u)$, we have from (4.107) the following radial constant,

$$\text{constant} = \frac{\partial \mathcal{L}}{\partial (x'(u))} = \frac{e^{3A(u)} x'(u)}{\sqrt{(x'(u))^2 + \frac{e^{2B(u)-2A(u)}}{u^4 h(u)}}} = \frac{e^{3A(u)}}{\sqrt{1 + \frac{e^{2B(u)-2A(u)}}{(x'(u))^2\, u^4 h(u)}}}. \tag{4.108}$$

Since (4.108) is a radial constant, we can choose to evaluate it at any convenient value of the radial coordinate u. Notice from Fig. 4.4 that at the turning point of γ_A, one has, $0 = u'(x=0) = (du/dx)_{x=0} = 1/(dx/du)_{u=u_c} = 1/x'(u=u_c)$, so that by evaluating (4.108) at $u = u_c$, one obtains,

$$\text{constant} = e^{3A(u_c)}. \tag{4.109}$$

By substituting (4.109) into (4.108) and then solving for $x'(u)$, one gets,

$$x'(u) = \frac{dx}{du} = \pm \frac{\mathrm{e}^{3A(u_c)} \mathrm{e}^{B(u)-A(u)}}{u^2 \sqrt{h(u)} \sqrt{\mathrm{e}^{6A(u)} - \mathrm{e}^{6A(u_c)}}}. \tag{4.110}$$

By noticing from Fig. 4.4 that by increasing x from 0 to $l/2$, u decreases from u_c to 0, one concludes that the derivative $x'(u)$ must be negative, so that one

must choose the minus sign in (4.110),

$$x'(u) = \frac{dx}{du} = -\frac{\mathrm{e}^{3A(u_c)}\mathrm{e}^{B(u)-A(u)}}{u^2\sqrt{h(u)}\sqrt{\mathrm{e}^{6A(u)}-\mathrm{e}^{6A(u_c)}}}, \tag{4.111}$$

which, akin to [126], actually has the opposite sign from what is written in [114], [117]. Indeed, by closely following the approach in [126], it follows from (4.111) that,

$$dx = -\frac{\mathrm{e}^{3A(u_c)}\mathrm{e}^{B(u)-A(u)}}{u^2\sqrt{h(u)}\sqrt{\mathrm{e}^{6A(u)}-\mathrm{e}^{6A(u_c)}}}\, du. \tag{4.112}$$

Integrating both sides of (4.112), we have,

$$\begin{aligned} x(u) = \int_{x(u_c)=0}^{x(u)} d\tilde{x} &= -\int_{u_c}^{u} d\tilde{u}\, \frac{\mathrm{e}^{3A(u_c)}\mathrm{e}^{B(\tilde{u})-A(\tilde{u})}}{\tilde{u}^2\sqrt{h(\tilde{u})}\sqrt{\mathrm{e}^{6A(\tilde{u})}-\mathrm{e}^{6A(u_c)}}} \\ &= +\int_{u}^{u_c} d\tilde{u}\, \frac{\mathrm{e}^{3A(u_c)}\mathrm{e}^{B(\tilde{u})-A(\tilde{u})}}{\tilde{u}^2\sqrt{h(\tilde{u})}\sqrt{\mathrm{e}^{6A(\tilde{u})}-\mathrm{e}^{6A(u_c)}}}. \end{aligned} \tag{4.113}$$

For $u = 0$, we have that $x(u = 0) = l/2$, therefore [114], [117],

$$\frac{l}{2} = \int_0^{u_c} du \frac{\mathrm{e}^{3A(u_c)}\mathrm{e}^{B(u)-A(u)}}{u^2\sqrt{h(u)}\sqrt{\mathrm{e}^{6A(u)}-\mathrm{e}^{6A(u_c)}}}. \tag{4.114}$$

Finally, we can substitute (4.111) into (4.106), so that

$$A(\gamma_A) = 2R^2 \int_0^{u_c} du\ \mathrm{e}^{3A(u)} \sqrt{\left(\frac{\mathrm{e}^{3A(u_c)}\mathrm{e}^{B(u)-A(u)}}{u^2\sqrt{h(u)}\sqrt{\mathrm{e}^{6A(u)}-\mathrm{e}^{6A(u_c)}}}\right)^2 + \frac{\mathrm{e}^{2B(u)-2A(u)}}{u^4 h(u)}}. \tag{4.115}$$

After simplifying, we have that [117]

$$A(\gamma_A) = 2R^2 \int_0^{u_c} du\ \frac{\mathrm{e}^{B(u)+2A(u)}}{u^2\sqrt{h(u)}} \sqrt{\frac{\mathrm{e}^{6A(u)}}{\mathrm{e}^{6A(u)}-\mathrm{e}^{6A(u_c)}}}, \tag{4.116}$$

where the above expression, corresponding to the hyperarea integral of the hypersurface γ_A, is ultraviolet divergent, that is, on the gravity side of the holographic duality this divergence is associated with the lower limit $u \to 0$ of (4.116), corresponding to the near-boundary part of the bulk geometry. Since ultraviolet (UV) divergences are independent of temperature [127], [128], they are the same in vacuum and at finite temperature (and chemical potential). In [114], [117], it was explicitly identified that the UV divergence of (4.116) in

the 1RCBH model takes the form R^2/ϵ^2, [8] where $u = \epsilon$ corresponds to a small finite UV cutoff near the boundary employed to regularize the integral (4.116). As expected from general properties of divergences in QFTs, this is, in fact, the very same UV divergence found in vacuum for the area functional of the hypersurface γ_A with the slab entanglement geometry illustrated in Fig. 4.4 in the case of the SYM theory at zero temperature and vanishing chemical potential — see e.g. [126].

Therefore, once the form of the UV divergence is known, we can subtract it from the regularized hyperarea integral of the hypersurface γ_A in order to *define* a finite difference as follows,[9]

$$\frac{\Delta\tilde{A}(\epsilon)}{R^2} \equiv \frac{A(\gamma_A;\epsilon)}{R^2} - \frac{1}{\epsilon^2} = \int_\epsilon^{u_c} du\; 2\,\frac{\mathrm{e}^{B(u)+2A(u)}}{u^2\sqrt{h(u)}}\sqrt{\frac{\mathrm{e}^{6A(u)}}{\mathrm{e}^{6A(u)}-\mathrm{e}^{6A(u_c)}}} - \frac{1}{\epsilon^2}. \quad (4.117)$$

Although formally finite, as we shall discuss in the next subsection, Eq. (4.117) is inconvenient for numerical calculations, since it comprises the subtraction of two large numbers, which is generally problematic to handle in numerical calculations with finite precision. In order to circumvent this numerical issue, we "des-integrate" the form of the subtracted UV divergence in (4.117), so that the delicate subtraction can be done inside the definite integral, what can be done by noticing that,

$$-\frac{1}{\epsilon^2} = \int_\epsilon^{u_c}\left(-\frac{2}{u^3}\right)du - \frac{1}{u_c^2}. \quad (4.118)$$

Substituting (4.118) into (4.117), we have

$$\frac{\Delta A(\epsilon)}{R^2} = \int_\epsilon^{u_c} du\;\left(2\,\frac{\mathrm{e}^{B(u)+2A(u)}}{u^2\sqrt{h(u)}}\sqrt{\frac{\mathrm{e}^{6A(u)}}{\mathrm{e}^{6A(u)}-\mathrm{e}^{6A(u_c)}}} - \frac{2}{u^3}\right) - \frac{1}{u_c^2}, \quad (4.119)$$

$$\Delta A \equiv \Delta A(\epsilon = 0), \quad (4.120)$$

where $\Delta\tilde{A}(\epsilon)$ in (4.117) and $\Delta A(\epsilon)$ in (4.119) are formally the same, but we denote them with different symbols in order to illustrate in the next subsection that Eq. (4.119) is numerically more well-behaved than Eq. (4.117). In fact, as

[8] Remember that we have set here the asymptotic AdS radius L to unity. We also remark that our notation differs from the one used in [114], [117], where they denoted the two large sizes of the slab geometry at the boundary by L (while we denote it by R), and the asymptotic AdS radius was denoted by R (while we denote it by L).

[9] This is finite as long as one does not consider the limit where the turning point u_c of the hypersurface γ_A approaches the boundary.

we shall see, we can safely remove the UV cutoff by setting $\epsilon = 0$ in (4.119), obtaining a finite and cutoff-independent expression ΔA, as defined in (4.120), while by progressively lowering the value of ϵ in (4.117) leads to a spurious numerical divergence for sufficiently small values of the UV cutoff.

Notice from Eqs. (4.117) and (4.119) that for $u_c \to \epsilon$, the considered integrals formally vanish and the hyperarea difference diverges with negative values. Therefore, the hyperarea difference ΔA is not positive-definite and cannot be geometrically interpreted as a hyperarea, corresponding instead to a difference between two divergent hyperareas. Consequently, by using the finite difference ΔA in Eq. (3.25), instead of the divergent extremal hypearea $A(\gamma_A)$, one obtains a quantity which, although finite, is not positive-definite. Therefore, in our opinion, one cannot physically interpret the corresponding result as the entanglement entropy of subregion A in Fig 4.4 (which is originally also a positive-definite and divergent quantity for a continuous QFT), and should instead interpret it as an entanglement entropy difference. This point has been overlooked in some previous works published in the literature.

We remark that in [114], [117], instead of evaluating the integrals numerically, it was employed a very laborious method which consists in expanding the integrand of (4.116) into several summations, eventually arriving at the following expression for the finite hyperarea difference,

$$\begin{aligned}
\frac{\Delta\mathcal{A}}{R^2} &= \frac{1}{u_c^2}\left\{\frac{3\xi}{2}\left(\frac{u_c}{u_H}\right)^2 - \left[1+\xi\left(\frac{u_c}{u_H}\right)^2\right]^{\frac{3}{2}} + \frac{1+\xi}{3\xi}\left(\frac{u_c}{u_H}\right)^2\left[\left(1+\xi\left(\frac{u_c}{u_H}\right)^2\right)^{\frac{3}{2}} - 1\right]\right\} \\
&+ \frac{1}{u_c^2}\left\{\sum_{k=2}^{\infty}\sum_{n=0}^{k}\sum_{m=0}^{\infty}\Lambda_{knm}\frac{\Gamma\left(m+\frac{1}{2}\right)\Gamma(k+n-1)}{\Gamma(k+n+m+1)}\left(\frac{u_c}{u_H}\right)^{2(k+n+m)}\right. \\
&\times\left.\left[(m+1)+(k+n-1)\left(1+\xi\left(\frac{u_c}{u_H}\right)^2\right)\right]\right\} \\
&+ \frac{1}{u_c^2}\left\{\sum_{k=0}^{\infty}\sum_{n=0}^{k}\sum_{m=0}^{\infty}\sum_{j=1}^{\infty}\Lambda_{knm}\frac{\Gamma\left(m+j+\frac{1}{2}\right)\Gamma(k+n+3j-1)}{\Gamma(j+1)\Gamma(k+n+m+3j+1)}\left(\frac{u_c}{u_H}\right)^{2(k+n+m)}\right. \\
&\times\left.\left[(m+1)+(k+n+3j-1)\left(1+\xi\left(\frac{u_c}{u_H}\right)^2\right)\right]\right\},
\end{aligned} \tag{4.121}$$

where $\xi \equiv Q^2 u_H^2$ and Λ_{knm} is given by,

$$\Lambda_{knm} \equiv \frac{(-1)^{k+n}\Gamma\left(k+\frac{1}{2}\right)}{\pi\Gamma(n+1)\Gamma(k-n+1)}\xi^{k-n+m}(1+\xi)^n\left[1+\xi\left(\frac{u_c}{u_H}\right)^2\right]^{-m-\frac{1}{2}}. \tag{4.122}$$

The approach we have chosen to implement is much faster and efficient than

using the above summations, and consists in numerically integrating (4.120) without performing any expansion of its integrand. In the next subsection, we are going to present some preliminary results for the numerical evaluation of the integral for the finite difference $\Delta A/R^2$ and compare it with the outcome obtained through the above formula for $\Delta\mathcal{A}/R^2$ in terms of summations. This will be more systematically approached in an upcoming work intended for publication, where we shall also numerically interpolate the dimensionless combination $\Delta A/LR^2$ as a function of μ/T and l/L,[10] providing explicit 3D and 2D plots to illustrate and discuss the physical behavior of the entanglement entropy difference for the 1RCBH model, a fundamental point which is simply missing in the previous works [114], [117].

4.3.3 Preliminary Results

Below we present some preliminary results concerning the numerical evaluation of Eq. (4.117) for $\Delta\tilde{A}(\epsilon)/R^2$ and Eq. (4.119) for $\Delta A(\epsilon)/R^2$, which are written in terms of the small UV cutoff ϵ, and compare them with the results obtained from Eq. (4.120) for $\Delta A/R^2$, which is independent of the UV cutoff, and from Eq. (4.121) for $\Delta\mathcal{A}/R^2$, which is also independent of the UV cutoff but depends on the order of the truncations done in the summations. All these area differences should give formally the same results, but in numerical calculations this will not be necessarily true due to the finite precision of the computations, and also due to the fact that the truncations for the summations in Eq. (4.121) for $\Delta\mathcal{A}/R^2$ will only provide an approximate expression for the area difference.

We have as control parameters in the gravity side of the holographic duality the pair of variables $(Q, u_H = 1/r_H)$, corresponding to the charge and the radial position of the black hole background solution, besides the turning point u_c of the extremal hypersurface γ_A. As discussed before, the pair (Q, u_H) controls the value of the dimensionless ratio μ/T in the dual 1RCBH plasma living at the boundary, while the turning point $u_c \in (\epsilon, u_H)$ controls the size of the characteristic length l of the slab entanglement geometry A in Fig. 4.4, through Eq. (4.114). Notice from Fig. 4.1(a) that $Qu_H \in [0, \sqrt{2}]$ in the thermodynamically stable branch of black hole solutions, while $Qu_H \in [\sqrt{2}, \infty)$ in the thermodynamically unstable branch of black holes.

[10] We will simply keep setting $L = 1$, but formally restore L in the labels of the plots to make it explicit that we are plotting dimensionless combinations, as appropriate for a CFT.

ϵ	$\Delta\tilde{A}(\epsilon)/R^2$	$\Delta A(\epsilon)/R^2$	$\Delta A/R^2$
10^{-2}	-128.068	-126.068	-126.679
10^{-3}	-126.691	-126.691	-126.679
10^{-4}	-142.337	-126.679	-126.679
10^{-5}	-142.351	-126.679	-126.679
10^{-6}	-142.353	-126.679	-126.679
10^{-7}	-142.344	-126.679	-126.679
10^{-8}	-152	-126.679	-126.679
10^{-9}	-6.50593×10^8	-126.679	-126.679

TABLE 4.1: Test case #1 with $(Q = 1, u_H = 0.08, u_c = 0.05)$.

Upper limit	$\Delta\mathcal{A}/R^2$
20	-162.90428323618872
90	-143.88841956721814
120	-141.59105516915363

TABLE 4.2: Test case #1 with $(Q = 1, u_H = 0.08, u_c = 0.05)$. The first column refers to the different values used as common upper limits for the summations in Eq. (4.121).

As a first test case, we chose $Q = 1$, $u_H = 0.08$ (so that we are in the stable branch of black holes), and $u_c = 0.05$. Then, we varied the value of the UV cutoff ϵ to analyze the numerical convergence of the expressions for $\Delta\tilde{A}(\epsilon)/R^2$ and $\Delta A(\epsilon)/R^2$, which depend on the cutoff. The results are shown in Table 4.1, where we also display the result obtained for the cutoff-independent ratio $\Delta A/R^2$ (where $\Delta A \equiv \Delta A(\epsilon = 0)$). On the other hand, in Table 4.2 we show the results for the calculation of $\Delta\mathcal{A}/R^2$ using different truncations (taking a common upper limit) for the summations in Eq. (4.121). One notices the following salient features in such a comparison:

- The regularization and subtraction schemes discussed in the previous subsection appear to be consistent. In fact, the divergent hyperarea in Eq. (4.116) returns, under numerical integration using the native routine `NIntegrate` in Wolfram's Mathematica, the enormous value $A(\gamma_A)/R^2 \sim 3.422937243317424 \times 10^{55897}$, which was made finite by subtracting the factor $1/\epsilon^2$ independently of the temperature or the chemical potential, as it should be;

- Although (4.117) is formally equivalent to (4.119), numerically, due to the dependence on the UV cutoff ϵ and the well-known issue with subtracting

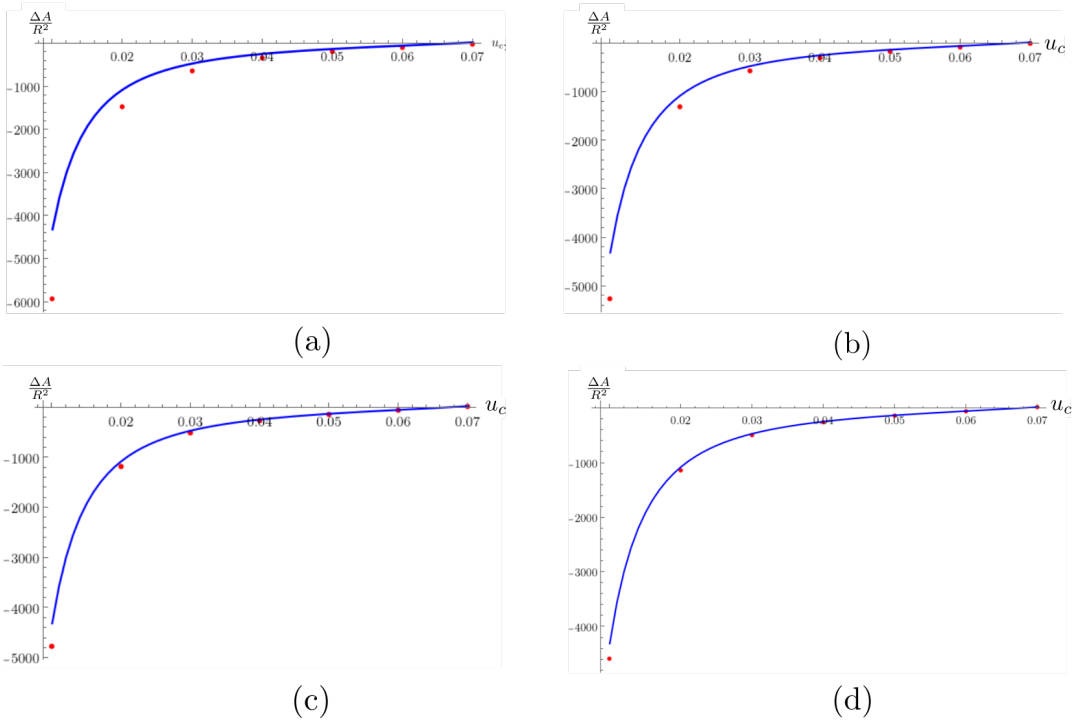

FIGURE 4.5: Numerical evaluation of the finite difference integral (continuous blue line) $\Delta A/R^2$, compared with the result obtained for $\Delta\mathcal{A}/R^2$ in terms of summations (red points), for the test case #1. In (a), we used 5 as a common upper limit for the summations in Eq. (4.121), which took 1 second to evaluate in Mathematica; in (b), we used 15 as a common upper limit, which took 15 seconds to evaluate; in (c), we used 65 as a common upper limit, which took 6h22min22s to evaluate; and in (d), we used 180 as a common upper limit, which took 37h3min39s to evaluate. In striking constrast, the numerical integral took just about 1 second to evaluate!

large numbers with finite numerical precision, we see from the tables above that, for the test case under consideration, in fact, (4.117) $\sim$ (4.119) for ϵ in the range between 10^{-2} and 10^{-3}. However, for progressively smaller values of ϵ, Eq. (4.117) becomes an inefficient expression from a numerical point of view and eventually diverges again (due to a purely numerical reason, involving the subtraction of large numbers with finite numerical precision);

- Eq. (4.119) converges rather fast to Eq. (4.120) within Mathematica's standard numerical precision, for ϵ of the order of 10^{-4} or less. Clearly, from a numerical point of view, Eq. (4.119) is a much better and efficient expression than Eq. (4.117) (even though both are formally identical). Moreover, it is clear that we can explicitly set $\epsilon = 0$ in Eq. (4.119) and

thus work directly with Eq. (4.120), without needing to use the UV cutoff ϵ (which was only necessary as an intermediate step to properly regularize the divergent integral of the hyperarea, before subtracting the corresponding UV divergence);

- Regarding the results for $\Delta\mathcal{A}/R^2$ in terms of the summations in Eq. (4.121), the corresponding calculations are extremely slow and time consuming, and even going up to 120 terms in Table 4.2, the results have not yet converged. In order to obtain a broader vision of the test case at hand, we plotted the comparison shown in Fig. 4.5. One sees that, for the present test case, by increasing the number of terms considered in the summations, indeed the red points slowly approach the blue curve corresponding to the much faster numerical integration method. However, even with 180 terms in the summations, the red points still not converged to the blue curve.

Curiously, the values obtained via summation with 90 or 120 terms are very close to (4.117) for ϵ between 10^{-4} and 10^{-7}, which seems to indicate that the expression via summations must be encountering a problem of subtracting large numbers as well (although, in this case, it does not explicitly involve the UV cutoff ϵ, which does not appear in the summations).

To confirm the presence of possible numerical issues (at least if no refinement is made in Mathematica's operating standards) in the calculation of the summations, another test case was also considered, corresponding to the choice $(Q = 1, u_H = 1, u_c = 0.9999)$, with the corresponding results shown in Tables 4.3 and 4.4.

ϵ	$\Delta\tilde{A}(\epsilon)/R^2$	$\Delta A(\epsilon)/R^2$	$\Delta A/R^2$
10^{-2}	4.45873	4.45873	4.45883
10^{-3}	2.6341	4.45883	4.45883
10^{-4}	2.63365	4.45883	4.45883
10^{-5}	2.63361	4.45883	4.45883
10^{-6}	2.63428	4.45883	4.45883
10^{-7}	2.59375	4.45883	4.45883
10^{-8}	-4786	4.45883	4.45883
10^{-9}	-1.02154×10^7	4.45883	4.45883

TABLE 4.3: Test case #2 with $(Q = 1, u_H = 1, u_c = 0.9999)$.

Upper limit	$\Delta\mathcal{A}/R^2$
20	1.824011004347724
90	$-6.573009973338912 \times 10^{24}$

TABLE 4.4: Test case #2 with $(Q = 1, u_H = 1, u_c = 0.9999)$. The first column refers to the different values used as common upper limits for the summations in Eq. (4.121).

This test case above is interesting, as it reveals some new nuances. Firstly, as in the previous case, (4.120) is completely finite and (4.119) converges to (4.120) even more rapidly than in the previous case. Again, (4.117) starts for $\epsilon = 10^{-2}$ equal to (4.119), but as we decrease ϵ, (4.117) starts to behave poorly and eventually diverges negatively (although for smaller values of ϵ, it is positive in the present case). A similar trend is seen in the expression via summations (although in this case we vary the number of terms considered in the summations, instead of ϵ, since the summations do not depend on the UV cutoff, but do depend on the corresponding truncations), but in this new test case there is no convergence at all and adding more terms to the summations considerably worsens the situation. This intriguing issue clearly requires further investigation to be fully understood and solved.

Chapter 5

2RCBH model

As previously mentioned in section 4.1, the STU model with three generic conserved R-charges has three Maxwell gauge fields (associated with each $U(1)$ of the Cartan subgroup of the $SU(4)$ R-symmetry group), two scalar fields, and the metric. Alongside with the 1RCBH model discussed in Chapter 4, we have another model originating from the same parent (the STU model) which, by taking one R-charge to be zero and keeping the other two R-charges nonzero but equal to each other, gives us what is called the 2 R-charge Black Hole (2RCBH) model [110], [111]. Similarly to the 1RCBH model, the 2RCBH model is also a rigorous top-down holographic construction defined at finite temperature and density, but that contrary to the 1RCBH model, it does not have a critical point in its phase diagram.

5.1 The 2RCBH Model

The 2RCBH model has not been as widely explored in the literature as its sibling, the 1RCBH model. In fact, up to now, just the structure of Fermi surfaces [111], some transport coefficients [110], the thermodynamics and the spectra of homogeneous quasinormal modes [55] have been analyzed for the 2RCBH model. It is our purpose to add to the literature by investigating information properties of this model, and comparing with the corresponding results for the 1RCBH model, since these are two top-down holographic constructions originating from the same parent model, but possessing different physical properties and phase diagrams.

The 2RCBH model [110], [111] is also described by the bulk action given by (4.1). The Maxwell-dilaton coupling for the 2RCBH model is different, while

the dilaton potential is the same as for the 1RCBH model in (4.2),

$$f(\phi) = \mathrm{e}^{\sqrt{\frac{2}{3}}\phi} \quad V(\phi) = -\frac{1}{L^2}\left(8\mathrm{e}^{\frac{\phi}{\sqrt{6}}} + 4\mathrm{e}^{-\sqrt{\frac{2}{3}}\phi}\right), \tag{5.1}$$

where L, as previously mentioned, is the asymptotically AdS_5 radius. For simplicity, again, we will consider $L = 1$. As stated before, any model of the EMD class satisfies the equations of motion given by (4.8), (4.9), and (4.10). Furthermore, as before, to describe a strongly coupled QFT on the boundary, dual to the EMD theory defined in the gravitational bulk, in a particular case where this QFT is in a homogeneous and isotropic configuration, in thermodynamic equilibrium at finite temperature and density, and in the absence of external electromagnetic fields, we use the following ansatz for the bulk fields,

$$ds^2 = \mathrm{e}^{2A(r)}\left(-h(r)dt^2 + d\vec{x}^2\right) + \frac{\mathrm{e}^{2B(r)}}{h(r)}dr^2, \quad \phi = \phi(r), \quad A^\mu = \Phi(r)\delta^\mu_0, \tag{5.2}$$

where the fields depend only on the holographic radial coordinate. The gauge field has only the nonzero temporal component, whose value at the boundary provides the chemical potential in the QFT. The metric, which has a blackening function, describes charged black hole backgrounds, which are the gravitational duals to thermal states at finite temperature and density in the boundary QFT in thermodynamic equilibrium.

Substituting (5.1) – which specifies the 2RCBH model within the class of EMD models – and (5.2) – which specifies that the system is in equilibrium – into the general equations of the EMD fields (4.8), (4.9), and (4.10), we will obtain a set of coupled ODEs for the bulk fields, whose solutions are of the form specified below [55], [110], [111],[1]

[1]The solutions presented were explicitly verified by direct substitution into the ODEs, thus showing that these functions do, in fact, solve the field equations. It is worth noting that there is a typo corresponding to an incorrect factor of 1/2, which should be $\sqrt{2}$ for $\Phi_2(r)$ in equation (14) of [111], and also a typo corresponding to an incorrect factor of 1/2 where it should be 1 for $\Phi_1(r)$ in equation (17) of [111], where $\Phi_1(r)$ and $\Phi_2(r)$ refer to the solutions for the Maxwell field in the 1RCBH and 2RCBH models, respectively. On the other hand, the signs of $\Phi_1(r)$ and $\Phi_2(r)$ in [110] are reversed compared to those used in this text and in [52], [55], [111]: these are still solutions to the field equations, but would instead imply negative R-charge chemical potentials. It is also worth mentioning the different notation used in [110], where the black hole mass M and the chemical potential of the dual gauge theory μ are instead denoted by $\sqrt{\mu}$ and Ω, respectively. There is also a typographical error in Equation (2.2) of [114] and in Equation (6) of [117] regarding the expression for $f(\phi)$ in the 1RCBH model.

$$A(r) = \ln r + \frac{1}{3}\ln\left(1 + \frac{Q^2}{r^2}\right), \tag{5.3}$$

$$B(r) = -\ln r - \frac{2}{3}\ln\left(1 + \frac{Q^2}{r^2}\right), \tag{5.4}$$

$$h(r) = 1 - \frac{M^2}{\left(r^2 + Q^2\right)^2}, \tag{5.5}$$

$$\phi(r) = \sqrt{\frac{2}{3}}\log\left(1 + \frac{Q^2}{r^2}\right), \tag{5.6}$$

$$\Phi(r) = \left(-\frac{\sqrt{2}MQ}{r^2 + Q^2} + \frac{\sqrt{2}MQ}{r_H^2 + Q^2}\right). \tag{5.7}$$

These solutions are specified in terms of two pieces of data that we can choose for the black holes: their mass, denoted by M, and their charge, denoted by Q. Each black hole solution generated in the gravitational bulk from the choices of the pair (M, Q) is dual, via the holographic dictionary, to a specific thermal state of the boundary QFT, located at $r \to \infty$. In the solutions given by (5.3) to (5.7), r_H is the radial location of the event horizon of the black hole solution, obtained by the condition that the g_{tt} component of the metric vanishes, which corresponds to the vanishing of the blackening function at $r = r_H$:

$$\left(1 - \frac{M^2}{\left(r_H^2 + Q^2\right)^2}\right) = 0. \tag{5.8}$$

Since the expression given above is a quartic equation for r_H, it therefore has four roots. As the holographic radial coordinate r is real and non-negative, we take from these four roots the one that corresponds to a real and non-negative value for the radial location of the event horizon, which is given by

$$r_H = \sqrt{M - Q^2}. \tag{5.9}$$

We can use (5.9) to express M as a function of r_H and Q. Alternatively to describing the black hole backgrounds in terms of (M, Q), we can describe them in terms of (r_H, Q), resulting in

$$M = Q^2 + r_H^2. \tag{5.10}$$

In the next section, we will discuss the calculation of thermodynamic observables, phase diagrams, and susceptibilities for the 2RCBH model.

5.2 Thermodynamics

5.2.1 Basic Thermodynamic Variables

We can also obtain the Hawking temperature of the black hole in terms of the charge Q and the radial location of the event horizon r_H for this model through (3.15) with the identification of the metric coefficients given below (5.11), which follows from (5.2):

$$T = \left.\frac{\sqrt{-\left(g_{tt}\right)'\left(g^{rr}\right)'}}{4\pi}\right|_{r=r_H} \tag{5.11}$$

where $g_{tt} = -\mathrm{e}^{2A(r)}h(r)$, $g^{rr} = \mathrm{e}^{-2B(r)}h(r)$, and $'$ denotes the respective derivative with respect to r.

Substituting into expression (5.11), we have that

$$T = \left.\frac{\sqrt{-\left(-\mathrm{e}^{2A(r)}h(r)\right)'\left(\mathrm{e}^{-2B(r)}h(r)\right)'}}{4\pi}\right|_{r=r_H} \tag{5.12}$$

$$= \left.\frac{\sqrt{\left(2\mathrm{e}^{2A(r)}h(r)A'(r) + \mathrm{e}^{2A(r)}h'(r)\right)\left(\mathrm{e}^{-2B(r)}h'(r) - 2\mathrm{e}^{-2B(r)}h(r)B'(r)\right)}}{4\pi}\right|_{r=r_H}, \tag{5.13}$$

applying (5.3), (5.4), and (5.5) after calculating the respective derivatives:

$$T = \left.\frac{\sqrt{-\frac{\frac{M^4(Q^4-9r^4)}{(Q^2+r^2)^4} - \frac{2M^2(Q^4+9r^4)}{(Q^2+r^2)^2} + Q^4 - 9r^4}{r^2}}}{6\pi}\right|_{r=r_H}. \tag{5.14}$$

Substituting (5.9) and (5.10) into the expression above, setting $r = r_H$, and simplifying, we have:

$$T = \frac{r_H}{\pi}. \tag{5.15}$$

For the $U(1)$ R-charge chemical potential, using (3.23), we have:

$$\mu = \lim_{r\to\infty}\Phi(r) = \lim_{r\to\infty}\left(-\frac{\sqrt{2}MQ}{r^2+Q^2} + \frac{\sqrt{2}MQ}{r_H^2+Q^2}\right), \tag{5.16}$$

where $\Phi(r)$ was given by (5.7). Calculating the limit, we have:

$$\mu = \frac{\sqrt{2}MQ}{r_H^2 + Q^2}. \tag{5.17}$$

Substituting (5.10) and simplifying, we obtain the chemical potential:

$$\mu = \sqrt{2}Q. \tag{5.18}$$

The entropy S can be obtained through the Bekenstein-Hawking formula (3.18),

$$S = \frac{A_H}{4G_5}, \tag{5.19}$$

where A_H is given by

$$\begin{aligned} A_H &= \int_{\mathcal{M}} \sqrt{|g|} d^3x, && (5.20)\\ &= \int_{\mathcal{M}} \sqrt{g_{xx}g_{yy}g_{zz}} d^3x, && (5.21)\\ &= \int_{\mathcal{M}} \sqrt{\mathrm{e}^{2A(r)}\mathrm{e}^{2A(r)}\mathrm{e}^{2A(r)}} d^3x, && (5.22)\\ &= \sqrt{\mathrm{e}^{6A(r)}} \int_{\mathcal{M}} d^3x, && (5.23) \end{aligned}$$

Substituting (5.3), evaluating at $r = r_H$, and simplifying, we have

$$A_H = r_H \left(Q^2 + r_H^2\right) \int_{\mathcal{M}} d^3x. \tag{5.24}$$

Since the integral is in three dimensions, we will have a volume denoted by V

$$A_H = r_H \left(Q^2 + r_H^2\right) V. \tag{5.25}$$

Substituting (5.25) into (5.19), we have

$$S = \frac{r_H \left(Q^2 + r_H^2\right) V}{4G_5}. \tag{5.26}$$

Dividing the entropy S by the volume V, we obtain the entropy density

$$s = \frac{r_H \left(Q^2 + r_H^2\right)}{4G_5}. \tag{5.27}$$

We can rewrite the five-dimensional Newton's constant as

$$\kappa_5^2 = 8\pi G_5 \Rightarrow 4G_5 = \frac{\kappa_5^2}{2\pi},$$

Thus, the entropy density is given by:

$$s = \frac{2\pi r_H}{\kappa_5^2}\left(Q^2 + r_H^2\right). \tag{5.28}$$

The R-charge density, given by the radially conjugate momentum, is again given by expression (3.24). Reproducing the steps described from (4.35) to (4.41), carefully substituting $f(\phi)$ with the expression given by (5.2), and substituting (5.3), (5.4), (5.6), and (5.7), and simplifying, results in

$$\rho = \frac{\sqrt{2}Q\left(Q^2 + r_H^2\right)}{\kappa_5^2}. \tag{5.29}$$

5.2.2 Phase Diagram and Equation of State

The 2RCBH black hole solutions can be parameterized by various values of the dimensionless ratio Q/r_H. To obtain this ratio, we divide (5.18) by (5.15), resulting in

$$\frac{\mu}{T} = \sqrt{2}\pi\frac{Q}{r_H}. \tag{5.30}$$

From (5.30), we obtain the quantity Q/r_H,

$$\frac{Q}{r_H} = \frac{1}{\sqrt{2}\pi}\frac{\mu}{T}. \tag{5.31}$$

Since the quantity Q/r_H is non-negative, this implies $\mu/T \in [0, \infty)$. Looking at the same expression, we see that for each value of the ratio $\mu/T \in [0, \infty)$, there exists only one corresponding value of Q/r_H, which in turn parameterizes only one solution branch, differently from the 1RCBH model where there are two branches of competing black hole solutions, as discussed before.

For a SYM plasma, the relation given by (4.53), when substituted into the entropy density relation (5.28), yields

$$s = \frac{N_c^2 r_H\left(Q^2 + r_H^2\right)}{2\pi}. \tag{5.32}$$

Isolating the charge Q from expression (5.18) and r_H from (5.15), and substituting above, we have

$$s = \frac{N_c^2 T^3}{4}\left(2\pi^2 + \left(\frac{\mu}{T}\right)^2\right). \tag{5.33}$$

Substituting (4.53) into the R-charge density relation (5.29), we have

$$\rho = \frac{N_c^2 Q\left(Q^2 + r_H^2\right)}{2\sqrt{2}\pi^2}. \tag{5.34}$$

Again, isolating the charge Q from expression (5.18) and r_H from (5.15), and substituting into the expression above and rearranging the terms, we obtain

$$\rho = N_c^2 T^3 \frac{(\mu/T)}{4}\left[1 + \frac{(\mu/T)^2}{2\pi^2}\right]. \tag{5.35}$$

Starting again from the Gibbs-Duhem thermodynamic relation, $dp = sdT + \rho d\mu$, it is possible to calculate the pressure. For this, it is necessary to obtain the entropy and chemical potential as presented below.

Starting from (5.33), we have

$$\left(\frac{\partial s}{\partial \mu}\right)_T = \left(\frac{\partial s}{\partial\left(\mu/T\right)}\right)_T \left(\frac{\partial\left(\mu/T\right)}{\partial \mu}\right)_T = \frac{1}{2} N_c^2 \mu T. \tag{5.36}$$

For the charge density, starting from (5.35), we have

$$\left(\frac{\partial \rho}{\partial T}\right)_\mu = \left(\frac{\partial \rho}{\partial T}\right)_{\mu/T} + \left(\frac{\partial \rho}{\partial\left(\mu/T\right)}\right)_T \left(\frac{\partial\left(\mu/T\right)}{\partial T}\right)_\mu = \frac{1}{2} N_c^2 \mu T. \tag{5.37}$$

From expressions (5.36) and (5.37), we again obtain the Maxwell relation

$$\left(\frac{\partial s}{\partial \mu}\right)_T = \left(\frac{\partial \rho}{\partial T}\right)_\mu. \tag{5.38}$$

Again, from the Gibbs-Duhem relation, the quantities s and ρ are partial derivatives of the pressure with respect to T and μ, respectively. Writing the pressure as a function of T and μ, we have

$$p = \int \left[s + \rho\left(\frac{\partial \mu}{\partial T}\right)_{\frac{\mu}{T}}\right] dT + F(\mu) = \int \rho T d\left(\mu/T\right) + G(T). \tag{5.39}$$

Let's define

$$I_1 = \int \left[s + \rho\left(\frac{\partial \mu}{\partial T}\right)_{\frac{\mu}{T}}\right] dT + F(\mu), \quad I_2 = \int \rho T d\left(\mu/T\right) + G(T). \tag{5.40}$$

where I_1 is an expression for the pressure, in which the first term of the integrand is the entropy density integrated with respect to temperature, resulting in

$$I_1 = \frac{N_c^2 T^4}{32\pi^2}\left(2\pi^2 + \left(\frac{\mu}{T}\right)^2\right)^2 + F(\mu). \tag{5.41}$$

For I_2, we also have an expression for the pressure, where we have in the integrand the charge density integrated with respect to the chemical potential, such that

$$I_2 = \frac{N_c^2 T^4}{32\pi^2}\left(\frac{4\pi^2\mu^2}{T^2} + \left(\frac{\mu}{T}\right)^4\right) + G(T). \tag{5.42}$$

Since I_1 and I_2 are different expressions for the pressure, subtracting $I_1 - I_2$ should result in zero

$$I_1 - I_2 = \frac{1}{8}N_c^2\pi^2 T^4 + F(\mu) - G(T) = 0. \tag{5.43}$$

If $F(\mu) = 0$, we have $G(T) = \frac{1}{8}N_c^2\pi^2 T^4$. Substituting $G(T)$ into (5.42) and simplifying the expressions, we obtain

$$p = \frac{N_c^2 T^4 \pi^2}{8}\left(1 + \frac{(\mu/T)^2}{2\pi^2}\right)^2. \tag{5.44}$$

Using (5.28), (5.35), and (5.44), we can calculate the internal energy density $\varepsilon = Ts - p + \mu\rho$, resulting in

$$\varepsilon = \frac{3\pi^2 N_c^2 T^4}{8}\left(1 + \frac{(\mu/T)^2}{2\pi^2}\right)^2. \tag{5.45}$$

As mentioned in the previous chapter, $\varepsilon - 3p$ is the trace of the energy-momentum tensor of the 4D boundary QFT, which is generally nonzero but vanishes for conformal theories. We verify again that $\varepsilon - 3p = 0$, which was expected since the 2RCBH is also a conformal model [53].

The specific heat at fixed chemical potential and constant volume is given by

$$C_\mu = \frac{1}{V}\left(\frac{\partial Q}{\partial T}\right)_{\mu,V} = T\left(\frac{\partial s}{\partial T}\right)_\mu = T\left(\left(\frac{\partial s}{\partial T}\right)_\mu + \frac{\mathrm{d}s}{\mathrm{d}(\mu/T)}\left(\frac{\partial(\mu/T)}{\partial T}\right)_\mu\right), \tag{5.46}$$

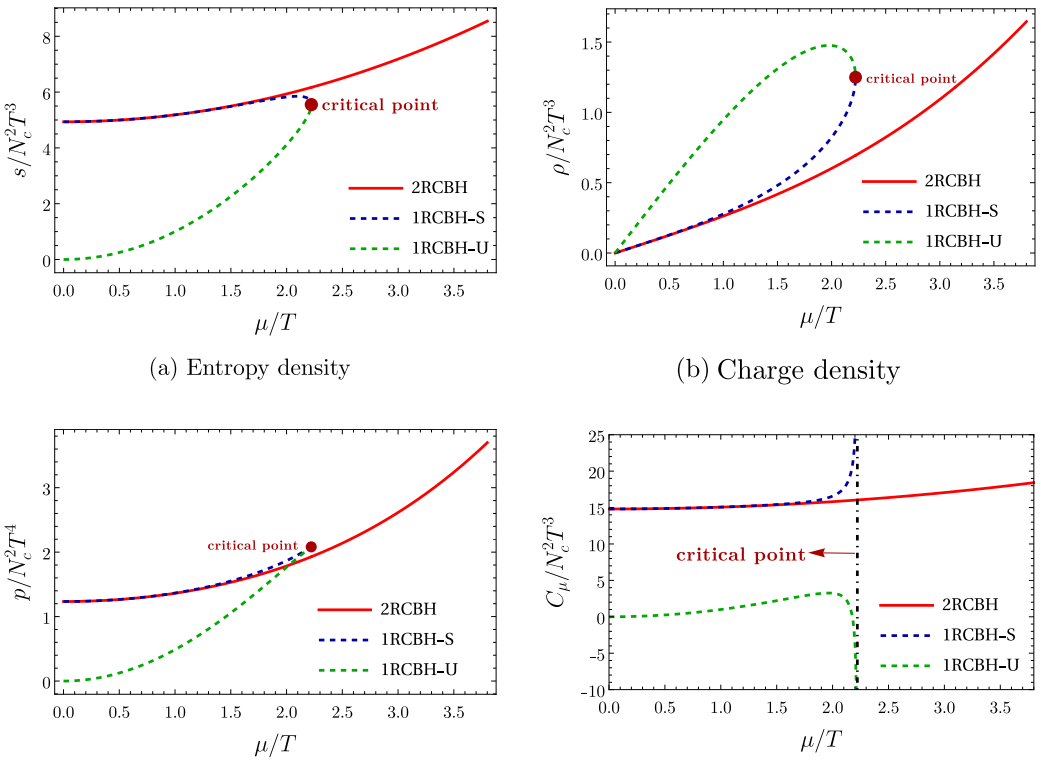

(a) Entropy density

(b) Charge density

(c) Pressure

(d) Specific heat

FIGURE 5.1: Distribution of thermodynamic quantities for the 2RCBH model along with the 1RCBH model. The solid line represents the phase diagram of the 2RCBH model. The dashed lines represent the stable and unstable branches of the 1RCBH model, denoted by the letters S and U, respectively.

and, substituting the expressions and performing the same mathematical manipulations as before for simplification, we have

$$C_\mu = \frac{N_c^2 T^3}{4}\left(6\pi^2 + \left(\frac{\mu}{T}\right)^2\right). \tag{5.47}$$

Considering that the $(n+1)$-th order R-charge susceptibility is given by

$$\chi_{n+1} = \left(\frac{\partial^n \rho}{\partial \mu^n}\right)_T = \left(\frac{\partial \chi_n}{\partial \mu}\right)_T, \tag{5.48}$$

where we calculate up to $n = 4$ and $\chi_1 = \rho$, as presented below,

$$\chi_2 = \left(\frac{\partial \rho}{\partial \mu}\right)_T = \left(\frac{\partial \rho}{\partial (\mu/T)}\right)_T \left(\frac{\partial (\mu/T)}{\partial \mu}\right)_T, \tag{5.49}$$

where, after performing the calculations, we have

$$\chi_2 = \frac{N_c^2 T^2}{8}\left(2 + \frac{3}{\pi^2}\left(\frac{\mu}{T}\right)^2\right). \tag{5.50}$$

Since we obtain (5.50) as a function of μ/T, we have $\partial/\partial\mu = T^{-1}\partial/\partial(\mu/T)$, and again, under the successive application of this operator, all other orders of susceptibilities below are obtained.

Thus, we have that χ_3 will be given by

$$\chi_3 = \frac{3N_c^2\mu}{4\pi^2}. \tag{5.51}$$

And finally, we have that χ_4 will be given by

$$\chi_4 = \frac{3N_c^2}{4\pi^2}, \tag{5.52}$$

since derivatives of order higher than 4 will result in zero.

The phase diagram of the 2RCBH model is a line segment that extends from the initial point $\mu/T = 0$, and grows indefinitely to infinity, unlike the 1RCBH model, which extends from the initial point $\mu/T = 0$ to the critical point at $\pi/\sqrt{2}$, where it ends abruptly. When $\mu/T = 0$ we recover from the 2RCBH model the purely thermal SYM theory, similarly to what happens in the thermodynamically stable branch of the 1RCBH model.

In figs. 5.1 and 5.2, we present the plots of the thermodynamic quantities of the 2RCBH model, comparing them with those of the 1RCBH model.

5.3 Aspects of Holographic Entanglement Entropy for the 2RCBH Model

In this section, we will present in detail the calculation of the holographic entanglement entropy (HEE) in the 2RCBH model. As already presented in the previous chapter for the 1RCBH model, the calculation will follow a very similar procedure to the one performed previously, with any differing detail duly noted.

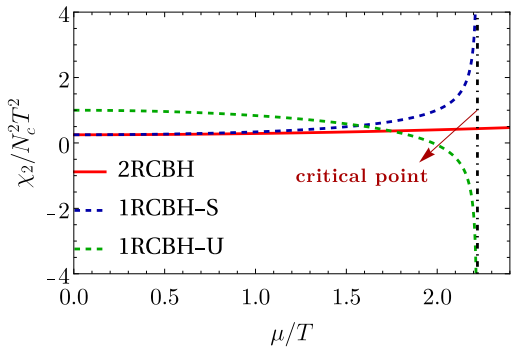

(a) 2nd-order susceptibility

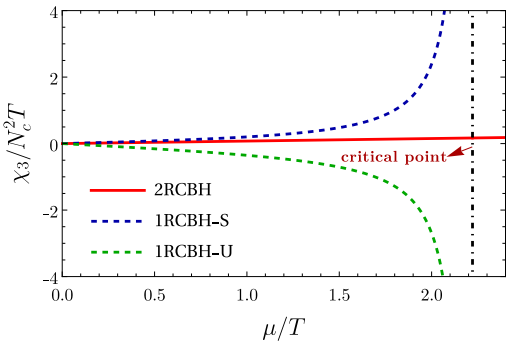

(b) 3rd-order susceptibility

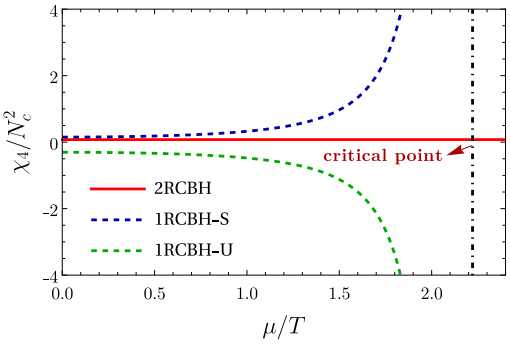

(c) 4th-order susceptibility

FIGURE 5.2: Susceptibilities up to the fourth order for the 2RCBH model along with the 1RCBH model. The solid line represents the phase diagram of the 2RCBH model. The dashed lines represent the stable and unstable branches of the 1RCBH model, denoted by the letters S and U, respectively.

5.3.1 Poincare Coordinates

It is convenient for the following discussion again in the so-called Poincaré coordinates, where the new holographic radial coordinate is defined as $u = 1/r$ and, therefore, the bulk fields in (5.2) now read as follows

$$ds^2 = \mathrm{e}^{2A(u)}\left(-h(u)dt^2 + d\vec{x}^2\right) + \frac{\mathrm{e}^{2B(u)}}{h(u)}\frac{1}{u^4}du^2, \quad \phi = \phi(u), \quad A^\mu = \Phi(u)\delta^\mu_0, \tag{5.53}$$

where the boundary $r \to \infty$ is at $u = 0$ in terms of the new holographic coordinate u.

Substituting (5.1) (which specify the 2RCBH model within the class of EMD models) and (5.53) (which specify that the system is in equilibrium in the new coordinate system) into the general EMD field equations (4.8), (4.9), and (4.10), we obtain a set of coupled ODEs for the bulk fields, whose solutions are of the

form specified below:

$$A(u) = \ln\left(\frac{1}{u}\right) + \frac{1}{3}\ln\left(1+Q^2u^2\right), \tag{5.54}$$

$$B(u) = -\ln\left(\frac{1}{u}\right) - \frac{2}{3}\ln\left(1+Q^2u^2\right), \tag{5.55}$$

$$h(u) = 1 - \frac{M^2}{\left((1/u)^2+Q^2\right)^2}, \tag{5.56}$$

$$\phi(u) = \sqrt{\frac{2}{3}}\ln\left(1+Q^2u^2\right), \tag{5.57}$$

$$\Phi(u) = \left(\frac{\sqrt{2}MQ}{(1/u_H)^2+Q^2} - \frac{\sqrt{2}MQ}{(1/u)^2+Q^2}\right). \tag{5.58}$$

In the solutions given by (5.54) to (5.58), we have that u_H is the radial location of the event horizon of the black hole solution, which is obtained by the condition that the g_{tt} component of the metric vanishes, which corresponds to the vanishing of the blackening function at $u = u_H$, so that

$$\left(1 - \frac{M^2}{\left((1/u_H)^2+Q^2\right)^2}\right) = 0. \tag{5.59}$$

Since the above expression is a quartic equation for u_H, it therefore has four roots. Since the holographic radial coordinate u is real and non-negative, we take from among these four roots the one that corresponds to a real and non-negative value for the radial location of the event horizon, which is given by

$$u_H = \frac{1}{\sqrt{M-Q^2}}. \tag{5.60}$$

We can use (5.60) to express M as a function of u_H and Q, and, alternatively to describing black hole backgrounds in terms of (M, Q), we can describe them in terms of (u_H, Q), resulting in

$$M = Q^2 + \frac{1}{u_H^2}. \tag{5.61}$$

5.3.2 Holographic Entanglement Entropy

The integral formulas are the same as those presented in Section 4.3.2 for the 1RCBH model, with the only change being the background black hole solutions. The corresponding results will be presented in an upcoming paper.

Chapter 6

Conclusions and perspectives

We reviewed the application of thermodynamics and information theory in the context of the gauge/gravity duality for two holographic toy-models: 1RCBH and 2RCBH.

In the case of the 1RCBH model, a top-down holographic construction defined at finite temperature and chemical potential, there is a critical point in its phase diagram. In contrast, the 2RCBH model is also a top-down holographic construction stemming from the same parent model (STU) as the 1RCBH model, but without a critical point in its phase diagram.

We also reviewed the calculation of the entanglement entropy of the 1RCBH model and presented some new preliminary results comparing the previous approach published in the literature, based on summations, with the direct numerical evaluation of the area integral involved in the calculation of the holographic entanglement entropy. Such a comparison revealed numerical issues, not considered in previous works, which require further investigation to be fully understood and solved. This is the main focus and perspective for the continuation of the present work, alongside with the analysis of the entanglement entropy in the 2RCBH model, which has not yet been considered in the literature. In fact, in previous works, not even the entanglement entropy of the 1RCBH model has been analyzed in detail, with just a formal expression being derived in the literature, without associated plots which should allow for a direct analysis of the physical behavior of the entanglement entropy in that model. The reason is likely related to the very inefficient formula based on summations, which is rather cumbersome and extremely slow to evaluate in practice. The more direct method we proposed here, based on numerical integration, is much faster and apparently displays no convergence issues like the summation method. We expect to report soon further developments in this direction in an upcoming paper intended for publication.

Bibliography

[1] M. M. Wilde, "From Classical to Quantum Shannon Theory," Jun. 2011. DOI: 10.1017/9781316809976.001. arXiv: 1106.1445 [quant-ph].

[2] T. M. Cover, *Elements of information theory*. John Wiley & Sons, 1999.

[3] M. M. Wilde, *Quantum information theory*. Cambridge university press, 2013.

[4] V. Vedral, *Introduction to quantum information science*. Oxford University Press, USA, 2006.

[5] R. L. Rivest, A. Shamir, and L. Adleman, "A method for obtaining digital signatures and public-key cryptosystems," *Communications of the ACM*, vol. 21, no. 2, pp. 120–126, 1978.

[6] R. Horodecki, P. Horodecki, M. Horodecki, and K. Horodecki, "Quantum entanglement," *Rev. Mod. Phys.*, vol. 81, pp. 865–942, 2009. DOI: 10.1103/RevModPhys.81.865. arXiv: quant-ph/0702225.

[7] J. Preskill, "Lecture notes for physics 229: Quantum information and computation," *California Institute of Technology*, vol. 16, no. 1, pp. 1–8, 1998.

[8] G. T. Landi, "Quantum information and quantum noise," *Lecture notes, July*, 2018.

[9] M. B. Plenio and S. Virmani, "An introduction to entanglement measures," *Quant. Inf. Comput.*, vol. 7, no. 1-2, pp. 001–051, 2007. DOI: 10.26421/QIC7.1-2-1. arXiv: quant-ph/0504163.

[10] E Schr *et al.*, "Die gegenw rtige situation in der quantenmechanik," *Die Naturwissenschaften*, vol. 23, no. 48, pp. 807–812, 1935.

[11] D. Bruß, "Characterizing entanglement," *Journal of Mathematical Physics*, vol. 43, no. 9, pp. 4237–4251, 2002.

[12] M. Horodecki, R. Horodecki, A. Sen(De), and U. Sen, "Common origin of no-cloning and no-deleting principles conservation of information," *Foundations of Physics*, vol. 35, no. 12, 2041–2049, Dec. 2005, ISSN: 1572-9516. DOI: 10.1007/s10701-005-8661-4. [Online]. Available: http://dx.doi.org/10.1007/s10701-005-8661-4.

[13] A. K. Ekert, J. G. Rarity, P. R. Tapster, and G. Massimo Palma, "Practical quantum cryptography based on two-photon interferometry," *Phys. Rev. Lett.*, vol. 69, pp. 1293–1295, 1992. DOI: 10.1103/PhysRevLett.69.1293.

[14] C. H. Bennett, G. Brassard, C. Crepeau, R. Jozsa, A. Peres, and W. K. Wootters, "Teleporting an unknown quantum state via dual classical and Einstein-Podolsky-Rosen channels," *Phys. Rev. Lett.*, vol. 70, pp. 1895–1899, 1993. DOI: 10.1103/PhysRevLett.70.1895.

[15] N. D. Mermin, "What is quantum mechanics trying to tell us?" *Am. J. Phys.*, vol. 66, p. 753, 1998. DOI: 10.1119/1.18955. arXiv: quant-ph/9801057.

[16] J. S. Bell, "On the Einstein-Podolsky-Rosen paradox," *Physics Physique Fizika*, vol. 1, pp. 195–200, 1964. DOI: 10.1103/PhysicsPhysiqueFizika.1.195.

[17] M. Horodecki, P. Horodecki, and R. Horodecki, "Separability of n-particle mixed states: necessary and sufficient conditions in terms of linear maps," *Phys. Lett. A*, vol. 283, no. 1-2, pp. 1–7, 2001. DOI: 10.1016/S0375-9601(01)00142-6.

[18] J. S. Bell, "AGAINST 'MEASUREMENT'," *Phys. World*, vol. 3, pp. 33–40, 1990.

[19] P. W. Shor, "Polynomial time algorithms for prime factorization and discrete logarithms on a quantum computer," *SIAM J. Sci. Statist. Comput.*, vol. 26, p. 1484, 1997. DOI: 10.1137/S0097539795293172. arXiv: quant-ph/9508027.

[20] D. Bruß, J. I. Cirac, P. Horodecki, F. Hulpke, B. Kraus, M. Lewenstein, and A. Sanpera, "Reflections upon separability and distillability," *Journal of Modern Optics*, vol. 49, no. 8, 1399–1418, Jul. 2002, ISSN: 1362-3044. DOI: 10.1080/09500340110105975. [Online]. Available: http://dx.doi.org/10.1080/09500340110105975.

[21] M. Horodecki, "Entanglement measures," *Quant. Inf. Comput.*, vol. 1, no. 1, pp. 3–26, 2001. DOI: 10.26421/QIC1.1-2.

[22] N. G. Almeida, *Introdução à Computação e Informação Quântica*. Livraria da Física, 2023.

[23] J. M. Maldacena, "The Large N limit of superconformal field theories and supergravity," *Adv. Theor. Math. Phys.*, vol. 2, pp. 231–252, 1998. DOI: 10.4310/ATMP.1998.v2.n2.a1. arXiv: hep-th/9711200.

[24] S. S. Gubser, I. R. Klebanov, and A. M. Polyakov, "Gauge theory correlators from noncritical string theory," *Phys. Lett. B*, vol. 428, pp. 105–114, 1998. DOI: 10.1016/S0370-2693(98)00377-3. arXiv: hep-th/9802109.

[25] E. Witten, "Anti-de Sitter space and holography," *Adv. Theor. Math. Phys.*, vol. 2, pp. 253–291, 1998. DOI: 10.4310/ATMP.1998.v2.n2.a2. arXiv: hep-th/9802150.

[26] ——, "Anti-de Sitter space, thermal phase transition, and confinement in gauge theories," *Adv. Theor. Math. Phys.*, vol. 2, L. Bergstrom and U. Lindstrom, Eds., pp. 505–532, 1998. DOI: 10.4310/ATMP.1998.v2.n3.a3. arXiv: hep-th/9803131.

[27] R. Rougemont, J. Grefa, M. Hippert, J. Noronha, J. Noronha-Hostler, I. Portillo, and C. Ratti, "Hot QCD phase diagram from holographic Einstein–Maxwell–Dilaton models," *Prog. Part. Nucl. Phys.*, vol. 135, p. 104 093, 2024. DOI: 10.1016/j.ppnp.2023.104093. arXiv: 2307.03885 [nucl-th].

[28] G. F. Chew and S. C. Frautschi, "Principle of Equivalence for All Strongly Interacting Particles Within the S Matrix Framework," *Phys. Rev. Lett.*, vol. 7, pp. 394–397, 1961. DOI: 10.1103/PhysRevLett.7.394.

[29] J. Greensite, *An introduction to the confinement problem*. 2011, vol. 821. DOI: 10.1007/978-3-642-14382-3.

[30] M. B. Green, J. H. Schwarz, and E. Witten, *Superstring Theory. Vol. 1: Introduction*, ser. Cambridge Monographs on Mathematical Physics. Jul. 1988, ISBN: 978-0-521-35752-4.

[31] ——, *Superstring Theory. Vol. 2: Loop Amplitudes, Anomalies And Phenomenology*. Jul. 1988, ISBN: 978-0-521-35753-1.

[32] J. Polchinski, *String theory. Vol. 1: An introduction to the bosonic string*, ser. Cambridge Monographs on Mathematical Physics. Cambridge University Press, Dec. 2007, ISBN: 978-0-511-25227-3, 978-0-521-67227-6, 978-0-521-63303-1. DOI: 10.1017/CBO9780511816079.

[33] ——, *String theory. Vol. 2: Superstring theory and beyond*, ser. Cambridge Monographs on Mathematical Physics. Cambridge University Press, Dec. 2007, ISBN: 978-0-511-25228-0, 978-0-521-63304-8, 978-0-521-67228-3. DOI: 10.1017/CBO9780511618123.

[34] K. Becker, M. Becker, and J. H. Schwarz, *String theory and M-theory: A modern introduction*. Cambridge University Press, Dec. 2006, ISBN: 978-0-511-25486-4, 978-0-521-86069-7, 978-0-511-81608-6. DOI: 10.1017/CBO9780511816086.

[35] O. Aharony, S. S. Gubser, J. M. Maldacena, H. Ooguri, and Y. Oz, "Large N field theories, string theory and gravity," *Phys. Rept.*, vol. 323, pp. 183–386, 2000. DOI: 10.1016/S0370-1573(99)00083-6. arXiv: hep-th/9905111.

[36] J. L. Petersen, "Introduction to the Maldacena conjecture on AdS / CFT," *Int. J. Mod. Phys. A*, vol. 14, pp. 3597–3672, 1999. DOI: 10.1142/S0217751X99001676. arXiv: hep-th/9902131.

[37] H. Nastase, "Introduction to AdS-CFT," Dec. 2007. arXiv: 0712.0689 [hep-th].

[38] M. Natsuume, *AdS/CFT Duality User Guide*. 2015, vol. 903, ISBN: 978-4-431-55441-7, 978-4-431-55440-0. DOI: 10.1007/978-4-431-55441-7. arXiv: 1409.3575 [hep-th].

[39] A. V. Ramallo, "Introduction to the AdS/CFT correspondence," *Springer Proc. Phys.*, vol. 161, C. Merino, Ed., pp. 411–474, 2015. DOI: 10.1007/978-3-319-12238-0_10. arXiv: 1310.4319 [hep-th].

[40] J. Polchinski, "Dirichlet Branes and Ramond-Ramond charges," *Phys. Rev. Lett.*, vol. 75, pp. 4724–4727, 1995. DOI: 10.1103/PhysRevLett.75.4724. arXiv: hep-th/9510017.

[41] ——, "Tasi lectures on D-branes," in *Theoretical Advanced Study Institute in Elementary Particle Physics (TASI 96): Fields, Strings, and Duality*, Nov. 1996, pp. 293–356. arXiv: hep-th/9611050.

[42] ——, "Dualities of Fields and Strings," *Stud. Hist. Phil. Sci. B*, vol. 59, pp. 6–20, 2017. DOI: 10.1016/j.shpsb.2015.08.011. arXiv: 1412.5704 [hep-th].

[43] J. de Boer, E. P. Verlinde, and H. L. Verlinde, "On the holographic renormalization group," *JHEP*, vol. 08, p. 003, 2000. DOI: 10.1088/1126-6708/2000/08/003. arXiv: hep-th/9912012.

[44] A. Adams, L. D. Carr, T. Schäfer, P. Steinberg, and J. E. Thomas, "Strongly Correlated Quantum Fluids: Ultracold Quantum Gases, Quantum Chromodynamic Plasmas, and Holographic Duality," *New J. Phys.*, vol. 14, p. 115 009, 2012. DOI: 10.1088/1367-2630/14/11/115009. arXiv: 1205.5180 [hep-th].

[45] G. T. Horowitz and V. E. Hubeny, "Quasinormal modes of AdS black holes and the approach to thermal equilibrium," *Phys. Rev. D*, vol. 62, p. 024 027, 2000. DOI: 10.1103/PhysRevD.62.024027. arXiv: hep-th/9909056.

[46] K. D. Kokkotas and B. G. Schmidt, "Quasinormal modes of stars and black holes," *Living Rev. Rel.*, vol. 2, p. 2, 1999. DOI: 10.12942/lrr-1999-2. arXiv: gr-qc/9909058.

[47] A. O. Starinets, "Quasinormal modes of near extremal black branes," *Phys. Rev. D*, vol. 66, p. 124 013, 2002. DOI: 10.1103/PhysRevD.66.124013. arXiv: hep-th/0207133.

[48] P. K. Kovtun and A. O. Starinets, "Quasinormal modes and holography," *Phys. Rev. D*, vol. 72, p. 086 009, 2005. DOI: 10.1103/PhysRevD.72.086009. arXiv: hep-th/0506184.

[49] E. Berti, V. Cardoso, and A. O. Starinets, "Quasinormal modes of black holes and black branes," *Class. Quant. Grav.*, vol. 26, p. 163 001, 2009. DOI: 10.1088/0264-9381/26/16/163001. arXiv: 0905.2975 [gr-qc].

[50] R. A. Konoplya and A. Zhidenko, "Quasinormal modes of black holes: From astrophysics to string theory," *Rev. Mod. Phys.*, vol. 83, pp. 793–836, 2011. DOI: 10.1103/RevModPhys.83.793. arXiv: 1102.4014 [gr-qc].

[51] R. A. Janik, J. Jankowski, and H. Soltanpanahi, "Quasinormal modes and the phase structure of strongly coupled matter," *JHEP*, vol. 06, p. 047, 2016. DOI: 10.1007/JHEP06(2016)047. arXiv: 1603.05950 [hep-th].

[52] S. I. Finazzo, R. Rougemont, M. Zaniboni, R. Critelli, and J. Noronha, "Critical behavior of non-hydrodynamic quasinormal modes in a strongly coupled plasma," *JHEP*, vol. 01, p. 137, 2017. DOI: 10.1007/JHEP01(2017)137. arXiv: 1610.01519 [hep-th].

[53] R. Critelli, R. Rougemont, and J. Noronha, "Homogeneous isotropization and equilibration of a strongly coupled plasma with a critical point," *JHEP*, vol. 12, p. 029, 2017. DOI: 10.1007/JHEP12(2017)029. arXiv: 1709.03131 [hep-th].

[54] R. Rougemont, R. Critelli, and J. Noronha, "Nonhydrodynamic quasinormal modes and equilibration of a baryon dense holographic QGP with a critical point," *Phys. Rev. D*, vol. 98, no. 3, p. 034 028, 2018. DOI: 10.1103/PhysRevD.98.034028. arXiv: 1804.00189 [hep-ph].

[55] G. de Oliveira and R. Rougemont, "New purely damped pairs of quasinormal modes in a hot and dense strongly-coupled plasma," *JHEP*, vol. 11, p. 079, 2024. DOI: 10.1007/JHEP11(2024)079. arXiv: 2408.09498 [hep-th].

[56] P. M. Chesler and L. G. Yaffe, "Horizon formation and far-from-equilibrium isotropization in supersymmetric Yang-Mills plasma," *Phys. Rev. Lett.*, vol. 102, p. 211 601, 2009. DOI: 10.1103/PhysRevLett.102.211601. arXiv: 0812.2053 [hep-th].

[57] ——, "Boost invariant flow, black hole formation, and far-from-equilibrium dynamics in N = 4 supersymmetric Yang-Mills theory," *Phys. Rev. D*, vol. 82, p. 026 006, 2010. DOI: 10.1103/PhysRevD.82.026006. arXiv: 0906.4426 [hep-th].

[58] ——, "Holography and colliding gravitational shock waves in asymptotically AdS_5 spacetime," *Phys. Rev. Lett.*, vol. 106, p. 021 601, 2011. DOI: 10.1103/PhysRevLett.106.021601. arXiv: 1011.3562 [hep-th].

[59] M. P. Heller, R. A. Janik, and P. Witaszczyk, "The characteristics of thermalization of boost-invariant plasma from holography," *Phys. Rev. Lett.*, vol. 108, p. 201 602, 2012. DOI: 10.1103/PhysRevLett.108.201602. arXiv: 1103.3452 [hep-th].

[60] W. van der Schee, "Holographic thermalization with radial flow," *Phys. Rev. D*, vol. 87, no. 6, p. 061 901, 2013. DOI: 10.1103/PhysRevD.87.061901. arXiv: 1211.2218 [hep-th].

[61] J. Casalderrey-Solana, M. P. Heller, D. Mateos, and W. van der Schee, "From full stopping to transparency in a holographic model of heavy ion collisions," *Phys. Rev. Lett.*, vol. 111, p. 181 601, 2013. DOI: 10.1103/PhysRevLett.111.181601. arXiv: 1305.4919 [hep-th].

[62] P. M. Chesler and L. G. Yaffe, "Numerical solution of gravitational dynamics in asymptotically anti-de Sitter spacetimes," *JHEP*, vol. 07, p. 086, 2014. DOI: 10.1007/JHEP07(2014)086. arXiv: 1309.1439 [hep-th].

[63] W. van der Schee, "Gravitational collisions and the quark-gluon plasma," PhD thesis, Utrecht U., 2014. arXiv: 1407.1849 [hep-th].

[64] M. Attems, J. Casalderrey-Solana, D. Mateos, D. Santos-Oliván, C. F. Sopuerta, M. Triana, and M. Zilhão, "Paths to equilibrium in non-conformal collisions," *JHEP*, vol. 06, p. 154, 2017. DOI: 10.1007/JHEP06(2017)154. arXiv: 1703.09681 [hep-th].

[65] R. Critelli, R. Rougemont, and J. Noronha, "Holographic Bjorken flow of a hot and dense fluid in the vicinity of a critical point," *Phys. Rev. D*, vol. 99, no. 6, p. 066 004, 2019. DOI: 10.1103/PhysRevD.99.066004. arXiv: 1805.00882 [hep-th].

[66] R. Rougemont, J. Noronha, W. Barreto, G. S. Denicol, and T. Dore, "Violation of energy conditions and entropy production in holographic Bjorken flow," *Phys. Rev. D*, vol. 104, no. 12, p. 126 012, 2021. DOI: 10.1103/PhysRevD.104.126012. arXiv: 2105.02378 [nucl-th].

[67] R. Rougemont, W. Barreto, and J. Noronha, "Hydrodynamization times of a holographic fluid far from equilibrium," *Phys. Rev. D*, vol. 105, no. 4, p. 046 009, 2022. DOI: 10.1103/PhysRevD.105.046009. arXiv: 2111.08532 [nucl-th].

[68] R. Rougemont and W. Barreto, "Holographic entropy production in a Bjorken expanding hot and dense strongly coupled quantum fluid," *Phys. Rev. D*, vol. 106, no. 12, p. 126 023, 2022. DOI: 10.1103/PhysRevD.106.126023. arXiv: 2207.02411 [hep-th].

[69] ——, "Stairway to equilibrium entropy," *Phys. Rev. D*, vol. 109, no. 12, p. 126 009, 2024. DOI: 10.1103/PhysRevD.109.126009. arXiv: 2402.04529 [hep-th].

[70] J. Erdmenger, N. Evans, I. Kirsch, and E. Threlfall, "Mesons in Gauge/-Gravity Duals - A Review," *Eur. Phys. J. A*, vol. 35, pp. 81–133, 2008. DOI: 10.1140/epja/i2007-10540-1. arXiv: 0711.4467 [hep-th].

[71] S. J. Brodsky, G. F. de Teramond, H. G. Dosch, and J. Erlich, "Light-Front Holographic QCD and Emerging Confinement," *Phys. Rept.*, vol. 584, pp. 1–105, 2015. DOI: 10.1016/j.physrep.2015.05.001. arXiv: 1407.8131 [hep-ph].

[72] J. Casalderrey-Solana, H. Liu, D. Mateos, K. Rajagopal, and U. A. Wiedemann, *Gauge/String Duality, Hot QCD and Heavy Ion Collisions*. Cambridge University Press, 2014, ISBN: 978-1-00-940350-4, 978-1-00-940349-8, 978-1-00-940352-8, 978-1-139-13674-7. DOI: 10.1017/9781009403504. arXiv: 1101.0618 [hep-th].

[73] Y. Kim, I. J. Shin, and T. Tsukioka, "Holographic QCD: Past, Present, and Future," *Prog. Part. Nucl. Phys.*, vol. 68, pp. 55–112, 2013. DOI: 10.1016/j.ppnp.2012.09.002. arXiv: 1205.4852 [hep-ph].

[74] O. DeWolfe, S. S. Gubser, C. Rosen, and D. Teaney, "Heavy ions and string theory," *Prog. Part. Nucl. Phys.*, vol. 75, pp. 86–132, 2014. DOI: 10.1016/j.ppnp.2013.11.001. arXiv: 1304.7794 [hep-th].

[75] C. Hoyos, N. Jokela, and A. Vuorinen, "Holographic approach to compact stars and their binary mergers," *Prog. Part. Nucl. Phys.*, vol. 126, p. 103 972, 2022. DOI: 10.1016/j.ppnp.2022.103972. arXiv: 2112.08422 [hep-th].

[76] S. A. Hartnoll, "Lectures on holographic methods for condensed matter physics," *Class. Quant. Grav.*, vol. 26, A. M. Uranga, Ed., p. 224 002, 2009. DOI: 10.1088/0264-9381/26/22/224002. arXiv: 0903.3246 [hep-th].

[77] C. P. Herzog, "Lectures on Holographic Superfluidity and Superconductivity," *J. Phys. A*, vol. 42, p. 343 001, 2009. DOI: 10.1088/1751-8113/42/34/343001. arXiv: 0904.1975 [hep-th].

[78] J. McGreevy, "Holographic duality with a view toward many-body physics," *Adv. High Energy Phys.*, vol. 2010, p. 723 105, 2010. DOI: 10.1155/2010/723105. arXiv: 0909.0518 [hep-th].

[79] G. T. Horowitz, "Introduction to Holographic Superconductors," *Lect. Notes Phys.*, vol. 828, pp. 313–347, 2011. DOI: 10.1007/978-3-642-04864-7_10. arXiv: 1002.1722 [hep-th].

[80] S. Sachdev, "What can gauge-gravity duality teach us about condensed matter physics?" *Ann. Rev. Condensed Matter Phys.*, vol. 3, pp. 9–33, 2012. DOI: 10.1146/annurev-conmatphys-020911-125141. arXiv: 1108.1197 [cond-mat.str-el].

[81] R.-G. Cai, L. Li, L.-F. Li, and R.-Q. Yang, "Introduction to Holographic Superconductor Models," *Sci. China Phys. Mech. Astron.*, vol. 58, no. 6, p. 060 401, 2015. DOI: 10.1007/s11433-015-5676-5. arXiv: 1502.00437 [hep-th].

[82] T. Nishioka, S. Ryu, and T. Takayanagi, "Holographic Entanglement Entropy: An Overview," *J. Phys. A*, vol. 42, p. 504 008, 2009. DOI: 10.1088/1751-8113/42/50/504008. arXiv: 0905.0932 [hep-th].

[83] M. Van Raamsdonk, "Lectures on Gravity and Entanglement," in *Theoretical Advanced Study Institute in Elementary Particle Physics: New Frontiers in Fields and Strings*, 2017, pp. 297–351. DOI: 10.1142/9789813149441_0005. arXiv: 1609.00026 [hep-th].

[84] B. Chen, B. Czech, and Z.-z. Wang, "Quantum information in holographic duality," *Rept. Prog. Phys.*, vol. 85, no. 4, p. 046 001, 2022. DOI: 10.1088/1361-6633/ac51b5. arXiv: 2108.09188 [hep-th].

[85] S. Chapman and G. Policastro, "Quantum computational complexity from quantum information to black holes and back," *Eur. Phys. J. C*, vol. 82, no. 2, p. 128, 2022. DOI: 10.1140/epjc/s10052-022-10037-1. arXiv: 2110.14672 [hep-th].

[86] G. W. Gibbons and S. W. Hawking, "Action Integrals and Partition Functions in Quantum Gravity," *Phys. Rev. D*, vol. 15, pp. 2752–2756, 1977. DOI: 10.1103/PhysRevD.15.2752.

[87] W. Greiner and J. Reinhardt, *Field quantization*. 1996.

[88] J. D. Bekenstein, "Black holes and entropy," *Phys. Rev. D*, vol. 7, pp. 2333–2346, 1973. DOI: 10.1103/PhysRevD.7.2333.

[89] S. W. Hawking, "Particle Creation by Black Holes," *Commun. Math. Phys.*, vol. 43, G. W. Gibbons and S. W. Hawking, Eds., pp. 199–220, 1975, [Erratum: Commun.Math.Phys. 46, 206 (1976)]. DOI: 10.1007/BF02345020.

[90] L. Bombelli, R. K. Koul, J. Lee, and R. D. Sorkin, "A Quantum Source of Entropy for Black Holes," *Phys. Rev. D*, vol. 34, pp. 373–383, 1986. DOI: 10.1103/PhysRevD.34.373.

[91] M. Srednicki, "Entropy and area," *Phys. Rev. Lett.*, vol. 71, pp. 666–669, 1993. DOI: 10.1103/PhysRevLett.71.666. arXiv: hep-th/9303048.

[92] P. Calabrese and J. L. Cardy, "Entanglement entropy and quantum field theory: A Non-technical introduction," *Int. J. Quant. Inf.*, vol. 4, p. 429, 2006. DOI: 10.1142/S021974990600192X. arXiv: quant-ph/0505193.

[93] A. Riera and J. I. Latorre, "Area law and vacuum reordering in harmonic networks," *Phys. Rev. A*, vol. 74, p. 052 326, 2006. DOI: 10.1103/PhysRevA.74.052326. arXiv: quant-ph/0605112.

[94] J. I. Latorre, "Entanglement entropy and the simulation of Quantum Mechanics," *J. Phys. A*, vol. 40, J. Sola, Ed., pp. 6689–6697, 2007. DOI: 10.1088/1751-8113/40/25/S13. arXiv: quant-ph/0611271.

[95] L. Amico, R. Fazio, A. Osterloh, and V. Vedral, "Entanglement in many-body systems," *Rev. Mod. Phys.*, vol. 80, pp. 517–576, 2008. DOI: 10.1103/RevModPhys.80.517. arXiv: quant-ph/0703044.

[96] J. Eisert, M. Cramer, and M. B. Plenio, "Area laws for the entanglement entropy - a review," *Rev. Mod. Phys.*, vol. 82, pp. 277–306, 2010. DOI: 10.1103/RevModPhys.82.277. arXiv: 0808.3773 [quant-ph].

[97] H. Casini and M. Huerta, "Entanglement entropy in free quantum field theory," *J. Phys. A*, vol. 42, p. 504 007, 2009. DOI: 10.1088/1751-8113/42/50/504007. arXiv: 0905.2562 [hep-th].

[98] P. Calabrese and J. Cardy, "Entanglement entropy and conformal field theory," *J. Phys. A*, vol. 42, p. 504 005, 2009. DOI: 10.1088/1751-8113/42/50/504005. arXiv: 0905.4013 [cond-mat.stat-mech].

[99] J. I. Latorre and A. Riera, "A short review on entanglement in quantum spin systems," *J. Phys. A*, vol. 42, p. 504 002, 2009. DOI: 10.1088/1751-8113/42/50/504002. arXiv: 0906.1499 [cond-mat.stat-mech].

[100] C. Holzhey, F. Larsen, and F. Wilczek, "Geometric and renormalized entropy in conformal field theory," *Nucl. Phys. B*, vol. 424, pp. 443–467, 1994. DOI: 10.1016/0550-3213(94)90402-2. arXiv: hep-th/9403108.

[101] P. Calabrese and J. L. Cardy, "Entanglement entropy and quantum field theory," *J. Stat. Mech.*, vol. 0406, P06002, 2004. DOI: 10.1088/1742-5468/2004/06/P06002. arXiv: hep-th/0405152.

[102] G. Vidal, J. I. Latorre, E. Rico, and A. Kitaev, "Entanglement in quantum critical phenomena," *Phys. Rev. Lett.*, vol. 90, p. 227 902, 2003. DOI: 10.1103/PhysRevLett.90.227902. arXiv: quant-ph/0211074.

[103] J. I. Latorre, E. Rico, and G. Vidal, "Ground state entanglement in quantum spin chains," *Quant. Inf. Comput.*, vol. 4, no. 1, pp. 48–92, 2004. DOI: 10.26421/QIC4.1-4. arXiv: quant-ph/0304098.

[104] H. Casini, "Geometric entropy, area, and strong subadditivity," *Class. Quant. Grav.*, vol. 21, pp. 2351–2378, 2004. DOI: 10.1088/0264-9381/21/9/011. arXiv: hep-th/0312238.

[105] M. Cramer, J. Eisert, M. B. Plenio, and J. Dreissig, "An Entanglement-area law for general bosonic harmonic lattice systems," *Phys. Rev. A*, vol. 73, p. 012 309, 2006. DOI: 10.1103/PhysRevA.73.012309. arXiv: quant-ph/0505092.

[106] S. Das and S. Shankaranarayanan, "How robust is the entanglement entropy: Area relation?" *Phys. Rev. D*, vol. 73, p. 121 701, 2006. DOI: 10.1103/PhysRevD.73.121701. arXiv: gr-qc/0511066.

[107] D. V. Fursaev, "Proof of the holographic formula for entanglement entropy," *JHEP*, vol. 09, p. 018, 2006. DOI: 10.1088/1126-6708/2006/09/018. arXiv: hep-th/0606184.

[108] K. Behrndt, M. Cvetic, and W. A. Sabra, "Nonextreme black holes of five-dimensional N=2 AdS supergravity," *Nucl. Phys. B*, vol. 553, pp. 317–332, 1999. DOI: 10.1016/S0550-3213(99)00243-6. arXiv: hep-th/9810227.

[109] M. Cvetic and S. S. Gubser, "Phases of R charged black holes, spinning branes and strongly coupled gauge theories," *JHEP*, vol. 04, p. 024, 1999. DOI: 10.1088/1126-6708/1999/04/024. arXiv: hep-th/9902195.

[110] O. DeWolfe, S. S. Gubser, and C. Rosen, "Dynamic critical phenomena at a holographic critical point," *Phys. Rev. D*, vol. 84, p. 126 014, 2011. DOI: 10.1103/PhysRevD.84.126014. arXiv: 1108.2029 [hep-th].

[111] ——, "Fermi surfaces in N=4 Super-Yang-Mills theory," *Phys. Rev. D*, vol. 86, p. 106 002, 2012. DOI: 10.1103/PhysRevD.86.106002. arXiv: 1207.3352 [hep-th].

[112] M. Asadi, H. Soltanpanahi, and F. Taghinavaz, "Critical behaviour of hydrodynamic series," *JHEP*, vol. 05, p. 287, 2021. DOI: 10.1007/JHEP05(2021)287. arXiv: 2102.03584 [hep-th].

[113] H. Ebrahim, M. Asadi, and M. Ali-Akbari, "Evolution of Holographic Complexity Near Critical Point," *JHEP*, vol. 09, p. 023, 2019. DOI: 10.1007/JHEP09(2019)023. arXiv: 1811.12002 [hep-th].

[114] H. Ebrahim and G.-M. Nafisi, "Holographic Mutual Information and Critical Exponents of the Strongly Coupled Plasma," *Phys. Rev. D*, vol. 102, no. 10, p. 106 007, 2020. DOI: 10.1103/PhysRevD.102.106007. arXiv: 2002.09993 [hep-th].

[115] B. Amrahi, M. Ali-Akbari, and M. Asadi, "Temperature dependence of entanglement of purification in the presence of a chemical potential," *Phys. Rev. D*, vol. 103, no. 8, p. 086 019, 2021. DOI: 10.1103/PhysRevD.103.086019. arXiv: 2101.03994 [hep-th].

[116] B. Amrahi, M. Asadi, and F. Taghinavaz, "Chaos near to the critical point: butterfly effect and pole-skipping," *Eur. Phys. J. C*, vol. 84, no. 5, p. 505, 2024. DOI: 10.1140/epjc/s10052-024-12854-y. arXiv: 2305.00298 [hep-th].

[117] D. Karan and S. Pant, "Entanglement and Chaos near critical point in strongly coupled Gauge theory," *Eur. Phys. J. C*, vol. 84, no. 2, p. 113, 2024. DOI: 10.1140/epjc/s10052-024-12463-9. arXiv: 2308.00018 [hep-th].

[118] J. W. York Jr., "Role of conformal three geometry in the dynamics of gravitation," *Phys. Rev. Lett.*, vol. 28, pp. 1082–1085, 1972. DOI: 10.1103/PhysRevLett.28.1082.

[119] E. Poisson, *A Relativist's Toolkit: The Mathematics of Black-Hole Mechanics*. Cambridge University Press, Dec. 2009. DOI: 10.1017/CBO9780511606601.

[120] H. Năstase, *Classical Field Theory*. Cambridge University Press, Mar. 2019, ISBN: 978-1-108-47701-7, 978-1-108-75321-0.

[121] R. C. Myers and O. Tafjord, "Superstars and giant gravitons," *JHEP*, vol. 11, p. 009, 2001. DOI: 10.1088/1126-6708/2001/11/009. arXiv: hep-th/0109127.

[122] S. S. Gubser, I. R. Klebanov, and A. W. Peet, "Entropy and temperature of black 3-branes," *Phys. Rev. D*, vol. 54, pp. 3915–3919, 1996. DOI: 10.1103/PhysRevD.54.3915. arXiv: hep-th/9602135.

[123] O. DeWolfe, S. S. Gubser, and C. Rosen, "A holographic critical point," *Phys. Rev. D*, vol. 83, p. 086 005, 2011. DOI: 10.1103/PhysRevD.83.086005. arXiv: 1012.1864 [hep-th].

[124] E. Quijada and H. Boschi-Filho, "Entanglement Entropy for D3-, M2- and M5-brane backgrounds," Nov. 2017. arXiv: 1711.08505 [hep-th].

[125] W. Fischler and S. Kundu, "Strongly Coupled Gauge Theories: High and Low Temperature Behavior of Non-local Observables," *JHEP*, vol. 05, p. 098, 2013. DOI: 10.1007/JHEP05(2013)098. arXiv: 1212.2643 [hep-th].

[126] E. Tonni, "Holographic entanglement entropy: near horizon geometry and disconnected regions," *JHEP*, vol. 05, p. 004, 2011. DOI: 10.1007/JHEP05(2011)004. arXiv: 1011.0166 [hep-th].

[127] M. L. Bellac, *Thermal Field Theory*, ser. Cambridge Monographs on Mathematical Physics. Cambridge University Press, Mar. 2011, ISBN: 978-0-511-88506-8, 978-0-521-65477-7. DOI: 10.1017/CBO9780511721700.

[128] A. K. Das, *Finite Temperature Field Theory*. New York: World Scientific, 1997, ISBN: 978-981-02-2856-9, 978-981-4498-23-4.